PHASE-RESOLVED FLUOROIMMUNOCHEMICAL METHODS FOR THE DETERMINATION OF PHENOBARBITAL

By

TERESA LYNN KEIMIG

Bachelor of Science
University of South Dakota
Vermillion, South Dakota
1982

Master of Science
University of Iowa
Iowa City, Iowa
1984

Submitted to the Faculty of the
Graduate College of the
Oklahoma State University
in partial fulfillment of
the requirements for
the Degree of
DOCTOR OF PHILOSOPHY
December, 1989

PHASE-RESOLVED FLUOROIMMUNOCHEMICAL
METHODS FOR THE DETERMINATION
OF PHENOBARBITAL

Thesis Approved:

Linda B. McGown
Thesis Adviser

Horacio A Mottola

Richard A. Bruce

Earl D. Mitchell, Jr

Norman N. Durham
Dean of the Graduate College

PREFACE

This thesis is divided into three main sections. The first part (Chapter II) is a literature review of time-resolved fluoroimmunochemical determinations. The next section (Chapter III) is a dicussion of phase-resolved fluorescence spectroscopy (PRFS) and a review of phase-resolved fluoroimmunochemical determinations. The following two chapters, IV and V, describe the approaches that were taken to develop a simplified and improved phase-resolved fluoroimmunoassay for phenobarbital in order to illustrate the applicability of PRFS to the determination of haptens.

I would like to acknowledge the National Institute on Drug Abuse (NIDA) and the National Science Foundation (NSF) for supporting this work. The financial support of the Department of Chemistry through teaching assistantships and summer scholarships is also appreciated.

I would also like to thank the members of my committee: Drs. Linda McGown, Horacio Mottola, Earl Mitchell and Richard Bunce for their time and efforts. You have each, in your own ways, provided me with examples of what a good chemist and a good person should be.

Dr. McGown, as my research advisor, has provided me with inspiration, guidance, support and friendship during my

graduate studies. For this I am very grateful. I would also like to thank her family and the members of her group at OSU for their help and camaraderie. Thank you Steve, Jenna, Mikey, Keith, Frank, Tyler, Kasem, Dave and Debbie.

I would also like to express my sincere appreciation to Dr. Mottola and the members of his research group: Sudha, Zach, Chris, Jianbo, Sun Gang and Paul for adopting me over the last two years. I really do not know if I would have finished without your friendship, support and understanding.

Finally, I would like to thank my parents, Joe and Cathy, and family for their love and encouragement. I know you have sometimes wondered if I would ever finish going to school, but I've learned that I can always count on your support.

TABLE OF CONTENTS

LIST OF TABLES

LIST OF FIGURES

Figure Page

CHAPTER I

INTRODUCTION

Immunochemical determinations belong to a broad class of analytical techniques called "binding assays". These techniques are defined as "any procedure in which quantitation of a material depends on the progressive saturation of a specific binder by that material and the subsequent determination of its distribution between bound and free phases" (1). In an immunochemical determination, the binder is an antibody (Ab) and the material being quantified is its antigen (Ag). Immunochemical determinations are very powerful analytical techniques due to their combination of high selectivity, low detection limits and wide applicability. They currently allow for the determination of femtomolar concentrations of analytes in highly complex samples.

The distribution of analyte between bound and free phases is usually followed by attaching a label, detectable by some physiochemical means, to either the antigen (Ag^*) or antibody (Ab^*). Labelled-antigen methods are called "immunoassays" and labelled-antibody methods are usually called "immunometric assays". The bound and free phases are usually physically separated before the label is measured;

however, if the signals of the bound and free labelled compounds are sufficiently different no separation step is necessary. Determinations requiring a separation step are "heterogeneous" and those that do not are "homogeneous". The label can be any material which can be measured precisely and accurately in very small quantities. Typical labels include radioisotopes, enzymes and fluorophores.

Radioactive isotopes are the most widely employed labels in immunochemical determinations. In recent years legal, social and logistical objections to their use have been raised. The use of radioisotopes involves potential environmental and health hazards, mainly in the preparation of the labelled reagent but also in its handling and disposal. The labelled reagent also has a relatively short shelflife due to the nature of the label. On the other hand, radioisotopes are not affected by variations in the chemical and physical microenvironments; the instrumentation used is reliable, relatively inexpensive and now widely available; and the label has a very high signal-to-noise ratio. Alternative labels generally have higher limits of detection and/or are not as easy to use except for the avoidance of radioactivity. They are widely applied to those analytes not requiring low detection limits or to determinations in which qualitative rather than quantitative results are desired.

Fluorescent labels are relatively inexpensive and have a reasonably long shelflife. The fluorescence measurement can usually be accomplished quickly and easily. The main

limitation of fluorescent labels is that many compounds present in biological fluids can cause problems in the measurement of the fluorescence of a fluorophore. These problems include light scattering, endogenous fluorophores, inner filter effects and quenching. The fluorophores most frequently used as labels in immunochemical determinations include fluorescein, the rhodamines, umbelliferone, fluorescamine and rare earth metal chelates. The fluorophore most widely used at the present time is fluorescein, which has a high molar absorptivity ($\sim 9 \times 10^4$ $M^{-1}cm^{-1}$) in the vis- ible region of the electromagnetic spectrum and a quantum yield approaching 1.00. It also has high photo-stability and chemical stability. Its main drawback is that it is very sensitive to background interferences, scattering from the sample and concentration quenching.

Immunochemical determinations employing fluorescent labels have been gaining widespread usage. This is due to the high sensitivity of fluorescence measurement and the sensitivity of the fluorescent label to changes in its chemical microenvironment. Because of the sensitivity to changes in its environment, simple, rapid heterogeneous and homogeneous fluoroimmunochemical determinations are possible. Determinations based on changes in fluorescence intensity, energy transfer, polarization and fluorescence lifetimes have been reported (2-5). Two different techniques have been developed to take advantage of changes in fluorescence lifetimes in fluoroimmunochemical determina-

tions. One is based upon time-resolved spectroscopy and the other on phase-resolved fluorescence spectroscopy.

In time-resolved spectroscopy, pulsed light is used to excite the sample and the fluorescence decay is monitored. When a fluorophore is excited by pulsed light, fluorescence is emitted following each pulse with an intensity which decays at a rate related to the excited-state lifetime of the emitting species. An electronically-gated detection system can be used to measure photons at any time interval after the excitation pulse has decayed to an undetectable level. Time-resolved fluoroimmunochemical determinations, based upon time-resolved methods of eliminating background fluorescence, employ fluorescent labels with lifetimes above 100 ns. The labels are usually some type of rare earth chelate and the determinations are usually heter- ogeneous. Two different commercially available time-resolved fluoro-immunoassay systems have been developed. Chapter II is a critical review of time-resolved fluoroimmunochemical determinations, including a discussion of the labels and instrumentation developed for use in them.

In phase-resolved fluorescence spectroscopy, sinusoidally-modulated light is used to excite the fluorescent sample. The resulting fluorescence emission is also sinusoidally modulated but is phase-shifted and demodulated with respect to the excitation beam. The emission signal, measured with a phase-sensitive detector, is dependent on the modulation frequency, the excitation and emission wavelengths, and the intensity, lifetime and concentration

characteristics of the emitting specie(s). The phase-resolved fluoroimmunochemical determinations that have been reported used fluorescent labels, fluorescein and two rhodamines, with short lifetimes (< 5 ns). These determinations were all homogeneous systems and were based on lifetime differences between the free and bound labelled species. Phase-resolved fluoroimmunochemical determinations are the only immunochemical determinations that use fluorescence lifetime selctivity as the basis of homogeneous detection. Chapter III contains a brief discusssion of the theory of phase-resolved fluorescence spectroscopy and a review of phase-resolved fluoroimmunochemical determinations.

The first phase-resolved immunochemical determination was developed for phenobarbital (6) and was based on very small changes in the intensity (< 10%) and lifetime (100 ps) of fluorescein-labelled phenobarbital when it was bound by the anti-phenobarbital antibody. Because of the very small changes in the fluorescence signal, the data collection and analysis was fairly complicated and time-consuming. It was also not very amenable to automation. The reagents were purchased in the form of a heterogeneous fluoroimmunoassay kit from a company that subsequently went out of business.

There was a need to simplify and improve the phenobarbital immunoassay, in order to better demonstrate the feasability of the phase-resolved approach to fluoroimmunassay of small molecules. The work presented in this thesis

describes various approaches that were taken towards this goal. The studies can be divided into two main categories as follows:

1) Studies of the effects of organized media on the fluorescence of fluorescein-labelled phenobarbital and antibody-bound labelled phenobarbital. The effects of various surfactants and cyclodextrins were evaluated and compared, with the idea that they might improve the discrimination between the free and antibody-bound labelled phenobarbital. This work is presented in Chapter IV.

2) Studies of the optimization of experimental conditions with respect to the various reagents used in the fluoroimmunoassay. In order not to eliminate the dependence on commercially-available kits, phenobarbital, fluorescein-labelled phenobarbital and anti-phenobarbital antibodies were obtained individually from commercial sources or synthesized here at Oklahoma State University. Thus, both reagent concentrations and instrumental conditions could be optimized. Effects of several different antibody preparations were studied and compared. Also, a different experimental approach to data collection and analysis was taken in order to facilitate the implementation of a flow system. These studies are presented in Chapter V.

CHAPTER II

A REVIEW OF TIME-RESOLVED FLUOROIMMUNOCHEMICAL DETERMINATIONS

Introduction

The first immunoassay was reported by Yalow and Berson (6) in 1960. They used 134I-labelled antigens to develop a radioimmunoassay for insulin. In a labelled-antigen immmunoassay (Figure 1), the labelled and unlabelled antigen compete for a limiting amount of antibody. The amount of labelled antigen bound by the antibody is controlled by the law of mass action. As the amount of unlabelled antigen in the sample increases, the amount of labelled-antigen bound to the antibody decreases. Thus the amount of labelled-antigen present in the bound phase is inversely proportional to the amount of antigen (analyte) in the sample. If the exact concentrations of labelled antigen and antibody and the affinity constant for the system are known, then the analyte concentration could be determined by calculation. In practice, a calibration curve of a series of antigen standards is almost always needed.

Miles and Hale (7) introduced the first "immunometric assay" in 1968. This technique used a radioisotope-labelled

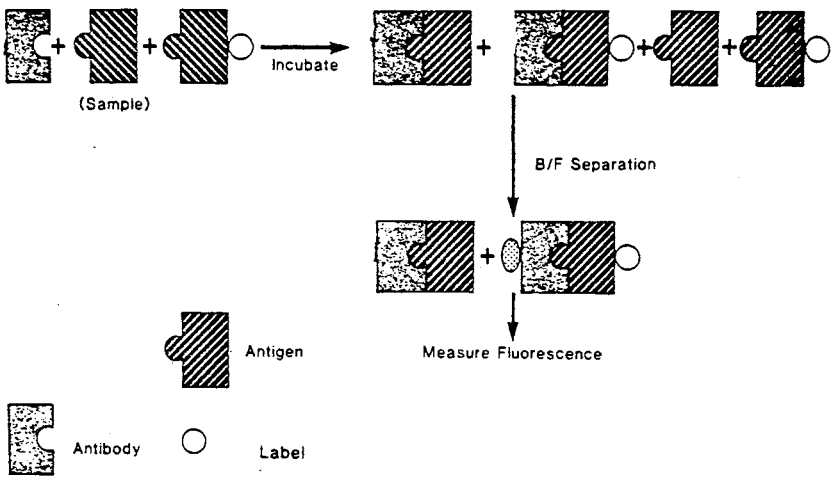

Figure 1. Schematic Representation of an Immunoassay Procedure. Adapted from Simonsen, M.G. In Nonisotopic Alternatives to Radioimmunoassay: Principles and Applications; Kaplan, L.A.; Pesce, A.J., Eds.; Marcel Dekker, Inc.: New York, 1981; p. 1.

antibody. The antigen was allowed to react with a fixed, excess amount of labelled antibody. Either the antigen-labelled antibody complex or the free labelled antibody may be determined.

Immunometric determinations (Figure 2), are divided into two main variations. In the first, the antigen in the sample competes with antigen immobilized on a solid phase for the labelled antibody. After a separation step, the amount of labelled antibody in one of the two phases is measured and the amount of analyte is determined from a calibration curve. The amount of labelled antibody in the solid phase is inversely proportional to the amount of analyte. This type of immunometric determination is also known as "one-site" since only one antigenic determinant is needed. In contrast, the other type of immunometric determination uses an antibody solid phase in addition to a labelled antibody. In this noncompetitive, "two-site" technique, the analyte is incubated with an excess of solid phase antibody and an excess of labelled antibody. The "two-site" immunometric determinations is are divided into "one-step" and "two-step" methods, depending on the number of incubation steps used. After the immunochemical reactions have occured, the solid phase is separated from the reaction medium. The amount of labelled antibody in the solid phase is directly proportional to the amount of antigen in the sample. The concentration of analyte is determined through the use of a calibration curve. If the

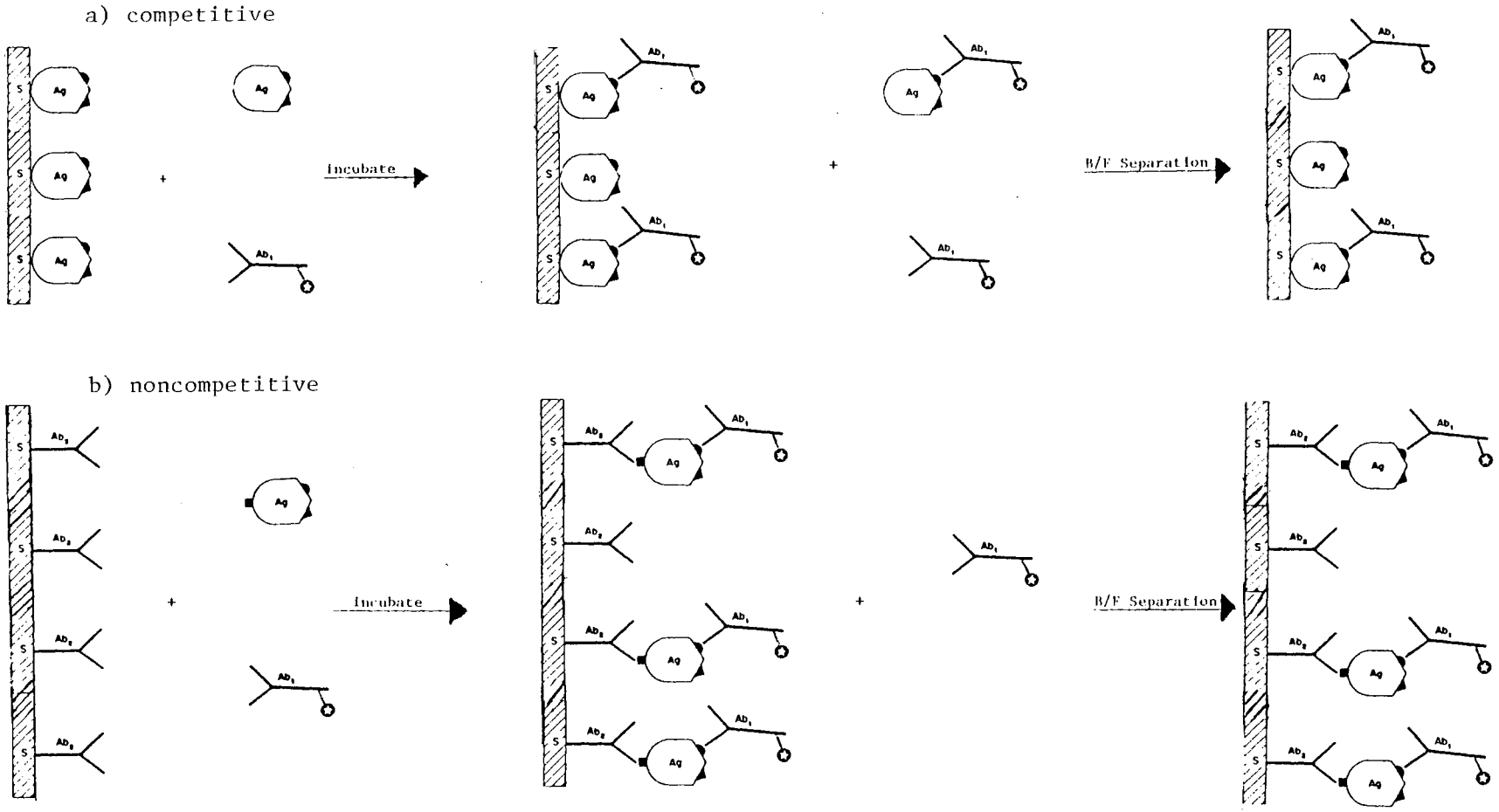

Figure 2. Schematic Representation of an Immunometric Procedure. a) competitive, b) noncompetitive.

two antibodies do not bind to separate antigenic determinants, or if the number of molecules with binding sites to only one of the antibodies is high, then the analyte should first be allowed to react with the solid phase antibody and then washed before the labelled antibody is added (a "two-step" method). The "two-site" immunometric determination is also known by the descriptive term "sandwich immunoassay".

Sensitivity, Detection limits and Selectivity

Sensitivity and Detection Limits

In clinical chemistry and biochemistry journals the terms sensitivity and detection limit are often misused in the eyes of analytical chemists. The American Chemical Society Committee on Environmental Improvement defines detection limit as "the lowest concentration of analyte that the analytical process can reliably detect" (9). They recommend that the detection limit be located at three standard deviations above the blank signal. It should be expressed in concentration units derived from the calibration curve. This method gives a 7% risk of false negatives and false positives. The sensitivity of a method is defined as " the ratio of change in instrumental response to the change in analyte concentration, i.e., the slope of the calibration curve." Note that detection limit and sensitivity are not interchangable. Most papers on

immunochemical determinations use some seemingly arbitrarily-chosen value as the detection limit and then proceed to use sensitivity as a synonym for detection limit. Some of this confusion becomes more understandable in light of the International Federation of Clinical Chemistry (IFCC) definitions of sensitivity and detection limit (10). They define sensitivity as " the ability of an analytical method to detect small quantities of the measured component." They state further that sensitivity has no numerical value. Detection limit is defined as "the smallest single result, which with a stated probability (commonly 95%), can be distinguished from a suitable blank." The limit of detection, according to the IFCC, may be either a concentration or an amount. The confusion that results from these radically different definitions of sensitivty can best be illustrated by Figure 3, taken from Ekins (8), who states that "the definition of sensitivity in terms of lower limit of detection has now been both universally and formally accepted". In this review the ACS definitions of sensitivity and limit of detection shall be used; alternative usages of these words have been translated into the appropriate terminology.

A significant improvement in the detection limit is one of the principal advantages of noncompetitive immunometric determinations over immunoassays (and competitive immunometric determinations). This improvement in the detection limits, according to Ekins and coworkers (8,11,12), is due

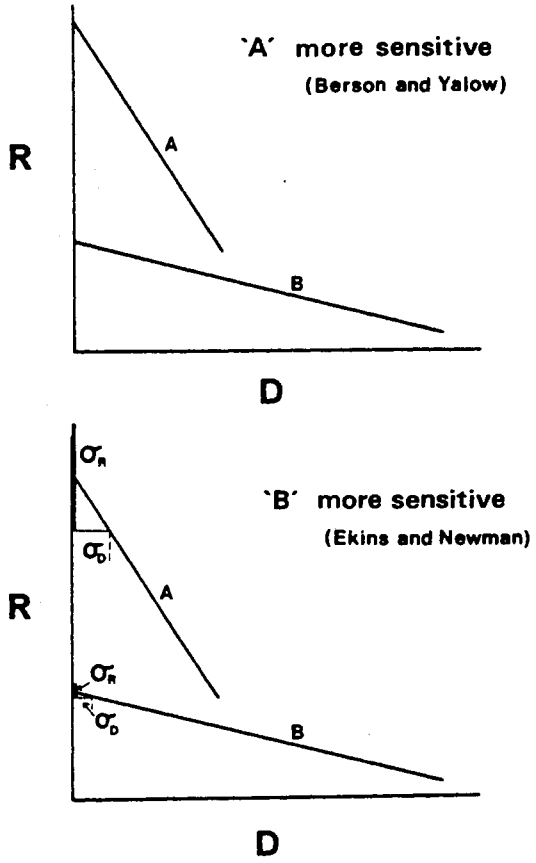

Assay dose-response curves for two assays (A and B) are shown. The Berson/Yalow concept of sensitivity defines assay A as of greater sensitivity. Ekins et al (8) define assay B as more sensitive since the random error in the zero dose measurement (σ_D) i.e. the lower limit of detection, is smaller. σR represents the random error in the response variable (R) at zero dose.

Figure 3. Sensitivity vs. Detection Limit for an Immunoassay. From Reference (8).

to the differences in the optimal reagent concentrations for the two types of immunochemical determinations. In any immunochemical determination, the overall detection limit of the method is influenced by the equilibrium constant of the immunochemical reaction, the detectability of the label, the extent of misclassification of the labelled reagent (bound versus free), and the precision of the required reagent manipulations (12). However, the relative importance of these factors differs significantly as a result of the contrasting amounts of antibody which are optimal in each type of determination.

Consider an ideal system in which the antibodies show negligible nonspecific binding and the label has an infinite detectability. In an immunoassay, the optimal antibody concentration tends toward zero when either the bound or free fraction of labelled antigen is measured. In a noncompetitive immunometric determination, the optimal antibody concentration tends toward zero when the free labelled antibody is measured and toward infinity when the bound labelled antibody is measured. In an immunoassy, because the optimal Ab concentration approaches zero, the equilibrium constant, K_{eq}, of the immunochemical reaction is the dominant factor in determining the extent of reaction and thus is a major constraint on the ultimate detection limit of the method. The precision of the reagent manipulations is also very critical. The ultimate detection

limit is defined by Ekins (8) as the relative error in the signal of the analyte blank (σ_R/R) divided by K_{eq}. The relative error is composed of an "experimental" error component (ε) and a signal measurement component, where ε is the error due to reagent and sample manipulations. Since the label has an "infinite detectability", the signal measurement component of the relative error should be essentially equal to zero. Thus, the detection limit is reduced to ε/K_{eq}. Ekins assumes that ε is limited in practice to approximately 1%. Equilibrium constants of antigen-antibody reactions are seldom higher than 10^{12} liters/mole (1). Thus the ultimate detection limit is around 10^{-14} M regardless of the choice of label. The best detection limits reported in the literature for this type of determination are around 10^{-10} M (12). In a noncompetitive immunometric determination where the amount of bound labelled reagent is measured, K_{eq} is of lesser importance because an excess of labelled antibody is used. However, using an excess of Ab* also increases the nonspecific binding. The optimal concentration of Ab* is dependent upon both the K_{eq} and the fractional nonspecific binding of Ab*. Hence, high antibody binding strength is advantageous but of lesser importance than in an immunoassay. When larger amounts of antibody are used, the pipetting precision is also improved.

Ekins and collegues (8) state that the ultimate limit of detection is defined by: a) the relative error of the

analyte blank signal (σ_R/R), b) the fractional non-specific binding of the antibody (k), and c) the equilibrium constant. The relative error in the analyte blank signal is equal to σ_n/n.s.b. , the error in the estimate of the non-specifically bound (n.s.b.) antibody. The resulting expression of the detection limit is given by

$$\frac{k\sigma_n}{K_{eq}\ (n.s.b.)} \qquad (1)$$

They assume that σ_n/n.s.b. and k are equal to 1% and that K_{eq} is once again equal to 10^{12} liters/mole. The minimum detection limit is then equal to 10^{-16} M, which is two orders of magnitude lower than the minimum detection limit of an immunoassay.

In the above calculations it was assumed that the detectability of the label was infinite. In actual practice this is not the case. The most commonly used radioisotope ^{125}I, has a detection limit of $\sim 10^7$ molecules/ml or $2x10^{-14}$ M (8). This is of the same order of magnitude as the minimum detection limit of an immunoassay. The use of a label with a lower detection limit than ^{125}I in an immunoassay would not yield much benefit in terms of detection limits. However, in a noncompetitive immunometric determination a gain of approximately two orders of magnitude (or more if n.s.b. is reduced below 1%) is possible.

Selectivity

Most substances with molecular weight greater than 5000 can elict an immune response (13). Substances with a smaller molecular weight usually need to be coupled to a large carrier molecule to stimulate the immune system. Substances that elicit an immune response are known as antigens. Small nonimmunogenic antigens are called haptens. Antibodies belong to a type of protein called immunoglobulins, which are divided into five classes. Most immunochemical determinations make use of immunoglobulin G (IgG), which has a molecular weight of 160,000 and consists of four peptide chains held together by disulfide bonds. The two longer heavy chains and the two shorter light chains are joined to form a Y-shaped structure, as seen in Figure 4. The N-terminal halves of each chain are variable in aminoacid sequence while the C-terminal halves are constant. The N-terminal region of one heavy and one light chain form a binding site that makes a complementary fit with the antigen.

The immune response will result in the production of large numbers of antibody molecules with slightly different variable regions. Some will fit the antigen closely and have a high binding strength while others will fit less closely and consequently have a lower binding strength. Cross-reactants are substances, usually with some close structural similarity to the antigen, that bind to the same antibody. Antibody binding strength is the result of the

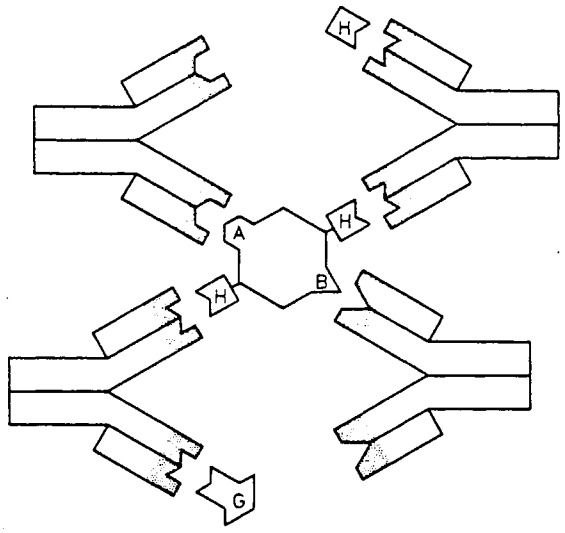

Schematic representation of antibody (immunoglobulin G) structure and some aspects of the immune response. An immunogenic molecule (center) has antigenic determinants A and B, and hapten groups (H) are covalently attached. The response to the immunogen results in the formation of Y-shaped antibody molecules whose variable sequence regions (shaded) form binding sites specific for A, B, or H. Antibodies against H will bind the free (nonimmunogenic) hapten (top). A structurally related hapten (G) will also bind (cross-react) with such antibodies (bottom).

Figure 4. Schematic Representation of Antibody Structure and Some Aspects of Immune Response. From Reference (4).

combined effects of all the noncovalent interactions between the antigen and the binding site (4). Most antibodies have association constants between 10^6 - 10^{12} liter/mole (4). Immunochemical determinations generally use antibodies with constants in excess of 10^9 liter/mole (1). Non-specificity in an immunochemical determination is mainly due to two factors, cross-reactants and other substances which affect the Ab/Ag equilibrium constant. The relative effects of these two factors depend upon the type of immunochemical determination employed.

The effect of cross-reactants is more pronounced in the case of noncompetitive immunometric determinations than in the case of immunoassays and competitive immunometric determinations (12). Cross-reactants compete with the analyte for the antibody binding sites. In an immunoassay, the strength of the cross-reactant relative to the analyte with respect to the antibody binding site is approximately equal to the ratio of their equilibrium constants (11). If the equilibrium constant of the antibody/antigen reaction is large, the effect of most cross-reactants is negligible. In a noncompetitive immunometric determination, the large excess of antibody lessens the effect of differences in binding strength. Equal amounts of analyte and cross-reactant tend to give equal responses; this effect can be reduced by immunopurification of the antibody or by use of the sandwich method (12).

Substances which alter the equilibrium constant of the immunochemical reaction have a pronounced effect on immunoassays and competitive immunometric determinations but not on noncompetitive immunometric determinations (11). Once again, this difference is due to the differences in the optimal reagent concentrations. In an immunoassay, the optimal concentration of antibody tends toward zero. In this situation the distribution of analyte between the free and bound phases is very dependent upon the equilibrium constant. Consequently small changes in K_{eq} can have large effects on the results of the determination. In a noncompetitive immunometric determination, the optimal concentration of Ab tends towards infinity and hte large excess of Ab drives the immunochemical reaction towards completion. Thus, small changes in K_{eq} will have a negligible effect on the results of the determination.

Lanthanide Chelate Labels and Labelling

Lanthanide Chelates

Several types of labels have been proposed for the development of immunometric determinations with very low detection limits. Immunoenzymatic determinations employing fluorescent or radioactive substrates have been reported to reach detection limits of 10^{-17} M and 10^{-18} M, respectively (14,15). Chemiluminescent labels can be detected at levels down to at least 10^{-18} molecules.(16). Although

commercially available instruments cannot reach this level, improvements in instrument design should make chemiluminescent techniques more competitive.

Conventional fluorescent labels are detectable at very low levels but, unfortunately, this has been limited in actual application by high background noise, which is primarily due to light scattering and the presence of other fluorophores in the solution. A wide range of biological materials exhibit fluorescence and may be present in sample solutions. Conventional fluoroimmunochemical determinations usually have a higher detection limit than radioisotopic methods. If the background fluorescence can be reduced, the detection limit of the fluoroimmunochemical determinations should improve.

The ideal fluorescent label should be stable, with high molar absorptivity and quantum yield in aqueous solution. It should also have excitation and emission wavelengths above those of most background materials (λ_{ex} > 360 nm and λ_{em} > 500 nm) and should not interfere with the antigen - antibody binding. Some rare earth metal ions, especially, Eu^{+3} and Tb^{+3}, form highly fluorescent chelates with organic ligands that fulfill many of these qualifications (17), including low detection limits ($\sim 10^{-14}$ M), long fluorescence lifetimes (10 to 1000 μs), large Stoke's shifts (>250 nm), broad excitation bands, and narrow emission lines (3). The long lifetimes of the metal chelates is very important, since the average decay time of background fluorescence is

less than 100 ns; thus, the background fluoresence can be significantly reduced by selectively detecting long-lived fluorescence.

Figure 5 depicts the generally accepted view of the energy transfer processes involved in lanthanide chelate fluorescence (18). Energy is absorbed by the organic ligand, which is then excited from the singlet ground state to the first excited singlet state. Intersystem crossing then occurs from the singlet excited state to the triplet excited state, followed by intermolecular energy transfer between the triplet state of the ligand and the resonance levels of the rare earth ion. Finally, the excited metal ion emits a photon; thus, the frequency of the emitted light is characteristic of the metal itself and independent of the nature of the ligand. The other charateristics of the fluorescence process, such as quantum efficiency, excitation maxima, intensity, lifetime, etc., are strongly dependent on the nature of the ligand and the solvents used (12). The ligand should be as highly absorbing as possible at a suitable wavelength so that the triplet state of the ligand is a little above the resonance line of the metal ion. Also, efficient intermolecular energy transfer requires a strong, stable bond between the metal ion and the ligand.

In time-resolved fluoroimmunochemical techniques, a bifunctional chelating agent is used to couple the metal ion to the molecule to be labelled (either Ab or Ag); the

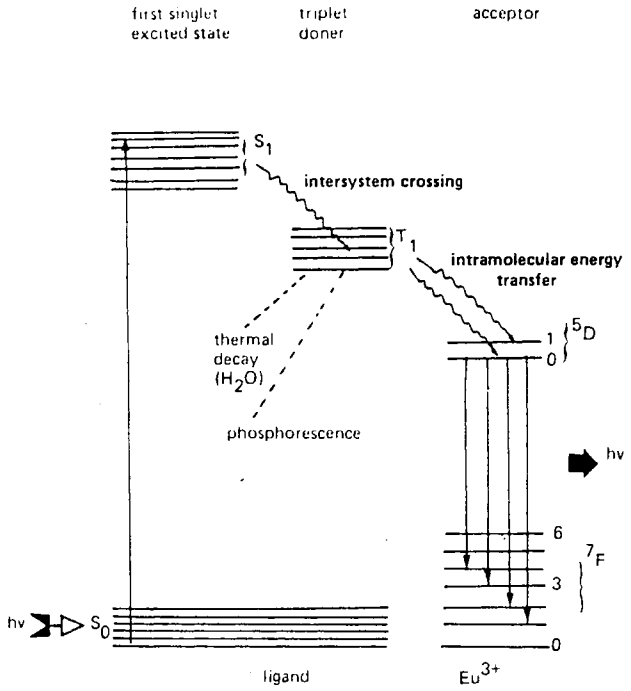

Figure 5. Energy Level Diagram of a Europium (III) Chelate. From Reference (12).

reagent must form a strong, stable metal chelate without disrupting the immunochemical reaction between the antibody and the antigen. The bifunctional reagents used in time-resolved fluoroimmunochemical determinations can be divided into two groups, depending on whether or not the final labelled complex is a strong fluorophore. Dakubu and coworkers (12) call them reagents of the first and second class, respectively. If the complex is of the second class, the fluorescence measurement is made after the immunochemical reaction by dissociating the metal ion from the complex into a solution containing chelating chromophores that are good energy donors. Bifunctional labelling reagents of the first class may be used like conventional fluorophores, but have the added advantage of very long lifetimes and large Stoke's shifts. There may also be some excitation energy transfer from a labelled protein molecule to the lanthanide chelate (19).

The use of a labelling reagent of the first class rather than of the second class seems to be advantageous. Additional reagents and an extra incubation step are required to get a fluorescence signal from a label of the second class; however, the chelates that form the most highly fluorescent lanthanide complexes (β-diketones) cannot be used as reagents of the first class because the stability of these complexes is not high enough (8,20). Certain europium β-diketone complexes have detection limits that are the same or better than the detection limit of ^{125}I (17).

These complexes can be used in an immunochemical determination designed for a labelling reagent of the second class.

In contrast to β-diketone complexes, polyaminopolycarboxylic acids form lanthanide complexes of very high stability (21). Most reagents of the first class are polyaminopolycarboxylic acids. Table I lists some labelling reagents of the first class used in time-resolved fluoroimmunochemical determinations and their fluorescence characteristics. Because of the lower fluorescence intensity of the polycarboxylic acid chelates, the detection limits for these labelling reagents are all higher than desired. Most reagents of this class have been combined with Tb^{+3} ions to form the fluorescent chelate, because Terbium forms more stable complexes in water and doesn't require the addition of other compounds to reduce fluorescence quenching by water molecules (17). However, the lower excitation wavelength may necessitate the use of quartz cells.

Europium polycarboxylic acid complexes are very sensitive to quenching by water molecules. Recently, Diamandis and coworkers (22-24) reported using a europium polycarboxylic acid complex, 4,7-bis(chlorosulfophenyl)-1,10-phenanthroline-2,9-dicarboxylic acid (BCPDA) as a labelling reagent of the first class. BCPDA forms a 1:1 complex with Eu^{+3} unless it is present in excess, in which case, complexes with more than one BCPDA can form. The chelating site consists of two carboxyl groups and two

TABLE I

FLUORESCENCE CHARACTERISTICS OF SOME BIFUNCTIONAL LABELLING REAGENTS OF THE 1st CLASS

Reagent	Metal Ion	λ_{ex} (nm)	λ_{em} (nm)	(ms)	LOD[f]	Reference
erythrosin	-	540	690	0.26	0.11 nM	50
transferrin	Tb+3	295	545	1.25	0.11 uM	46
pAS-DTPA [a]	Tb+3	312	545	1.58	<0.5 nM	48,79
diazophenyl-EDTA[b]	Tb+3	325	550	1.01	0.3 nM	49
aminophenyl-PPTA[c]	Tb+3	-	545	-	-	78
BCPDA [d]	Eu+3	337	613	0.76	10 pM	25
W-1174 [e]	Eu+3	355	613	0.42	-	27

[a] p-aminosalicylatediethylenetriaminepentaacetic acid.

[b] 1-(p-benzenediazoniumethylenediaminetetraacetic acid.

[c] 2,6-bis[(N,N-dicarboxymethyl)aminomethyl]-4-[2-methoxyphenyl]pyridine tetraacetic acid.

[d] 4,7-bis(chlorosulfophenyl)-1,10-phenanthroline-2,9-dicarboxylic acid.

[e] New compound from Wallac Organic Laboratories, not yet commercially avaliable.

[f] Limit of Detection.

heteroaromatic nitrogens. When BCPDA is immobilized on a solid surface in the presence of excess Eu^{+3}, the normal washing steps of an immunometric determination will not remove Eu^{+3} from the labelling reagent. A detection limit of $2x10^{-12}$ M was achieved for the 1:1 complex by adding a phenanthroline group to the polycarboxylic acid to get more effective energy transfer to the europium ion, and by measuring the fluorescence of the complex on a dry solid surface. There are, however, instrument design and reproducibility problems associated with measuring fluorescence from nonuniform solid surfaces (17).

A new labelling reagent of the first class was used in two recently published homogeneous TRFIAs (27,28). The europium chelate (W-1174) was prepared by Wallac Organic Chemistry Laboratory and is not yet commercially avaliable. The labelling reagent has excitation and emission maxima at 355 and 613 nm, respectively, and a fluorescence lifetime of 428 us. The structure of the chelate was not given, but the chelate was reported to have a stable complexing moiety, a functional group with a spacer arm for conjugation reactions, and a light absorbing aromatic structure. The excitation and energy-donating properties of the aromatic structure are sensitive to changes in the chelate's micro-environment that take place when the labelled species is bound in an immunochemical reaction. In the presence of albumin or detergents, the fluorescence of the free fraction

of the labelled species is higher than that of the bound fraction.

All of the labelling reagents of the second class that have been reported in the literature are polyamine polycarboxylates. The chelates all contain either an isothiocyanate or a diazo group to facilitate attachment to the molecule being labelled. The most commonly-used labelling reagents in this class are isothiocyanatophenyl-EDTA and isothiocyanatophenyldiethylenetriaminetetraacetate. After the immunochemical reaction, the metal ion in the bound phase can be dissociated from the chelator by lowering the pH to 2 or 3 (21). This is usually done with an acidic "enhancement" solution containing a β-diketone, "synergistic" compounds, and a nonionic detergent.

Because of their rigidity and good pi-electron delocalization, β-diketones ($R_1COCH_2COR_2$) form highly fluorescent complexes with lanthanide ions (12). The fluorescence characteristics of the complexes can be changed by varying the nature of the functional groups in the R_1 and R_2 positions. Fluorescence intensity can be enhanced by using bulky substituents and good electron donors in these positions. The β-diketone forms a tris chelate with the metal ion as show in Figure 6. The Eu^{+3} ion has a coordination number of eight (29). Six oxygen atoms are available for coordination from the β-diketone. If the coordination is completed by filling the last two positions

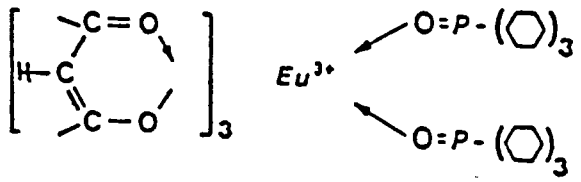

Figure 6. Structure of a Europium (III) -Diketone Synergist Complex.

with the oxygens of water molecules, then the fluorescence will be severely quenched. The "synergist", a Lewis base, is added to the enhancement solution to reduce the quenching. The best of these compounds are neutral molecules that have a lone oxygen atom for coordination to the metal, combined with a bulky, saturated hydrocarbon tail directed away from the metal ion. Tri-n-octylphosphine oxide (TOPO) is the most commonly used "synergist". A nonionic detergent, such as Triton X-100, is also added to the enhancement solution to solubilize the -diketone and the "synergist", and to provide a more hydrophobic environment for the chelate.

Fluorinated aromatic β-diketones produce the most intense fluorophores with europium and samarium ions (17). The lifetimes of the samarium chelates are shorter than that of the europium chelates and their detection limit is two orders of magnitude higher (30). Terbium does not form highly fluorescent chelates with aromatic β-diketones, probably because the excited state triplet levels of the β-diketone are slightly lower than the emission level of Tb^{+3} (31). Fluorinated, aliphatic β-diketones in acidic TOPO and detergent solution give good signals for both europium and terbium. Table II shows some β-diketone complexes and their fluorescence charateristics.

Double-label methods involving the simultaneous measurement of two different lanthanide ions are feasible if both ions form fluorescent complexes with the same ligand

TABLE II

FLUORESCENCE CHARACTERISTICS OF SOME LANTHANIDE β-DIKETONE COMPLEXES

β-diketone	Conditions	Metal Ion	λex(nm)	λem(nm)	τ(us)	LOD	Ref.
TTA	TOPO,TX-100, pH 3.2	Eu+3	354	618	300	2 pM	20,80
β-NTA	TOPO,TX-100, pH 3.5	Eu+3	337	613	430	10 fM	30
		Eu+3	340	613	430	50 fM	17
		Sm+3	340	643	41	0.7 pM	30
PTA	TOPO,TX-100, pH 4.0	Eu+3	308	614	1020	1 pM	32
		Tb+3	307	544	148	40 pM	32

Abbreviations

LOD - limit of detection
TTA - thenoyltrifluoroacetone
TOPO - tri-n-octylphosphine oxide
TX-100 - Triton X-100
-NTA - naphthoyltrifluoroacetone
PTA - pivaloyltrifluoroacetone

under the same reaction conditions. The pairs (Eu^{+3}, Tb^{+3}) and (Eu^{+3}, Sm^{+3}) meet this requirement. In 1987 Bador et al. (30) suggested the use of europium and samarium in a double-label system. Earlier, Hemmila and coworkers (17,31) suggested the europium, terbium pair, and late in 1987 the first report of an actual double-label time-resolved immunofluorimetric determination was published (32). The limits of detection found by Hemmila and coworkers for their europium and terbium complexes are shown in Table II, along with the detection limits found by Bador et al. (30) for their europium and samarium comlexes.

The Eu^{+3}, Sm^{+3} system has lower detection limits than the Eu^{+3}, Tb^{+3} system. The detection limits of both labels in the Eu^{+3},Tb^{+3} system are significantly higher than that of ^{125}I. In the Eu^{+3},Sm^{+3} system, the detection limit of the samarium label is an order of magnitude higher than that of ^{125}I. The Eu^{+3},Tb^{+3} system also has a higher excitation wavelength, which would allow the use of disposable plastic cells or microtitration strips. The aliphatic β-diketone used by Hemmila and coworkers has an excitation wavelength just above 300 nm; all available disposable glass or plastic containers absorb light in this region. In addition, normal glass contains rare earth ions which have been found to emit strong long-lived fluorescence (31). The type of microtitration strips used by Hemmila et al.(32) in their double-label determination was not reported, but were probably polystyrene as this was the type used in their

earlier determination with terbium labels (31). The terbium label was found to cause a slight interference (1%) with the determination of the europium label due to the minor spectral overlap of the terbium emission at 621 nm near the main emission peak of europium. The overlap of the europium and samarium chelates (30) seems to be larger than that of the europium and terbium chelates but no mention was made of any interference. The difference in fluorescence lifetimes of the europium/samarium system is larger so minor spectral overlap may be less critical.

Labelling

In most immunochemical determinations, each molecule is labelled with just one ^{125}I atom to avoid the possiblility of the radioactive tracer damaging the labelled reagent (1) or disrupting the antigen-antibody binding. In fluoroimmunochemical determinations, the possibility of multilabelling exists as long as the immunochemical reaction is not disrupted. Increasing the number of fluorophores per labelled molecule should result in an increase in the total fluorescence per labelled molecule, which in turn should lower the detection limit. However, concentration quenching can result when several fluorophores are immobilized close together. Fluorescein, the most commonly used conventional fluorophore, is very susceptible to this phenomenon (4).

Multilabelling is relatively simple in immunometric techniques because the antibody is a large protein. In

immunoassays the labelled molecule may not be a large, easily labelled molecule; thus, several indirect multilabelling techniques have also been developed. In the first technique, a multilabelled carrier molecule, usually a large protein, may be attached to the analyte or antibody. This method is especially good for haptens like steroids which have a unique or restricted number of sites at which labels may be attached. The second type of indirect labelling involves another binding system such as Protein A, avidin/biotin, streptavidin/biotin or a second-antibody (33). Protein A binds to the constant region of the heavy chain of IgG. Its binding constant is slightly lower than that of most Ab/Ag complexes. Avidin and streptavidin bind biotin molecules. This system has a very high equilibrium constant (10^{15} M^{-1}). Each avidin can bind two biotin molecules and each streptavidin can bind one biotin. The second-antibody system uses another antibody directed against the antibody that binds the analyte. In each of these cases, the new binder is a large protein which can be multilabelled. In the avidin/biotin and streptavidin/biotin systems, antibodies are usually biotinylated; thus, avidin or streptavidin would be multilabelled. In another system, steptavidin is indirectly labelled via a thyroglobulin carrier molecule. As many as 160 chelating agents may be attached to the thyroglobulin (34). Protein A and avidin are universal labels in that they may be used in any system

once they are labelled. The second-antibody technique requires a series of animal species-specific antibodies.

Lanthanide chelates are usually attached to the antigen or antibody with an isothiocyanate, diazo or sulfonyl chloride group. Isothiocyanate reacts under mildly basic conditions with primary and secondary amine groups. The diazo group reacts with free tyrosine residues and to a lesser extent with histidine, lysine, arginine, and tyrptophan residues. Sulfonyl chloride groups react primarily with the amine groups on proteins under relatively mild conditions. Attachment via the isothiocyanate or sulfonyl chloride groups, rather than the diazo groups, usually allows for more fluorophores per molecule without loss of immunoreactivity. For example, Hemmila et al. (17) found that the optimal conjugation ratio of Eu^{+3} labels per antibody molecule was 3-5 with the diazo group but up to 50 with the isothiocyanate group in an immunofluorimetric determination of IgG. Diamandis and coworkers (15) reported the attachment of up to 20 lanthanide chelates per antibody with SO_2Cl.

There have been nine reports of indirect labelling in time-resolved immunochemical determinations. One was in an immunoassay of progesterone that used Horseradish Peroxidase as a carrier molecule (35). The second was a competitive immunometric determination of cortisol (24), which used multilabelled bovine serum albumin to label the anti-cortisol antibody. The remaining papers (22,23,34,36-39)

used a biotin/streptavidin system to label antibodies in immunometric determinations. All of the reports of indirect labelling, except the immunoassay, used labelling regents of the first class. The lanthanide chelate labels of the first class do not seem to be very sensitive to concentration quenching; in fact, fluorescence intensity enhancement has been reported with the BCPDA chelates. When thyroglobulin was multilabelled and complexed with Eu^{+3}, a six-fold fluorescence enhancement was observed (34). Concentration quenching is not a consideration with labelling reagents of the second class because the fluorescent chelate is not formed until the lanthanide ion is dissociated from the labelled molecule. Therefore, multilabelling sould be advantageous for labels of the second class, also.

Instrumentation

The achievable detection limit in fluoroimmunochemical determinations is mainly limited by the background fluorescence and, thus, a technique that could distinguish the fluorescence of the label from the background would significantly improve the limit of detection. Most background fluorescence has a decay time in the ten nanosecond range. As noted in the last section, lanthanide metal chelates have lifetimes in the microsecond to millisecond range. In conventional fluorescence, the background is reduced primarily by careful selection of excitation and emission wavelengths with filters or

monochromators; however, these techniques cannot entirely eliminate the background fluorescence.

When a fluorophore is excited by pulsed light, fluorescence is emitted following each pulse with an intensity which decays exponentially at a rate governed by the speed of the electronic transitions involved (40). As shown in Figure 7 , an electronically-gated detection system can be used to accumulate photons over any selected time interval after the excitation pulse and background signals have decayed to zero. This system may be used to measure the signal from a long-lived fluorophore by permitting the short-lived fluorescence to decay to zero before starting photon measurement. Conventional fluorphores cannot be used in this technique because their fluorescence lifetimes are too short. Table III shows the lifetimes of some conventional fluorophores used as labels in immunochemical determinations. Even if N-(3-pyrene)-maleimide, with a lifetime of 100 ns, is used, a significant contribution from the background would be expected if a substantial portion of the specific fluorescence from the fluorophore was within the measurement interval of the detection system (8). The fluorescence of the lanthanide chelates has a much longer lifetime and therefore all the nonspecific background will have decayed before the majority of the chelate's fluorescence has decayed. The lanthanides also have a large Stoke's shift (>200 nm). These two characteristics have permitted the construction of simple and relatively

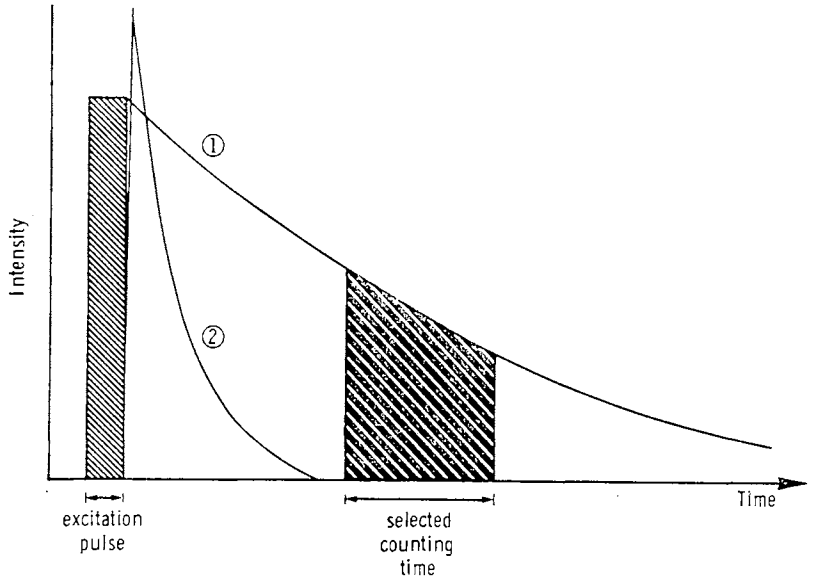

Discrimination of fluorescence signal from fluorescence of shorter lifetime by selection of photon counting time.

Figure 7. Schematic Representation of Time-Gated Detection. Showing Discrimination of fluoresence signal, ① , from fluorescence of shorter lifetime, ② , by photon counting time. From Reference (12).

TABLE III

FLUORESCENCE LIFETIMES OF SOME CONVENTIONAL FLUOROPHORES

Fluorophore	Lifetime	Reference
Fluorescein isothiocyanate (FITC)	4.5 ns	3
Rhodamine B isothiocyanate (RITC)	3.0 ns	3
Dansyl Chloride	14.0 ns	3
Fluorescamine	7.0 ns	3
N-3-pyrene maleimide (NPM)	100 ns	3

inexpensive pulsed-light, time-resolving fluorometers which are capable of yielding high signal-to-noise ratios.

Soini and Kojola (41) have developed a manually operated fluorometer for time-resolved fluoroimmunochemical determinations with lanthanide chelates as labels. A block diagram of their instrument is shown in Figure 8. The source is a xenon flashtube with a flash duration of 0.5 μs. Because the intensity of the flashes was not very reproducible, an integrator for a semiconductor photodiode was used as a stabilizer for the flashlamp. The detector is a photomultiplier tube operated in the single-photon mode. The pulse generater activates both the flashlamp and the timing of the emission counter. Interference band-pass filters mounted inside the sample compartment are used for excitation and emission wavelength selection. This design is also the basis for the commercially available computer-operated 1230 Arcus time-resolved fluorometer from LKB-Wallac. The intensity of the excitation beam in this type of instrument could possibly be increased by using a more intense source, such as a pulsed laser.

Another time-resolved fluorometer, shown in Figure 9, was developed in 1985 by Kuo and coworkers (42) specifically for use with terbium labels. They used a helium-cadmium laser with a continuous output at 325 nm for the excitation source. The excitation beam was pulsed by periodically interrupting the beam with a variable frequency chopper, and the fluorescence was detected by a PMT after passing through

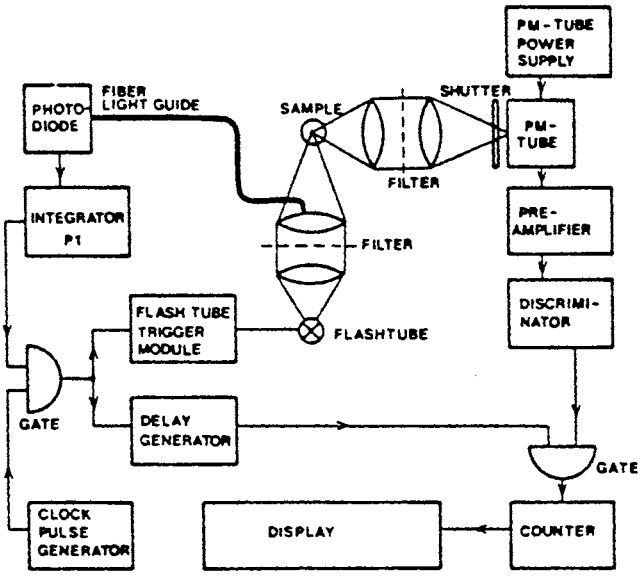

Figure 8. Block Diagram of the Time-Resolved Fluorometer Developed by Soini and Kojola from Reference (41).

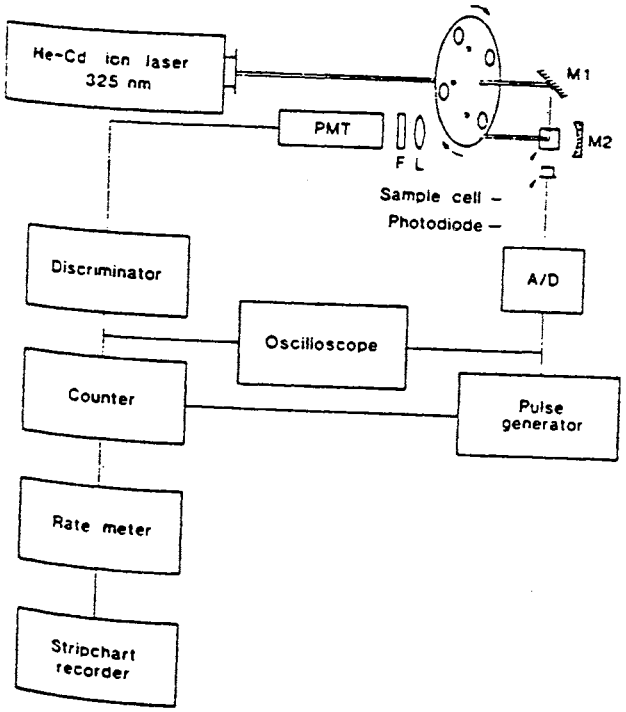

M, mirror; F, filter; PMT, photomultiplier tube; and A.D., analog-to-digital converter.

Figure 9. Schematic Diagram of the Time-Resolved Fluorometer Built by Kuo and Coworkers. From Reference (42).

an interference filter. A fast photodiode was used to monitor the beam and to trigger a pulse generator to open the gate of the photon counter after a set period. The chopper and the optical system are designed to block the PMT while the sample is exposed to the laser beam, to prevent PMT saturation by stray light or short-lived fluorescence. An oscilloscope was used to monitor the photodiode and PMT output in order to optimize the timing sequence and duration. The use of a laser and chopper eliminates the need for a complicated system, such as was used by Soni and Kojola to maintain the reproducibility of the xenon flash-tube. The main disadvantage of the laser system is the lack of wavelength selection. This particular instrument can only be used for compounds that absorb very near 325 nm.

In 1986, Dechaud et al. (43) reported the developement of a simple time-resolved fluorometer with a pulsed laser as the source. A block diagram of the instrument is shown in Figure 10. The laser emits at 337.1 nm and wavelength selection is accomplished by interference and sharp-cut filters; the emission filters could be replaced by a monochromator for spectroscopic studies. The detector is a PMT operated in the photon-counting mode with processing of the signal by a fast pre-amplifier and a discriminator. The start of the timing sequence is triggered by the control unit of the laser. The high output of the laser is very near the wavelength of maximum absorbance for the β-naphthoyltrifluoroacetone chelates; the high intensity

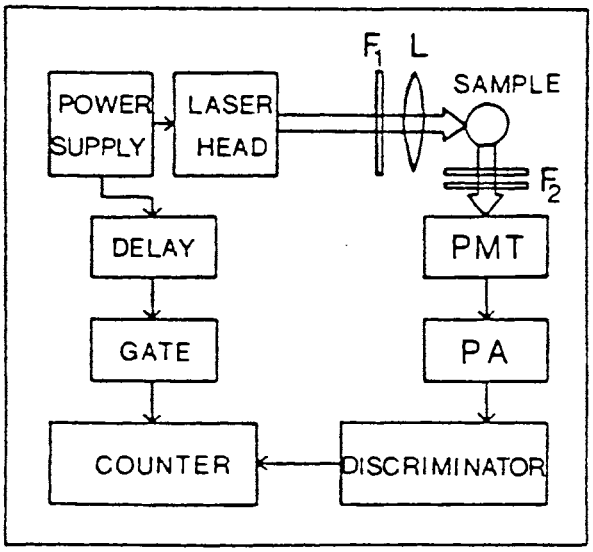

F_1, excitation filter; L, lens; F_2, emission filter; PMT, photomultiplier tube; PA, pre-amplifier

Figure 10. Block Diagram of a Pulsed Laser Time-Resolved Fluorometer. From Reference (43).

source may very well be the reason for the lower detection limit of the europium β-naphthoyltrifluoroacetone complex (30) using this instrument (see Table II). The pulsed laser in this instrument has very stable pulses, which eliminates the need for a chopper. On the other hand, pulsed lasers are larger and more expensive than continuous wave lasers, which may limit their application for clinical use.

A fourth type of time-resolved fluorometer was used by Diamandis and coworkers (22-24,44) to detect fluorescence from dry, solid surfaces. The instrument was a CyberFluor 615 gated fluorometer, which uses a pulsed nitrogen laser that laser has a pulse duration of 3-4 ns and a repetition rate of 20 pulses per second. A diagram of the CyberFluor 615 optical system is shown in Figure 11. This instrument measures 2000 to 3000 samples per hour in an automated design.

Time-Resolved Fluoroimmunochemical Determinations

The first papers reporting the use of time-resolved fluoroimmunometric determinations were published in 1982. Since then, determinations of many species of clinical interest using time-resolved fluoroimmunochemical techniques have been published. The techniques fall into two major categories, immunoassays and immunometric determinations, depending upon whether the label is attached to the antigen or the antibody. The labelled antibody category is further

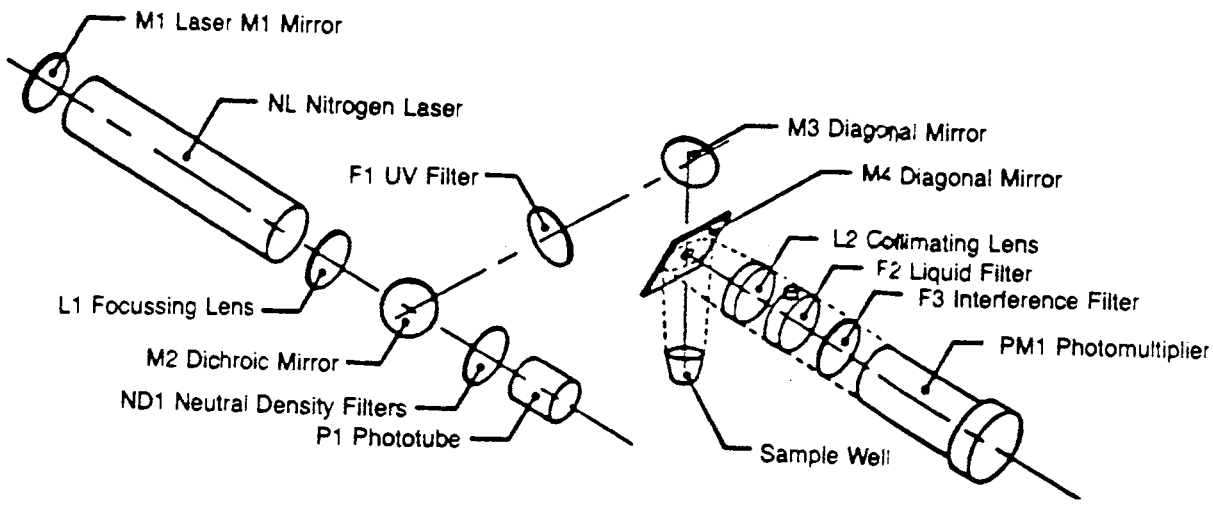

Figure 11. The Optical System of the CyberFluor 615 Time-Resolved Fluorometer. From Reference (44).

divided into competitive and noncompetitive techniques; the bulk of the determinations that have been reported fall into the noncompetitive labelled antibody category. Table IV lists the determinations that have been reported in each category according to the type of species determined and the labelling reagent employed.

As reported in a previous section, noncompetitive immunometric determinations are theoretically capable of reaching lower limits of detection than either immunoassays or competitive immunometric determinations. The detection limit, working range, coefficient of variation, and analysis times of the competitive time-resolved fluoroimmunochemical determinations and the noncompetitive time-resolved immunofluorometric determinations are reported in Table V and Table VI, respectively. These parameters are very similar for competitive immunometric determinations and immunoassays, which are both competitive techniques.

Most haptens can not be determined using the "sandwich" immunometric technique because they are too small to have two well-separated determinants. All of the competitive determinations that have been published are either for haptens or a model analyte. The first time-resolved immunochemical determinations were reported by a group of scientists at the Wallac Biochemical Laboratory. They originally focused on the time-resolved approach to fluoroimmunochemical determinations as a means of reaching lower detection limits than were possible with

TABLE IV

ANALYTES DETERMINED BY TIME-RESOLVED IMMUNOCHEMICAL METHODS

Analyte	Type[a]	Labelling Reagent	Class[b]	Reference
Model Analytes				
IgG	TRFIA	diazophenyl-EDTA-Tb	1	42
HSA	TRFIA	pAS-DTPA-Tb	1	46
Drugs				
Gentamicin	TRFIA	Transferrin-Tb2	1	61
CBZ	TRPhIA	erythrosin	1	48
Digoxin	cTRIFMA	pSCN-DTTA-Eu	2	52
Bases				
5-MedCyd	TRFIA	SCN-phenyl-EDTA-Eu	2	47
5-MedCyd	cTRIFMA	SCN-phenyl-EDTA-Eu	2	51
Steroid Hormones				
Progesterone	TRFIA	DTPA-Eu	2	35
E-3-G	TRFIA	W-1174	1	28
Testosterone	cTRIFMA	SCN-EDTA-Eu	2	49,61
Cortisol	cTRIFMA	SCN-phenyl-EDTA-Eu	2	50,61
Cortisol	cTRIFMA	BSA-BCPDA-Eu	1	24
Cortisol	cTRIFMA	streptavidin-BCPDA-Eu	I	36
Glycoprotein Hormones				
Thyrotropin	ncTRIFMA	SCN-phenyl-EDTA-Eu	2	57-63
Thyrotropin	ncTRIFMA	SA-TG-BCPDA-Eu	1	37
hCG	ncTRIFMA	diazophenyl-EDTA-Eu	2	53,56,57
free hCG	ncTRIFMA	SCN-phenyl-EDTA-Eu	2	58
hCG	ncTRIFMA	streptavidin-BCPDA-Eu	1	22
Lutropin	ncTRIFMA	SCN-EDTA-Eu	2	61,65
Lutropin	ncTRIFMA	SCN-DTTA-Eu	2	32
Lutropin	ncTRIFMA	streptavidin-BCPDA-Eu	1	38
Follitropin	ncTRIFMA	SCN-DTTA-Tb	2	32
Follitropin	ncTRIMFA	DTPA-Eu	2	30
Follitropin	ncTRIFMA	DTPA-Sm	2	30
Polypeptide Hormones				
ACTH	ncTRIFMA	Scn-phenyl-EDTA-Eu	2	54
Prolactin	ncTRIFMA	DTPA-Eu	2	43
Thyroxin	TRFIA	W-1174	1	27
Insulin	ncTRIFMA	SCN-phenyl-DTTA-Eu	2	66
EGF	ncTRIFMA	SCN-phenyl-EDTA-Eu	2	67

TABLE IV (Continued)

Analyte	Type[a]	Labelling Reagent	Class[b]	Reference
Viral Analytes				
HBsAg	ncTRIFMA	diazophenyl-EDTA-Eu	2	69
Rubella Ab	ncTRIFMA	diiazophenyl-EDTA-Eu	2	68
Rotavirus	ncTRIFMA	diazophenyl-EDTA-Eu	2	55
Adenovirus	ncTRIFMA	diazophenyl-EDTA-Eu	2	55
RSV	ncTRIFMA	diazophenyl-EDTA-Eu	2	55
Influenzavirus	ncTRIFMA	diazophenyl-EDTA-Eu	2	55
p-influenzavirus	ncTRIFMA	diazophenyl-EDTA-Eu	2	55
Misc. Proteins				
a-fetoprotein	ncTRIFMA	SCN-phenyl-EDTA-Eu	2	70
a-fetoprotein	ncTRIFMA	streptavidin-BCPDA-Eu	1	23
a-fetoprotein	ncTRIFMA	SA-TG-BCPDA-Eu	1	34
Phospholipase A2	ncTRIFMA	SCN-phenyl-EDTA-Eu	1	74
CA 125	ncTRIFMA	SCN-phenyl-DTTA-Eu	2	72
SHBG	ncTRIFMA	SCN-phenyl-DTTA-Eu	2	71,76
34 kDa SmBP	ncTRIFMA	SCN-phenyl-EDTA-Eu	2	73
a-interferon	ncTRIFMA		2	75
ferritin	ncTRIFMA	streptavidin-BCPDA-Eu	1	39
PP5	ncTRIFMA	SCN-phenyl-EDTA-Eu	2	77
CEA	ncTRIFMA	SCN-PPTA-Tb	1,2	78
CEA	ncTRIFMA	p-nitrophenoxy-DTPA-Eu	2	78

[a] Type of determination, cTRIFMA is competitive, ncTRIFMA is noncompetitive.
[b] Class of Labelling Reagent.

Analytes
IgG - Immunoglobulin G
HSA - Human Serum Albumin
CBZ - Carbemazepine
5-MedCyd - 5-methyl-2'-deoxycytidine
E-3-G - Estrone-3-glucuronide
hCG - Choriogonadotropin
ACTH - Corticotropin
CA 125 - Ovarian carcinoma-associated antigen determinate
HBsAg - Hepatitis B surface antigen
RSV - Respiratory syncytial virus
SHBG - Sex-hormone binding protein
SmBP - Somatomedin binding protein
PP5 - Placental Protein 5
CEA - Carcinoembryonic antigen
EGF - Epidermal growth factor

For labelling reagents of the first class see Table I.

Labelling Reagents
SCN - isothiocyanate
EDTA - ethylenediaminetetraacetic acid
DTPA - diethylenetriaminepentaacetic acid
DTTA - diethylenetriaminetetraacetic acid
SA - streptavidin
TG - thyroglobulin

radioimmunochemical methods. Their work is the basis of a commercially available immunochemical system from LKB-Wallac called Dissociation-Enhanced Lanthanide Fluoroimmunoassay (DELFIA). The DELFIA system uses a polyaminepolycarboxylate labelling reagent of the second class and an enhancement solution, added after the immunochemical reaction, containing β-naphthoyltrifluoroacetone (β-NTA), TOPO, and Triton X-100 at approximately pH 3. Because of the step involving a highly fluorescent secondary chelate, the DELFIA system is susceptable to contamination from free europium in the environment. Homogeneous determinations are also not possible with this system. Most of the immunometric determinations that have been reported use this system.

Recently, a group of scientists, at CyberFluor Inc., has developed a new lanthanide labelling reagent of the first class, whose a detection limit which seems to be only slightly higher than the europium chelate used by LKB-Wallac. The fluorescence of the bound fraction of the labelled species is measured on the dry solid phase after the separation step. In all instances, this label has been used with some type of indirect labelling technique, usually involving biotin and streptavidin, to increase the number of fluorophores per labelled molecule. This is almost the only label of the first class that has been used in a time-resolved immunometric determination. Conversely, all but two of the time-resolved immunoassays reported have used a label of the first class. Because most of the

immunometric determinations have used the DELFIA system, the determinations of any particular type of analyte are very similar. Most of the pertinent information on these determinations is presented in Tables V and VI. The general characteristics of the determination of each type of analyte will be reviewed and any new or unique approaches are discussed in the following sections of this chapter.

Labelled-Antigen Methods

All immunoassys are competitive techniques. In general, time-resolved fluoroimmunoassays (TRFIA) have higher detection limits and shorter working ranges but are less susceptible to cross-reactants and have shorter analysis times than noncompetitive time-resolved immunofluorometric assays (TRIFMA). Immobilization of the antibody makes the separation step simpler and more efficient if it is needed. Judging by the analysis times in Table V, all TRFIAs seem to be nonequilibrium techniques. The first TRFIA was reported in 1984 (45). Between 1984 and November of 1988 only four more TRFIAs were published and, as stated above, two of these were for model analytes (42,46). No subsequent applications of either of these two systems have been reported. Since November of 1988, three more TRFIAs have been reported, two of which were homgeneous systems. The lowest TRFIA detection limit was for the determination of progesterone (35), which is also the only reported use of the DELFIA system in an immunoassay. A carrier molecule was

TABLE V

COMPARISON OF THE WORKING RANGES, PRECISION, ANALYSIS TIMES AND LABELLING METHODS OF TRFIAs AND COMPETITIVE TRIFMAs

Species	Working Range	#[a]	RSD[b]	Time[c]	Labelling Method	Reference
TRFIA						
Gentamicin	NR	NR	NR	NR	direct	61
HSA[d]	25 - 50 g/l	20	5%	1.0 hr	direct	46
IgG[e]	50 - 2000 nM	NR	5%	1.5 hr	direct	42
Carbamazepine	0.8 - 300 uM	12	<10%	0.5 hr	direct	48
Progesterone	0.6 - 200 nM	10	<4%	3.5 hr	indirect	35
E-3-G[f]	10 - 458 nM	24	3%	2.5 hr	direct	28
Thyroxin	50 - 300 nM	12	<5%	1.0 hr	direct	27
5-MedCyd[g]	18 - 12500 nM	8	<5%	0.5 hr	direct	47
Competitive TRIFMA						
Testosterone	0.3 - 10 nM	9	<10%	2.0 hr	direct	49,61
Cortisol	3 - 2000 nM	12	<8%	2.5 hr	direct	50,61
Cortisol	30 - 1000 nM	10	<10%	1.5 hr	indirect	24
Cortisol	28 - 1300 nM	12	11%	1.5 hr	indirect	51
Digoxin	0.3 - 5 nM	10	<7%	1.0 hr	direct	52
5-MedCyd[g]	0.5 - 25000 nM	NR	11%	2.0 hr	direct	51

NR Not reported.
a Number of replicates used to calculate the RSD.
b Relative Standard Deviation, in percent.
c Analysis Time.
d Human Serum Albumin.
e Immunoglobulin G.
f Estrone-3-Glucuronide.
g 5-methyl-2'-deoxycytidine.

used to increase the Eu/Ag ratio to five and the antibody was immobilized on the polystyrene sample tubes. The main reason this TRFIA has the lowest detection limit is that it used the label with the lowest detection limit. The detection limit of the label in this TRFIA is several orders of magnitude lower than that of any of the other labels used for TRFIAs.

The two new homogeneous TRFIAs, one for the determination of thyroxin (27) and the other for the determination of estrone-3-glucuronide (28), used a new labelling reagent of the first class (W-1174). They are the first homogeneous time-resolved fluoroimmunochemical determinations to be published. Both are based upon quenching of the fluorescence of labelled antigen when it is antibody-bound. No lifetime selectivity between Ag* and Ag*-Ab is possible with the TRFIAs; the time discrimination is still just used to eliminate background fluorescence. In the TRFIA of thyroxin ~90% of the fluorescence was quenched by anti-thyroxin antibodies. An amount of Ab large enough to bind most of the Ag* was used in order to reduce the incubation time. Both determinations had short analysis times and good reproducibility. The developement of homogeneous TRFIAs is an important step. It should make TRFIAs a viable alternative to the popular TDX fluorescence polarization immunoassay system in the area of therapuetic drug monitoring.

The TRFIA of 5-methyl-2'-deoxycytidine is unique in that it used polylysine as a bridge between the europium chelate and the anigen (47). This base is the only modified or minor base in mammalian DNA, and is thought to be a regulator of eucaryotic gene transcription. The tracer was labelled 5-methylcytidine, and an immobilized second antibody directed at IgG was used to separate the bound fraction from the free fraction. The TRFIA had a working range of three orders of magnitude, which is very wide for an immunoassay.

One of the most interesting time-resolved determinations is not technically a TRFIA since the label is phosphorescent rather than fluorescent, but the technique is very similar (48). The label is erythrosin, a tetraiodo-fluorescein derivative, the phosphorescence of which was measured at room temperature in aqueous solution after chemical removal of oxygen with sodium sulfite. The phosphorescence of the label is quenched by about 80% upon antibody binding, so that no separation step is needed. Although this immunoassay doesn't have a very low detection limit ($\sim 8 \times 10^{-7}$ M) it is low enough for some applications such as therapeutic drug monitoring. Sidki et al. (48) have found that the phosphorescence of this label on a variety of haptens is quenched by all of the antisera they studied.

Competitive Labelled-Antibody Methods

All six competitive TRIFMAs that have been reported involve the use of a solid phase antigen along with the labelled antibody. Competitive TRIFMAs have similar detection limits, working ranges, precision, and analysis times to TRFIAs. Like TRFIAs, the competitive TRIFMAs are nonequilibrium methods for the determination of haptens. The determinations of digoxin, testosterone, 5-methyl-2'-deoxycytidine and one of the cortisol determinations (49-52) used the DELFIA system. The other two cortisol determinations (24,36) employed indirect labelling with BCPDA-Eu and solid phase detection (the CyberFluor system).

Two different types of indirect labelling were reported for the CyberFluor system. The first involved using a large carrier molecule (BSA) labelled with up to 40 BCPDA molecules (24). The second involved the use of biotinylated antibodies and streptavidin labelled with 15 BCPDA molecules (36). Each biotin binds one streptavidin, while the antibody may have up to 16 biotin groups bound to it. This method has been proposed by CyberFluor as a universal detection system. A schematic depiction of the process is shown in Figure 12a.

The digoxin TRIFMA has a narrow working range but the therapeutic range of this drug is only 1.0 - 2.0 nM, with toxcicity starting at doses above 3 nM. The steroid TRIFMAs also cover the normal serum values of these compounds. The determination of cortisol using the DELFIA system (50) has a

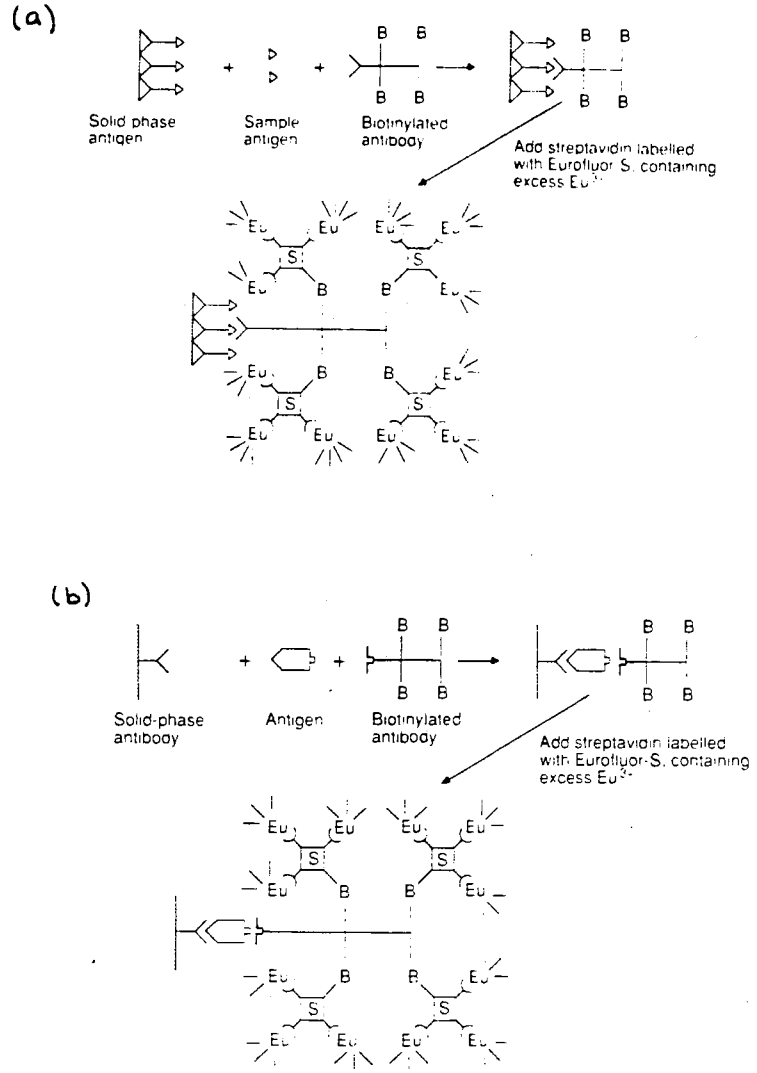

B = biotin. S = streptavidin. The fluorescence of the final product is measured on the dry solid phase.

Figure 12. Schematic Depiction of the CyberFluor Systems for Haptens (a) and Larger Anigens (b). From Reference (44).

lower detection limit than either of the cortisol determinations using the CyberFluor systems, but the analysis time is also longer - approximately 2.5 hours versus about 1.5 hours. All of these determinations showed at least fair correlation with their corresponding RIAs, with correlation coefficients (r) ranging from 0.93 for DELFIA cortisol to 0.98 for the other cortisol determinations and the testosterone TRIFMA. Most competitive immunochemical techniques use polyclonal antibodies because of their higher binding strength, but in the cortisol determination with indirect labelling better results were produced with a monoclonal antibody. Perhaps the polyclonal antibody was partially directed against the carrier molecule and the bridging group.

Noncompetitive Labelled Antibody Methods

All of the noncompetitive TRIFMAs use a solid-phase antibody and a free labelled antibody. At least one of the antibodies used in these methods, if not both, is usually monoclonal. The analyte must have at least two antigenic determinants spaced far enough apart to allow two antibodies to bind simultaneously. The analysis can be accomplished in one or two incubation steps. One-step noncompetitive determinations frequently suffer from a "high dose hook effect", in which the fluorescence signal reaches a maximum and then decreases as the analyte concentration increases.

TABLE VI

COMPARISON OF THE WORKING RANGES, PRECISION, ANALYSIS TIMES AND LABELLING METHODS OF NONCOMPETITIVE TRIFMAs

Species	# of Steps	Working Range	#[a]	RSD[b]	Time[c] (hr)	Labelling Method	References
Glycoprotein Hormones							
Thyrotropin	1	0.03 - 324 mIU/l	12	<5%	2.0	direct	59,61
Thyrotropin	1	0.03 - 100 mIU/l	12	<10%	5.0	BN:SA:TG[d]	37
hCG	1	0.1 - 135 IU/l	10	<10%	2.0	direct	56
hCG	2	0.7 - 350 IU/l	10	<10%	4.0	direct	56
hCg	1	1.0 - 500 IU/l	15	<10%	3.5	BN:SA[d]	22
hCG	2	1.5 - 500 IU/l	15	<7%	4.5	BN:SA[d]	22
hCG	2	0.13 - 5000 IU/l	12	<10%	4.5	direct	58
free -hCG	2	1.0 - 200000 ng/l	12	<10%	4.5	direct	58
Lutropin	2	0.04 - 125 IU/l	NR	<8%	3.5	direct	61
Lutropin	1	0.5 - 240 IU/l	15	<10%	2.5	BN:SA[d]	38
Lutropin	2	1 - 250 IU/l	NR	10%	0.5	direct	65
Lutropin	2	0.1 - 250 IU/l	12	<10%	3.5	direct	32
Follitropin	2	4 - 250 IU/l	12	<15%	3.5	direct	32
Follitropin	1	1.2 - 135 IU/l	12	<10%	4.0	direct	30
Follitropin	1	10 - 135IU/l	12	<15%	4.0	direct	30
Polypeptide Hormones							
ACTH	2	25 -1000 ng/l	10	<10%	6.0	direct	54
Prolactin	1	1 - 100 mg/l	10	<6%	4.0	direct	43
Insulin	1	2.4 - 2400 mIU/l	12	<10%	3.0	direct	66
Insulin	2	2.4 - 2400 mIU/l	12	<10%	4.0	direct	66
EGF	2	2.5 - 5000 ng/l	8	<10%	4.0	direct	67
Viral Analytes							
HBsAg	1	NR	NR	NR	3.0	direct	69
Rubella Ab		cut off	10	<7%	3.5	direct	68

TABLE VI (Continued)

Species	# of Steps	Working Range	#[a]	RSD[b]	Time[c] (hr)	Labelling Method	References
Rotavirus		1 - 10 ng/ml	NR	NR	3.5	2nd Ab	55
Adenovirus		1 - 100 ng/ml	NR	NR	3.5	2nd Ab	55
RSV		1 - 1000 ng/ml	NR	NR	19	2nd Ab	55
Influenzavirus A&B		1 - 1000 ng/ml	NR	NR	19	2nd Ab	55
P-influenzavirus 1,2&3		1 - 1000 ng/ml	NR	NR	19	2nd Ab	55
Misc. Proteins							
SHBG	1	8pM - 200 nM	10	<6%	3.0	direct	71
CA 125	2	1.5 - 7200 U/ml	5	<10%	19	direct	72
34 kDa SmBP	2	0.25 - 250 ug/l	12	<8%	4.5	direct	73
PLA2	1	0.02 - 100u g/l	12	<12%	2.5	direct	74
hAFP	1	0.1 - 1000 IU/ml	12	<12%	2.5	direct	70
hAFP	2	0.2 - 1000 IU/ml	12	<10%	3.5	direct[d]	70
hAFP	2	0.1 - 1030 IU/ml	21	<8%	3.0	BN:SA[d]	23
hAFP	1	5.0 - 500 ng/ml	NR	NR	2.5	direct[d]	34
hAFP	1	1.0 - 500 ng/ml	NR	NR	2.5	BN:SA[d]	34
hAFP	1	0.2 - 500 ng/ml	NR	NR	2.5	BN:SA:TG[d]	34
2-interferon		0.020 - 100 nM	NR	NR	NR	direct[d]	75
ferritin	1	1.1 - 1100 uM	12	<10%	2.0	BN:SA	39
PP5	2	0.05 - 1000 ug/l	20	<10%	3.5	direct	77
CEA	1	1.0 - 400 ng/ml	5	<3%	2.0	direct	78
CEA	1	1.5 - NR ng/ml	5	<3%	1.5	direct	78
CEA	1	1.0 - NR ng/ml	5	<3%	2.0	direct	78

a Number of replicates used to calculate the RSD.
b Relative Standard Deviation.
c Analysis time.
d Method of indirect labelling, biotin:streptavidin and biotin:streptavidin:thyroglobulin.

A typical two-step calibration curve and a one-step calibration curve showing the hook effect are shown in Figure 13. If a one-step TRIFMA suffers from the hook effect, the samples need to be run at more than one dilution in order to determine the analyte concentration. If no hook effect occurs, then the one-step method is advantageous because the second incubation step can be eliminated and the analysis time shortened. Two-step methods usually have a wider working range but frequently show higher limits of detection than one-step methods. Most noncompetitive sandwich methods use monoclonal antibodies to reduce nonspecific binding even though they generally have lower binding constants than polyclonal antibodies. High binding constants are not as important in noncompetitive immunometric determinations because they are reagent-excess techniques.

It is difficult to compare time-resolved fluoroimmunochemical determinations to other types of labelled immunochemical determinations strictly on the basis of the type of label used because the particular antibody preparations used are so critical to the outcome. Fortunately, some reports of immunometric determinations using different labels but the same antibodies have been published (46,53-55). For the purposes of this review, the noncompetitive TRIFMAs have been divided into groups according to the type of compound determined, including glycoprotein

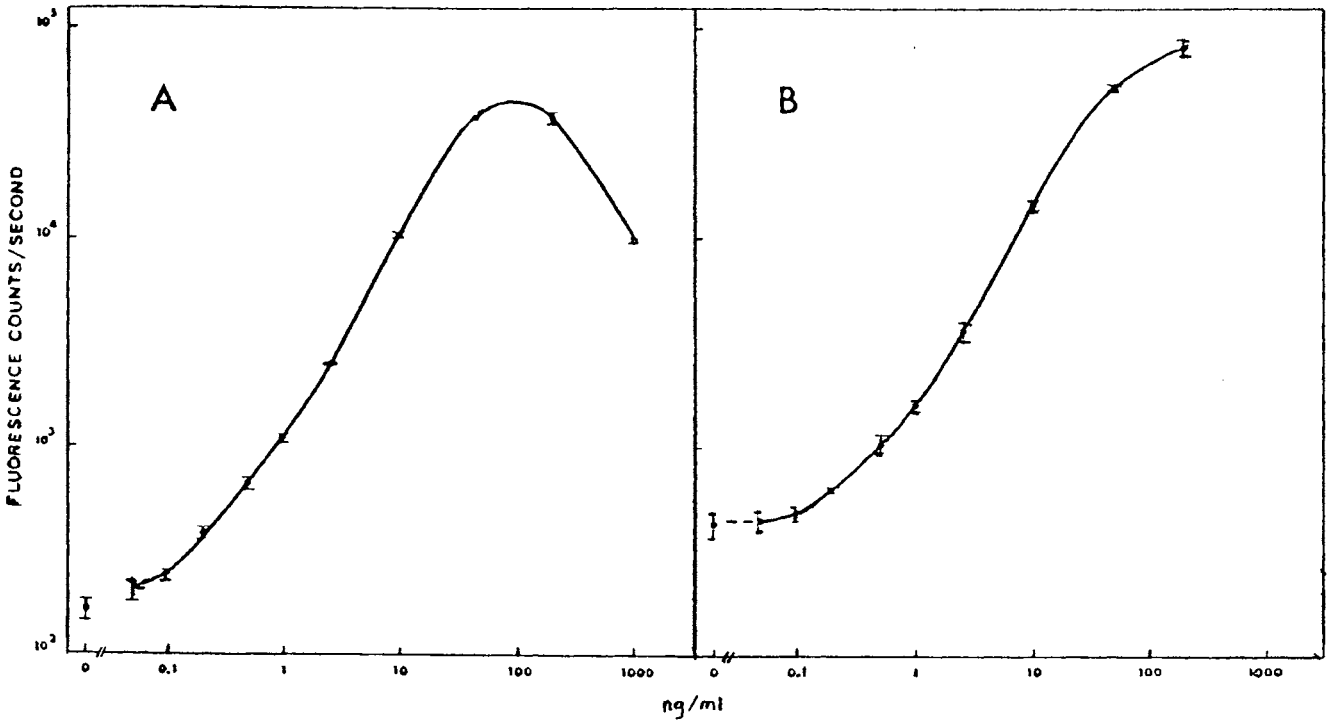

Figure 13. Typical Immunometric Calibration Curves With (a), and Without (b), a Hook Effect. From Reference (56).

hormones, polypeptide hormones, viruses and their related antigens and antibodies, and other miscellaneous proteins.

Determination of Glycoprotein Hormones. The glycoprotein hormones, human choriogonadotropin (hCG), thyrotropin (TSH), lutropin (LH), and follitropin (FSH) have all been determined by noncompetitive TRIFMA. These hormones are all composed of two subunits. The α subunits of each hormone are almost identical, while the β subunits are similar but differ somewhat in their amino acid sequences. Typically, a monoclonal antibody directed against either the whole hormone or one of the subunits is used as the solid-phase capture antibody. Another monoclonal antibody directed against the other subunit is labelled with the lanthanide chelate. The majority of papers discussed in this section are determinations of hCG and TSH and these methods are therefore discussed in greater detail.

Human choriogonadotropin (hCG) is primarily determined for early detection and monitoring of pregnancy and pregnancy-related disorders (22). The first TRIFMA of hCG was reported in 1983 by Pettersson et. al (56). It used the DELFIA system. Purified anti-hCG was immobilized on the surface of microtiter strip wells. Purified anti-LH was labelled with diazophenyl-EDTA-Eu. Both one- and two-step procedures were developed. The one-step procedure showed a high dose hook effect. The two-step method has a wide working range, which is beneficial since the normal range of

hCG values is also quite wide. Stenman and coworkers (57) developed a very rapid (20 minute) variation of this determination, as a rapid pregnancy test, with a working range of 1.7 - 300 IU/l. (An international unit (IU) is a quantity of a biological substance, in this case a hormone, that produces a specific internationally accepted biological effect.) An immunoradiometric determination (IRMA) was developed using the same antibodies and standards as the TRIFMA of hCG (53). Each labelled antibody had approximately five europium chelates or two ^{125}I atoms attached to it. The TRIFMA had a slightly lower detection limit than the IRMA (0.2 IU/l vs. 0.4 IU/l). Radiolabelled antibody with a higher ^{125}I-to-antibody ratio was also studied, and was found to have a lower immunoreactivity and higher detection limit. The ^{125}I-labelled antibody lost 50% of its potency in just four weeks while the europium labelled antibody was found to be stable for at least one year. The ^{125}I-labelled antibody showed greater instability than is normal for a radioactive immunoreagent because the ^{125}I level was 10-100 times greater than normal and thus, the damage to the labelled reagent was also greater.

The DELFIA system was also used to determine the concentration of the free β subunit (βhCG) of hCG as well as the intact hCG (58). Choriocarcinoma patients with a therapy resistant disease have increased levels of βhCG. A monoclonal Ab reacting with both free βhCG and hCG was used as the solid-phase capture Ab. For the determination of hCG

an antibody directed against the α subunit of hCG was labelled, and for the determination of βhCG, an antibody that reacted only with the free β subunit was labelled. This antibody probably binds a site covered by the α subunit in intact hCG. Both determinations were two step procedures. The detection limit for the hCG determination was similar to that previously reported using the DELFIA sysytem. The working range was at least an order of magnitude larger than any other TRIFMA for hCG. The determination of βhCG had a smaller working range but otherwise was similar to the hCG determination. The results were verified by first separating βhCG and intact hCG in a sample using hydrophobic-interaction HPLC and then running the TRIFMAs. No interference of hCG in the determination of βhCG was seen at hCG concentrations below 1800 IU/l. Some cross-reaction (about 0.6%) did occur at higher concentrations, and the degree of cross-reaction increased with increasing incubation times.

In 1987, Khosravi and Diamandis (22) reported a new type of TRIFMA for hCG. The second antibody was labelled with biotin instead of a europium chelate. Streptavidin was multilabelled with BCPDA-Eu. The fluorescence of the resulting complex, Ab_1-hCG-Ab_2-biotin-streptavidin-BCPDA-Eu, was measured directly on the dried solid-phase by excitation with a nitrogen laser. Once again, both one- and two-step procedures were developed and the one-step procedure again showed a hook effect. The detection limit of

this hCG determination was slightly higher than that found in the DELFIA system of Pettersson et. al (56), although the analysis times and imprecision were similar. The DELFIA hCG determination also showed good correlation (r = 0.99) with this method.

The measurement of TSH in serum is one of the essential tests of thyroid function (59). The lower limit of normal TSH values is about 0.4 mIU/l, while hyperthyroid levels are less than 0.1 mIU/l (60). Radioimmunoassays cannot distinguish between these two concentrations. A one-step TRIFMA of TSH was reported by Lovgren and coworkers (61) in 1984. They reported a sufficiently low detection limit to detect hyperthyroidism, and a wide working range, as shown in Table 6. The commercial DELFIA kit developed from this system has been evaluated by several groups (59,60,62-64). The evaluations were generally favorable; reporting low detection limits, good precision and good calibration. Lawson et. al (62), however, found the TRIFMA more expensive to perform than the standard free thyroxin and total thyroxin determinations, with only marginally better detection limits.

TSH has also been determined using the CyberFluor TRIFMA system (37). A schematic representation of their basic immunometric system using indirect labelling with the streptavidin/biotin reaction is shown in Figure 12b. The determination of TSH uses a modification of this approach, in which streptavidin is indirectly labelled using thyroglobulin as a carrier molecule. Up to 160 BCPDA

molecules could be attached to each thyroglobulin. The detection limit was the same as in the DELFIA system; however, the working range was shorter and the analysis time was doubled.

The determination of lutropin (LH) and follitropin (FSH) values is often needed when the pathological abnormalities of male and female reproductive systems are investigated. The normal ranges of LH and FSH are 1 - 100 IU/l and 4 - 250 IU/l, respectively. A two-step TRIFMA of LH using the DELFIA system was reported by Lovgren and coworkers (61). The method had a good working range, detection limit and precision, but showed high cross-reactivity with hCG. Stenman et. al (65) developed a rapid (30 minute) version of this TRIFMA. No mention was made of the previously reported cross-reaction but the same antibodies were apparently used.

A TRIFMA for LH using the CyberFluor system with a thyroglobulin carrier molecule was also reported (38). Two variations of the TRIFMA were given. One used longer incubation times (2 hours) and had a lower detection limit (0.5 IU/l). The other, more rapid determination, used shorter incubation times and had a higher detection limit (1.0 IU/l), but could be preformed in less than one hour. The working ranges and precisions were similar to the other determinations of LH. Some cross-reaction (5%) with hCG was reported and thus this TRIFMA is not recommended for samples from pregnant patients or new mothers. There was good

correlation ($r = \sim 0.96$) of the TRIFMA with DELFIA and IRMA kits for LH determinations.

The first FSH TRIFMA was reported in 1987 by Bador et. al (30). They actually developed two different determinations, one with a europium label and another with a samarium label. The samarium-labelled TRIFMA had a ten-fold higher detection limit than the europium-labelled method and its coefficient of variation increased rapidly for concentrations below 10 IU/l. Double-label TRIFMA methods for LH and FSH (32) were also reported in 1987. In this approach, purified anti-LH monoclonal antibody was labelled with a europium chelate and purified anti-FSH monoclonal antibody was labelled with a terbium chelate. The enhancement solution contained PTA instead of β-NTA for reasons discussed earlier. The two-step, double-label TRIFMA showed low cross-reactivity, but higher sample volumes and concentrations of labelled antibody had to be used to compensate for the higher detection limits of these fluorophores (see Table II). The detection limits of the determination were still higher than the single-label DELFIA kits but lower than commercial, double-label RIA kits (32).

Determinations of Polypeptide Hormones. The polypeptide hormones prolactin (LTH), corticotropin (ACTH), insulin, and human epidermal growth factor (hEGF) have all been determined by noncompetitive DELFIA-type TRIFMAs (43,54,66,67). The techniques, analysis times, and imprecisions are similar for all of the determinations. The

determinations of LTH and ACTH were both compared to IRMAs using the same antibodies and standards. The determination of LTH (43) easily covered the whole range of normal values (2 - 22 mg/l) and was well correlated (r = 0.98) to the corresponding IRMA over the entire normal and pathological concentration range. The determinations of ACTH (54) by TRIFMA and IRMA showed similar working ranges and detection limits, although the analysis time of the TRIFMA was considerably shorter than the 23 hours required for the IRMA. The imprecision of the TRIFMA was higher than that of the IRMA but still less than 10%.

Toivonen and coworkers (66), in their determination of human serum insulin, noted that the use of EDTA as an anticoagulant in plasma samples interfered with the one-step TRIFMA but not with the two-step procedure. EDTA will more than likely interfere with all of the competitive time-resolved fluoroimmunochemical determinations and one-step noncompetitive TRIFMAs using a DELFIA type system.

Determination of Antiviral Antibodies, Viral Antigens, and Viruses. The first reported TRIFMAs were for the determination of Rubella antibodies (68) and hepatitis B surface antigen (69). Shortly thereafter, the determinations of rotavirus, adenovirus, respiratory syncytial virus (RSV), influenzavirus types A and B, and parainfluenzavirus types 1, 2, and 3 were reported (55). The TRIFMA for Rubella virus is a noncompetitive technique even though it uses solid-phase antigen because the analyte is an

antibody. In this determination, the Rubella virus is immobilized on polystyrene beads and anti-human IgG is labelled with a europium chelate. The immobilized virus is used to capture the Rubella antibodies in the sample. After incubation and washing steps, the labelled second antibody is added. No detection limit was reported since this qualitative TRIFMA just uses a cutoff between positive and negative samples.

Hepatitis B surface antigen (HBsAg) is the most common immunological marker of hepatitis B virus infections (69). A high dose hook effect was noted in the one-step TRIFMA of HBsAg. The detection limit, reported as twice the signal level of the blank, was ~0.5 mg/l. The determination of viruses in stool and nasopharyngeal secretions by Halonen et. al (55) used the indirect labelling method shown in Figure 14. These determinations were compared to IRMAs that were identical to the TRIFMAs except that the last antibody was labelled with ^{125}I instead of a europium chelate. The TRIFMAs and IRMAs were reported to have similar detection limits, but the sensitivities of the former were generally higher than those of the latter.

Determination of Miscellaneous Proteins. The remaining TRFIAs that have been developed (23,70-75,39, 77,78) are for human alpha-fetoprotein (hAFP), sex-hormone binding globulin (SHBG), ovarian carcinoma-associated antigen determinant (CA 125), a 34 kDa somatomedin binding protein (34 kDa SmBP), pancreatic phospholipase A_2 (PLA_2 EC 3.1.1.4),

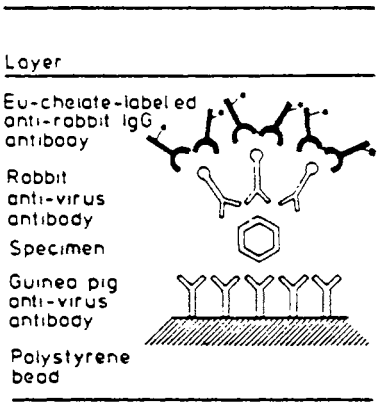

Principle of the indirect time-resolved fluoroimmunoassay for the detection of rotavirus and adenovirus in stool and RSV, parainfluenzavirus types 1, 2, and 3, influenza virus types A and B, and adenovirus in aspirates of nasopharyngeal secretions (*nps*)

Figure 14. Schematic Diagram of the TRIFMA Procedure for the Determination of Viruses. From Reference (55).

α_2-interferon, ferritin, placental protein 5 (PP5), and carcinoembryonic antigen (CEA). The determination of PLA_2, published in 1983, was among the first TRIFMAs reported (74). It is unique in that it uses the same purified polyclonal antibody for both roles in the sandwich complex in a one-step procedure. No hook effect was reported although the imprecision was a little high (12%) at some points.

Alpha-fetoprotein is a glycoprotein produced mainly in the yolk sac and the liver. It is normally present at very low concentrations in adult serum and in large amounts in maternal serum and amniotic fluid. Elevated levels are also seen in certain fetal disorders and in carcinomas of the liver, germ cells, and gastrointestinal tract (70). A DELFIA-type noncompetitive TRIFMA for hAFP in serum and amniotic fluid was reported in 1985 (70). Purified monoclonal antibodies directed at two different antigenic determinants were employed. Both one- and two-step procedures were developed. The one-step procedure showed a hook effect at concentrations above 5000 IU/ml; all maternal serum samples are below this level so the one-step procedure can be used for them. Human AFP levels in amniotic fluid and tumor cancer patient specimens are often much higher than this, and should be measured with the two-step procedure. Chan and coworkers (23) developed a two-step TRIFMA for hAFP that uses the same biotin/ streptavidin CyberFluor system that was employed by Khosravi

and Diamandis (22) for the determination of hCG. The determination correlated well with the DELFIA hAFP determination (r = 0.98). The detection limits, working ranges, precisions, and analysis times of both TRIFMAs were very similar. Quite recently, a new CyberFluor TRIFMA of AFP was reported (34), in which streptavidin was indirectly labelled with BCPDA via a thyroglobulin carrier molecule. The analytical parameters for this TRIFMA were similar to those for the other CyberFluor TRIFMA for AFP. The only improvement was that the new TRIFMA was a faster, one-step procedure. No hook effect was observed.

A one-step TRIFMA for SHBG, without a hook effect, has been reported (71) and compared to several other immunometric determinations of SHBG with respect to precision (76). The imprecision of both LKB and Farmos TRIFMAs was high compared to an IRMA. Only 77% and 82% of the respective TRIFMA samples had a coefficient of variation less than 8%, while 100% of the IRMA samples fell into this category.

Ferritin is a major intracellular iron-storage protein and its serum levels are a useful indicator of iron status in the body. The ferritin molecule consists of a protein shell of 24 very similar subunits and an interior core of ferric oxyhydroxide. Serum ferritin is usually measured by RIA or IRMA. A TRIFMA for the determination of ferritin which utilizes the CyberFluor system has been reported (39). The determination is a one-step procedure using monoclonal antibodies. A hook effect was observed at ferritin concen-

trations above 22 nM. A very low detection limit (1.1 pM) and low imprecision (<5%) were reported. The method was well correlated (r = 0.99) with an RIA technique based on double antibody separation.

A DELFIA TRIFMA has been used for the determination of placental protein 5 (PP5) in serum (77) using polyclonal antibodies. PP5 is a glycoprotein that binds heparin and inhibits the action of plasmin and thrombin. Its action is linked to the blood coagulation system. The low levels of PP5 in the serum and plasma of nonpregnant individuals are not detectable by RIA (detection limit around 1.2 μg/l). The two-step TRIFMA was able to detect PP5 down to a level of 0.05 μg/l with good precision. Good correlation (r = 0.97) with RIA was found for higher concentrations of PP5.

A TRIFMA for the determination of carcinoembryonic antigen (CEA) using a new terbium label has been reported (78). The fluorescence of the terbium can either be measured with the label bound to a solid surface while still in solution or after washing and an extraction step similar to the DELFIA system. Thus the labelling reagent (Tb-PPTA) can be used both as reagent of the first class and as a reagent of the second class. The fluorescence from the solid phase is an order of magnitude lower than that from the enhancement solution, which, is not used unless a lower detection limit is needed. The same antibodies were labelled with Eu(III)-(p-nitrophenoxy- carbonyl)DTPA in an effort to compare the two labels. The labelled antibodies

were found to have 8 Eu^{+3} and 11 Tb^{+3} per antibody. In enhancement solution, TRIFMA employing the Tb labelling reagent had a signal about 23% lower than that using the Eu labelling reagent.

Conclusions

This chapter has reviewed the use of time-resolved fluorescence in immunochemical determinations of species of clinical interest. Time-resolved fluorescence is based on the application of time-gated detection of long-lived fluorescence in order to eliminate background signals. This technique was applied to immunochemical determinations in order to develop immunometric methods with detection limits below those currently achievable with radiochemical labels. Current TRIFMAs have detection limits that are the same as IRMAs or just slightly lower. TRIFMA detection limits should improve as the use of both indirect labelling systems with high fluorophore-to-antibody ratios and pulsed laser instruments increases. It is also quite conceivable that new fluorophors, with detection limits lower than those of currently used fluorophores, will be developed.

The cost of changing the methods employed in clinical laboratories is very high. Switching to time-resolved fluoroimmunochemical methods is not currently justifiable if the decision is based solely on slight decreases in detection limits. On the other hand, if a laboratory is upgrading its facilities or just starting up, TRIFMAs are a

promising alternative to radioimmunochemical methods, especially since the handling of radioactive materials can be avoided. As the number of analytes that can be determined by commercially avaliable TRIFMA kits increases, more labs will probably begin to use this system.

The DELFIA system has been applied to all three of the main types of immunochemical determinations. No other type of labelling system has reported a lower detection limit than that of $Eu(\beta NTA)_3(TOPO)_2$ in TX-100. The CyberFluor system of TRIFMA seems to have only one advantage over the DELFIA system and this is its insensitivity to contamination by environmental europium. Otherwise its detection limits, working ranges and analysis times are about the same or a little worse than those of the DELFIA system. The new indirect labelling system used by CyberFluor should have lowered detection limits in its TRIFMAs but this was not evident from their data. Until just recently, TRIFMA kits were available commercially from only one company, LKB-Wallac, but Farmos Diagnostica and CyberFluor, Inc. are now producing TRIFMA kits, also. Perhaps a little competition will result in a reduction in the price of these relatively expensive kits.

Lastly, the use of TRPhIA for therapeutic drug monitoring should be compatible with the instrumentation developed for TRIFMA. If methods are found to increase the quantum yield of erythrosin, the detection limit of this method should decrease. TRPhIAs for haptens other than

drugs could then become commercially viable. The homogeneous TRFIA for haptens should soon become avaliable from LKB-Wallac and can be performed on the same instrument as the DELFIA kits. This should make the time-resolved approach to immunochemical determinations even more attractive to clinical laboratories.

CHAPTER III

PHASE-RESOLVED FLUORESCENCE SPECTROSCOPY AND ITS APPLICATION TO FLUOROIMMUNOCHEMICAL DETERMINATIONS

Theory of Phase-Resolved Fluorescence Spectroscopy

Phase-resolved fluorometry is based upon the phase-modulation approach to fluorescence lifetime determinations, in which the fluorescent sample is excited with sinusoidally-modulated light and observed with a phase-sensitive detector. The theory and instrumentation of phase-modulation and phase-resolved fluorometry have been described in detail elsewhere (81-85).

If a fluorescent sample is excited with sinusoidally-modulated light, the resulting fluorescence emission is also sinusoidally modulated, but the is phase-shifted and demodulated to an extent that depends on the fluorescence lifetime of the sample. The sinusoidal excitation has the form:

$$E(t) = A (1 + m_{ex} \sin \omega t) \qquad (2)$$

where E(t) is the time-dependent intensity of the exciting light, ω is the angular modulation frequency ($\omega = 2\pi f$, where

f is the linear modulation frequency), A is the d.c. intensity component of the exciting light and m_{ex} is the degree of modulation of the exciting light (the a.c.-to-d.c. intensity ratio). The resulting fluorescence emission has the form:

$$F(t) = A' [1 + m_{ex} m \sin (\omega t - \phi)] \quad (3)$$

where F(t) is the time dependent intensity of the fluorescence emission, A' is the d.c. intensity component of the emitting light, ϕ is the phase-shift of the emitting species and m is the demodulation factor. The relationship of the phase-shift and demodulation to the excitation and emission waveforms is shown in Figure 15.

The lifetime (τ) of the fluorescent species can be calculated from either the measured phase-shift (ϕ)

$$\tau_p = (1 / \omega) \tan \phi \quad (4)$$

or the demodulation

$$\tau_m = 1 / \omega [(1 / m^2) - 1]^{1/2} \quad (5)$$

The excitation phase and modulation are calibrated by the use of a reference fluorophore solution of known lifetime or a scattering solution ($\tau = 0$).

In phase-resolved fluorescence spectroscopy (PRFS) the time dependent (a.c.) component of the emission signal is observed with a phase-sensitive detector and integrated over a variable-phase half-cycle, followed by a nonintegration

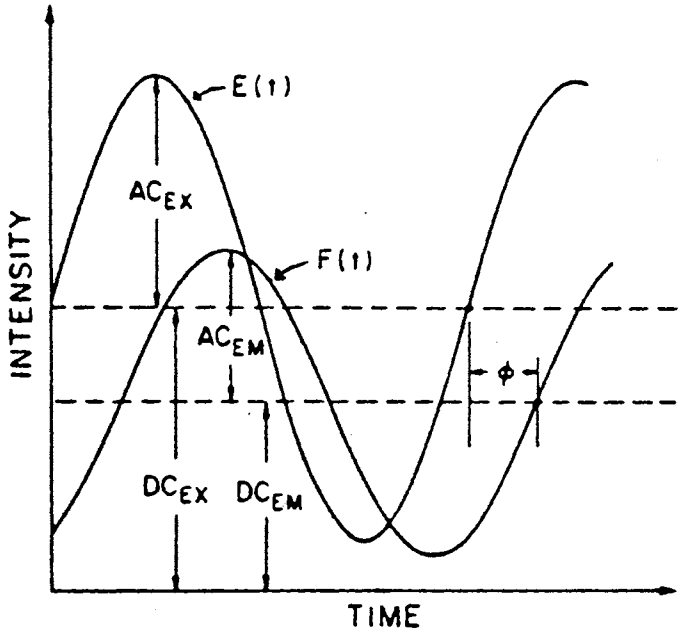

Figure 15. Schematic Representation of the Excitation E(t) and Fluorescence F(t) Waveforms. From Reference (83).

half-cycle. The phase of the half-cycle is continuously variable between 0° and 360°. The resulting phase-resolved fluorescence intensity (PRFI) has the form:

$$F(\phi_D) = A' m_{ex} m \cos(\phi_D - \phi) \qquad (6)$$

where ϕ_D is the position of the integration half-cycle (the detector phase angle setting). If ϕ_D equals the phase of the time-dependent fluorescence emission (F(t)), the maximum PRFI is observed; if ϕ_D is 90° out-of-phase with F(t), the PRFI is zero; if ϕ_D is between these two settings, intermediate values of PRFI are obtained. This is shown in Figure 16. $F(\phi_D)$ is dependent on the wave- lengths and modulation frequency and is a function of the intensity, lifetime and concentration of the emtting species. For a multicomponent system of independent emitters, the PRFI contributions are additive.

Review of Phase-Resolved Fluoroimmunochemical Determinations

In Chapter II, the use of fluorescence lifetime differences between free and bound forms of fluorescent labelled immunochemicals in TRFIA and TRIFMA was described. Phase-resolved fluorescence spectroscopy was first applied to immunochemical determinations by Bright and McGown (86). They described the use of PRFS to determine free and

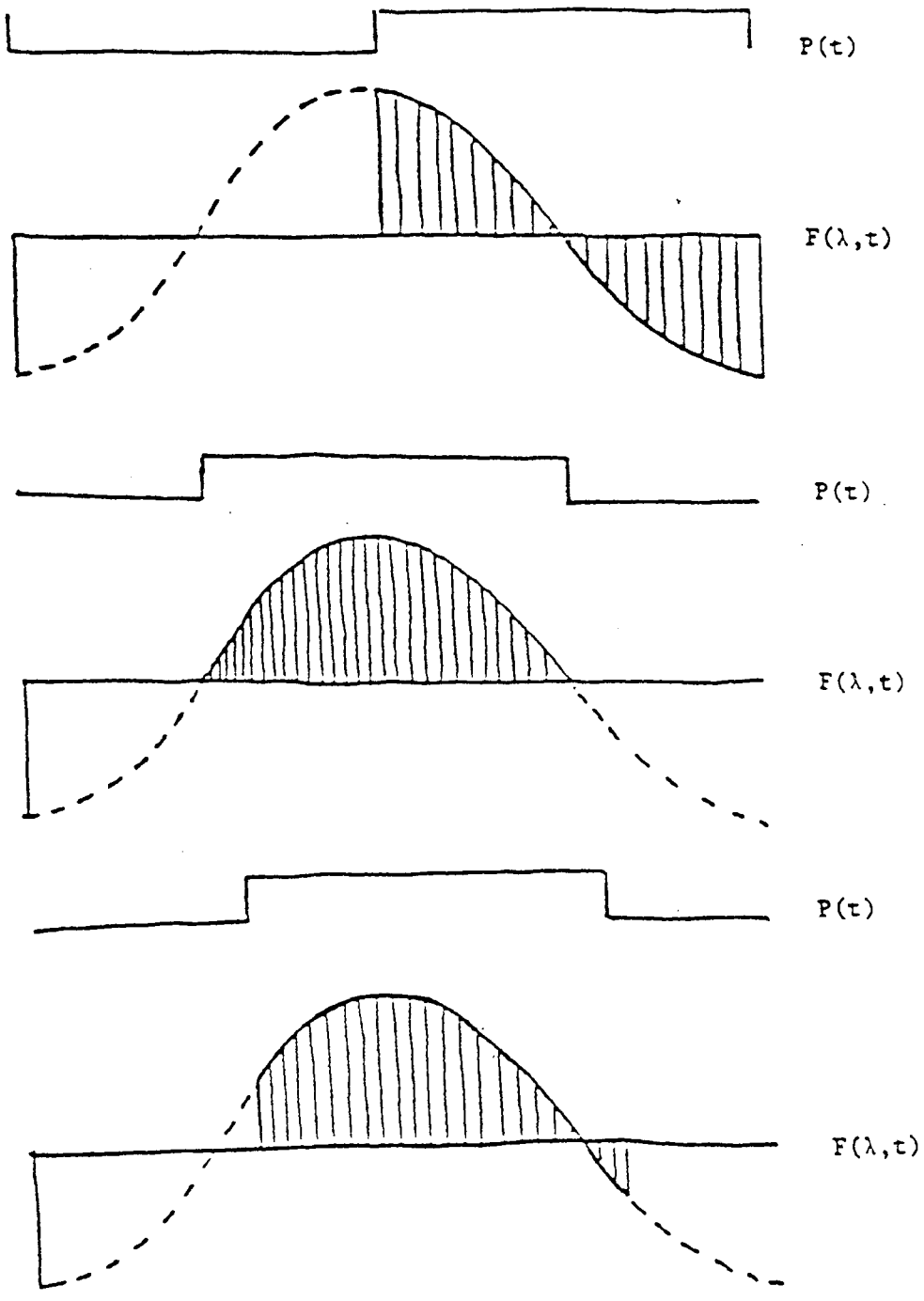

Figure 16. Depiction of the Periodic Interval Relative to F(t). From Reference (84).

antibody-bound fluorescein-labelled phenobarbital (Ag*) simultaneously in a homogeneous phase-resolved fluoroimmunoassay (PRFIA). The determination was based upon a small lifetime difference of 100 ps and a very small intensity change (< 10%) between the free and bound Ag*. The PRFIA involved measurements made at a series of five non-nulling detector phase angles. Because PRFI contributions of non-interacting emitters are additive, a series of linear equations were generated, of the form:

$$\begin{aligned} I_{\phi_1}^{PRF} &= I_{\phi_1}^{F}\ C_{Ag^*} + I_{\phi_1}^{B}\ C_{Ag^*\text{-}Ab} \\ &\cdot \quad\quad \cdot \quad\quad \cdot \\ &\cdot \quad\quad \cdot \quad\quad \cdot \\ &\cdot \quad\quad \cdot \quad\quad \cdot \\ I_{\phi_n}^{PRF} &= I_{\phi_n}^{F}\ C_{Ag^*} + I_{\phi_n}^{B}\ C_{Ag^*\text{-}Ab} \end{aligned} \qquad (7)$$

where $I_{\phi_1}^{PRF}$ is the PRFI of a solution, $I_{\phi_1}^{F}$ is the PRFI of a solution containing only free Ag* and $I_{\phi_1}^{B}$ is the PRFI of a solution containing only antibody bound Ag* for the first equation generated at $\phi_D = \phi_1$. The set of equations is only valid if the total concentration of labelled antigen (C_{A^*}) is held constant for all of the solutions. In matrix form, these equations appear as:

$$\begin{bmatrix} I_{\phi_1}^{F} & I_{\phi_1}^{B} \\ \cdot & \cdot \\ \cdot & \cdot \\ \cdot & \cdot \\ I_{\phi_n}^{F} & I_{\phi_n}^{B} \end{bmatrix} \begin{bmatrix} C_{Ag^*} \\ C_{Ag^*\text{-}Ab} \end{bmatrix} = \begin{bmatrix} I_{\phi_1}^{PRF} \\ \cdot \\ \cdot \\ \cdot \\ I_{\phi_n}^{PRF} \end{bmatrix} \qquad (8)$$

The over-determined matrix was "solved" for the fractions of free and bound Ag* using a least squares approach that included the constraint that the %free Ag* plus the %bound Ag* equal 100%. A typical calibration curve for the PRFIA determination of phenobarbital is shown in Figure 17. The PRFIA had a relative standard deviation of 6.7% for a set of four calibration curves. The limit of detection was found to be 3 μg/ml of phenobarbital in the undiluted sample. A homogeneous steady-state quenching approach was also tried, and the results obtained for the free Ag* were poorly correlated with the standard concentrations.

A homogeneous PRFIA for the determination of human serum albumin was also reported (87). This work demonstrated the applicability of PRFIA to the determination of macromolecules as opposed to haptens such as phenobarbital. Texas Red, a sulfonyl chloride derivative of sulforhodamine-101, was used as the label. This species has a high molar absorptivity and quantum yield and a lower rate of photobleaching than fluorescein. Also, its excitation and emission maxima are at 590 and 610 nm, respectively; these wavelengths are long enough to avoid most spectral interference from fluorescent species in serum.

Because PRFI contributions are additive for independent emitters, the PRFI of an immunoassay standard or unknown solution takes the form of Eqn. 6. When the amount of Ag in a solution containing constant amounts of Ag* and Ab is

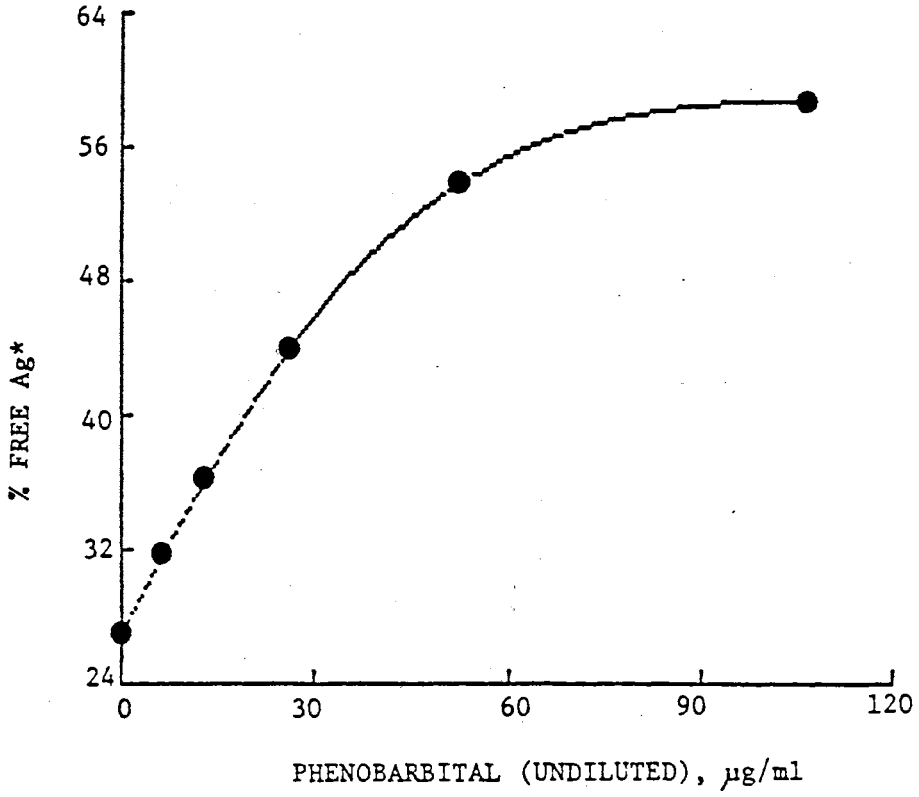

Figure 17. Typical PRFIA Calibration Curve for Phenobarbital. From Reference (84).

increased, the C_{Ag*} will increase by ΔC and C_{Ag*-Ab} will decrease by ΔC. Thus:

$$I'_{\phi n} = I^F_{\phi_n} (C_{Ag*} + \Delta C) + I^B_{\phi_n} (C_{Ag*-Ab} - \Delta C) \quad (9)$$

Subtraction of Eqn. 7 from Eqn. 9 gives

$$\Delta C = [I'_{\phi n} - I_{\phi n}] / (I^F_{\phi_n} - I^B_{\phi_n}) \quad (10)$$

Calibration curves were obtained by plotting ΔC as a function of C_{Ag} for a series of standard solutions.

A fluorescence lifetime difference between the free and bound HSA of 0.090 ns was observed. No sample matrix effects were seen with serum samples, possibly due to the high dilution factor (7×10^{-6}). A relative standard deviation of 5.8% was obtained for four calibration curves run on four consecutive days. The method was well correlated with values obtained for 24 serum samples at a local hospital's clinical chemistry laboratory, using the bromocresol green method (88) on a Technicon RA-1000 autoanalyzer.

The only other phase-resolved fluoroimmunochemical determination reported is a homogeneous, noncompetitive immunofluorometric determination of human lactoferrin (89). The method was based on energy transfer from fluorescein-labelled anti-lactoferrin (Ab^*F) to tetramethylrhodamine-labelled anti-lactoferrin (Ab^*R) when both antibodies were bound to lactoferrin (Ag). The PRFI of the donor species (Ab^*F) was measured and was found to decrease because of the energy transfer to Ag^*R, in the presence lactoferrin, as a

function of the resulting decreases in both Ag*F intensity and lifetime. Energy transfer was not observed in the absence of lactoferrin. The data analysis was much less involved than in the previous PRFIA's: PRFI's were measured at only one detector phase angle, and the ratio of the PRFI of Ab^*F in the presence of Ag to the PRFI in the absence of Ag was plotted as a function of C_{Ag} or log C_{Ag}. A pooled standard deviation of 8.39×10^{-3} intensity ratio units was calculated for the points in a set of four cali- bration curves. The relative standard deviation was <2%. A hook effect was observed at high concentrations of Ag, so samples would need to be run at two different dilutions in order to get unambiguous results.

CHAPTER IV

EFFECTS OF ORGANIZED MEDIA ON FREE AND ANTIBODY-BOUND FLUORESCEIN LABELLED PHENOBARBITAL

Introduction

Surfactants and cyclodextrins have been widely studied in recent years. Their ability to change the fluorescence characteristics of some molecules has been recognized as a valuable property and has potential applicability for immunoassays and immunometric determinations.

Common surfactants are amphiphilic molecules with a hydrophilic head group and a long, hydrophobic tail; they can be classified as cationic, anionic, nonionic or zwitterionic, depending on the nature of the hydrophilic group. Above a certain concentration, called the critical micelle concentration (CMC), surfactant monomers associate to form spherical particles of colloidal dimensions. In aqueous solution, the interior of the micelle contains the hydrophobic moieties while the hydrophilic head groups are located at the surface of the sphere. Interaction between fluorophores and micelles can cause large changes in the fluorescence characteristics of the fluorophore. Fluorophores generally associate with micelles in one of two ways,

depending on their relative hydrophobicity. They can adsorb on the exterior of the micelles in a primarily electrostatic interaction with the surfactant head groups, or they can be absorbed into the hydrophobic interior of the micelles to some degree (90).

Cyclodextrins are cyclic oligosacachrides composed of α-(1,4)-linkages of D(+)-glucopyranose units. The most common members of this family are α-, β-, and γ-cyclodextrins composed of six, seven, or eight glucose units, respectively. These molecules are torus shaped with a hydrophobic interior cavity. As the number of glucose units in the cyclodextrin increases, the diameter of the cavity increases from 4.5-6.0 (6 units) to 6.0- 8.0 (7 units) to 8.0-10.0 Å (8 units) (91). The cyclodextrins can form inclusion complexes with organic molecules of suitable size and shape. Larger molecules can form inclusion complexes if they have an aromatic moiety or other group that can fit into the cyclodextrin cavity. The interactions between the cyclodextrin and the included compound are largely due to van der Waals forces and hydrophobic interactions. Absorption spectra of aqueous solutions of the inclusion complexes are often different than those of the unbound solutes in aqueous solutions. Cyclodextrins are believed to enhance the fluorescence of certain fluorophores by inhibiting the quenching effects of aqueous solutions.

In heterogenous fluoroimmunochemical determinations, micelles or cyclodextrins could be used to increase the fluorescence intensity of the free fraction of the

fluorescent-labelled species after removal of the bound fraction in order to improve the detection limits. This approach was used in the TRIFMA systems reviewed in Chapter II. Micelle-induced spectral shifts could be of value in avoiding spectral interferences due to constituents in the sample matrix. The modification of fluorescence properties by micelles or cyclodextrins could also be exploited for homogeneous fluoroimmunochemical determinations to improve the discrimination between the free and bound fractions of the labelled species. For example, the use of sodium dodecyl sulfate, an anionic micellar species, to increase the fluorescence intensity and polarization differences between free and Ab-bound fluorescein-labelled gentamicin has been incorporated into a solvent-perturbation FIA technique (92). A similar approach was used for the determination of methamphetamine (93). If micelles and cyclodextrins increase the differences in the fluorescence characteristics of free and antibody-bound fluorescein-labelled phenobarbital, they could be used in the PRFIA of phenobarbital.

Experimental

Reagents

Fluorescein-labelled phenobarbital (Ag^*) was prepared *in situ* by Bright, Bunce and McGown (94). The dodecylamine hydrochloride (DAC) and dodecyltrimethyl-ammonium chloride (DTAC) were purchased from Eastman, and

the hexadecyltrimethylammonium chloride (CTAC), tetradecyltrimethylammonium bromide (TTAB) and N,N-dimethyldodecylamine-N-oxide (LDAO) from Fluka. Triton X-100 (TX-100) and beta-cyclodextrin (β-CD) were purchased from Sigma and gamma-cyclodextrin (γ-CD) was purchased from ICN Biochemicals. Sheep anti-phenobarbital antibodies (Ab) were purchased from Cambridge Medical Diagnostics. A protein concentration was not supplied with the Ab; thus, all concentrations of Ab in solution are reported as μl added of 1:500 dilution of Ab in 0.010 M, pH 7.4 phoshate buffer. All compounds were used without further purification.

Demineralized, distilled water was used for all preparations. The Ag* stock solution was prepared by 100-fold dilution of the chromatographically purified reaction product. The concentration of the stock solution was estimated to be 30 μM by using a calibration curve generated with fluorescein isothiocyanate (Sigma). Unbuffered solutions of all surfactants were prepared at concentrations above their reported CMC values (95,96) and mixed by ultrasonic treatment for 30 minutes. Cyclodextrin solutions were similarly prepared. The concentrations of these solutions are given in Table VII. Buffered solutions of the surfactants were prepared at the same concentrations as the unbuffered solutions, in 0.010 M sodium phosphate buffers ranging in pH from 5.8 to 7.8. Constant ionic strength (μ = 0.10 M) buffered solutions of TTAB were

prepared by addition of the appropriate amount of sodium chloride.

For the studies of free Ag*, the analytical concentration of Ag* in the cuvette was calculated to be 0.21 μM from the estimated concentration of the Ag* stock (see above). In the Ag*-Ab studies, Ag* stock solutions (3 x 10^{-6} M, 3 x 10^{-7} M) were prepared by diluting the the appropriate volume of Ag* with phosphate buffer.

Apparatus and Procedures

All fluorescence measurements, including steady-state intensities and dynamic phase-shifts and demodulations, were made with an SLM 4800S Spectrofluorometer in ratiometric modes, with a portion of the excitation beam diverted to a reference photomultiplier to compensate for fluctuations in the source output and (for dynamic measurements) excitation modulation. A 450-W xenon arc lamp was used for excitation, Hamamatsu R928 photomultipliers for detection and an Apple II+ microcomputer for on-line aquisition of fluorescence spectral and lifetime data and for lifetime calculations. A block diagram of the SLM 4800S is shown in Figure 18.

For dynamic measurements, slits were set at 16 nm and 0.5 nm band-pass for the excitation monochromator entrance and exit, respectively, 0.5 nm for the modulation tank exit, and 16 nm for both the entrance and exit of the emission monochromator. In studies where low concentrations of fluorophore were used (nanomolar levels), a 530 nm band pass

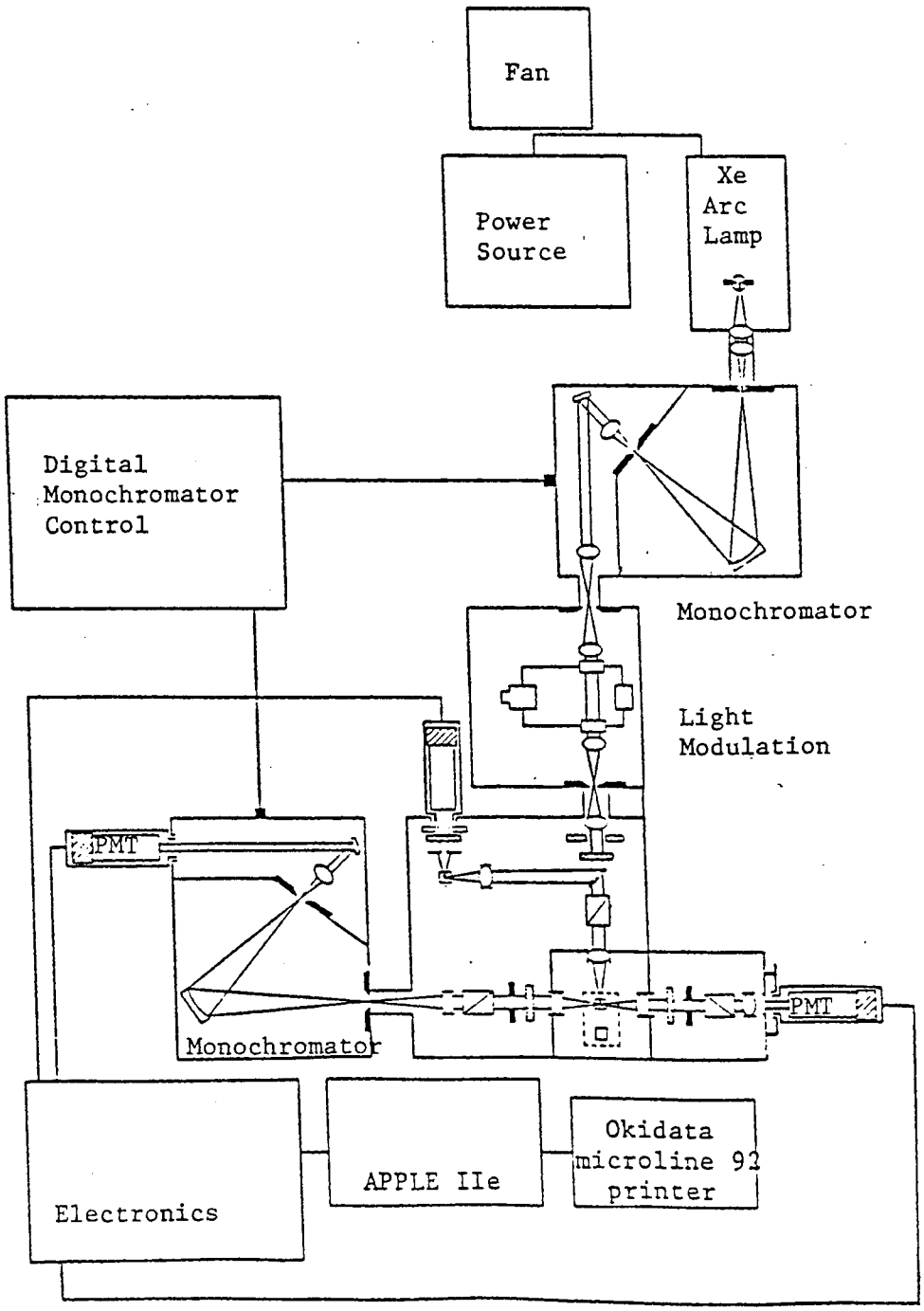

Figure 18. Block Diagram of the SLM 4800S Spectrofluorometer.

filter (10 nm half-width, Oriel) was used instead of the emission monochromator. In the micellar studies, all slits were set at 2 nm band-pass for steady-state intensity measurements, except for the excitation monochromator entrance slit which was set at 16 nm. An excitation polarizer set at 35° from the vertical axis was also used in the micelle studies. In the cyclodextrin studies, steady-state excitation and emission spectra were obtained with slit settings of 8 nm for the excitation monochromator entrance and exit and the modulation tank exit, and 16 nm for the emission monochromator entrance and exit.

Polarization studies were performed with an excitation polarizer set at 0° from the vertical axis and an emission polarizer set first at 0° and then at 90° from the vertical. Slits were set at 8 nm for the excitation entrance and exit and 4nm for the modulation tank exit. The 530 nm bandpass filter was used instead of the emission monochromator. Polarization was calculated using the following equation:

$$P = (I_{\parallel} - I_{\perp}) / (I_{\parallel} - I_{\perp}) \qquad (11)$$

where P is the fluorescence polarization, $I_{\parallel}$ is the fluorescence emission intensity with the excitation and emission polarizer parallel to each other and $I_{\perp}$ is the fluorescence emission intensity with the excitation and emission polarizers set perpendicular to each other.

Temperatures in the fluorometer sample chamber were maintained at 25° ± 0.1° with a Haake A81 temperature control unit. Disposable polyethylene cuvettes (Precision Cells)

were used to contain solutions for fluorescence measurements.

Unless otherwise noted, the fluoresence lifetimes of Ag* were determined relative to a reference solution of Acridine Orange in absolute ethanol (U.S. Industrial Chemical Co.), which was found (from phase-shift measurements) to have a lifetime of 3.19 $\pm$ 0.02 ns relative to a scattering solution, at the wavelengths used in this work. Equations for these calculations were described in Chapter III. All fluorescence lifetimes are reported as the average of five measurements taken in the "100 average" mode, in which each measurement is the average of 100 samplings performed internally by the spectrofluorometer.

Absorption spectra were acquired with a Perkin-Elmer Lambda Array 3840 Spectrophotometer.

Effects of Micelles and Cyclodextrins on Fluorescein-Labelled Phenobarbital

Results and Discussion

All of the fluorescence lifetimes reported here had standard deviations in the 5-50 ps range . A lifetime of 4.04 ns had previously been found for Ag* by using phase-shift measurements (86).

The effects of five micelle-forming species and of β- and γ-cyclodextrin are summarized in Table VII. The pH values of each of the unbuffered micellar solutions are also listed. All five micellar species caused red shifts ranging

TABLE VII

EFFECTS OF MICELLES AND CYCLODEXTRINS ON THE FLUORESCENCE PROPERTIES OF FLUORESCEIN-LABELLED PHENOBARBITAL (Ag*)

Added Species[a]	$\lambda_{em, max}$ [b]	Intensity Ratio	τ_p [d]	τ_m [e]	pH [f]
none	516	1.00	4.00[g]	4.00[g]	-
CTAC (3.0)	526	2.64	4.39	4.45	6.0
DAC (15)	523	1.36	4.07	4.23	4.6
DTAC (22)	526	2.54	4.28	4.30	6.6
LDAO (4.0)	522	1.05	3.68	3.86	7.1
TTAB (7.0)	525	2.72	4.40	4.44	6.0
β-CD[g] (2.0)	516	2.05	4.15	4.12	-
γ-CD[g] (2.0)	517	1.57	4.23	4.07	-

a Concentration in parentheses, mM.
b Emission maximum, using excitation at 490 nm, given in nm.
c Ratio of intensity in presence of the added species to that in its absence, each measured at its emission maximum.
d Fluorescence lifetime calculated from phase-delay, in ns, determined using the Ag* solution as a reference (τ = 4.00 ns).
e Fluorescence lifetime calculated from the demodulation, in ns, determined in the same manner as p.
f pH of the cuvette solution. Dash indicates pH not determined.
g Fluorescence lifetimes determined using a scattering solution as the reference.

from 5 to 10 nm in the emission of Ag*. No shifts in the emission maximum were observed with the cyclodextrins. Fluorescence enhancement was observed with all species, and was highest with CTAC, DTAC, and TTAB. All species except LDAO, which was the only nonionic micelle used, caused increases in the observed lifetime. CTAC, TTAB and β-cyclodextrin were chosen for further studies.

A shift in the emission maximum of Ag* to 526 nm was observed with both CTAC and TTAB at all pH values studied, indicating an absence of pH-dependence. Fluorescence enhancements of Ag* in CTAC and TTAB as a function of pH are shown in Table VIII. Enhancements are expressed as peak-to-peak values (i.e., the ratio of the intensity of micelle-Ag* to that of Ag*, each measured at its emission maximum). A small trend towards increased enhancement was observed as the pH decreased, with a dramatic increase at pH 5.8.

Absorption spectra of Ag* and TTAB-Ag* at pH 5.8 are shown in Figure 19. The spectra show a definite increase in absorptivity in the presence of TTAB, indicating that the so-called fluorescence enhancement is at least partially due to absorption rather than quantum yield changes. For simplicity, the fluorescence intensity increases will continue to be referred to as enhancements.

The fluorescence lifetime difference of 0.3 ns between micelle-Ag* and Ag* remained fairly constant over the pH range studied for Ag* in the presence of both CTAC and TTAB.

TABLE VIII

RATIOS OF THE INTENSITY OF Ag* IN THE PRESENCE OF MICELLES TO THE INTENSITY IN THE ABSENCE OF MICELLES AS A FUNCTION OF pH

pH	Intensity Ratio (CTAC)	Intensity Ratio (TTAB)
5.8	6.24	5.12
6.0	2.29	1.35
6.2	1.39	1.80
6.4	1.17	1.30
6.6	1.41	1.39
6.8	1.03	1.26
7.0	1.05	1.20
7.2	1.01	1.07
7.4	0.91	0.91

Ratios of intensities measured at λ_{ex} = 490 nm and at the emission maxima for that solution, both measured under the same buffer and pH conditions.

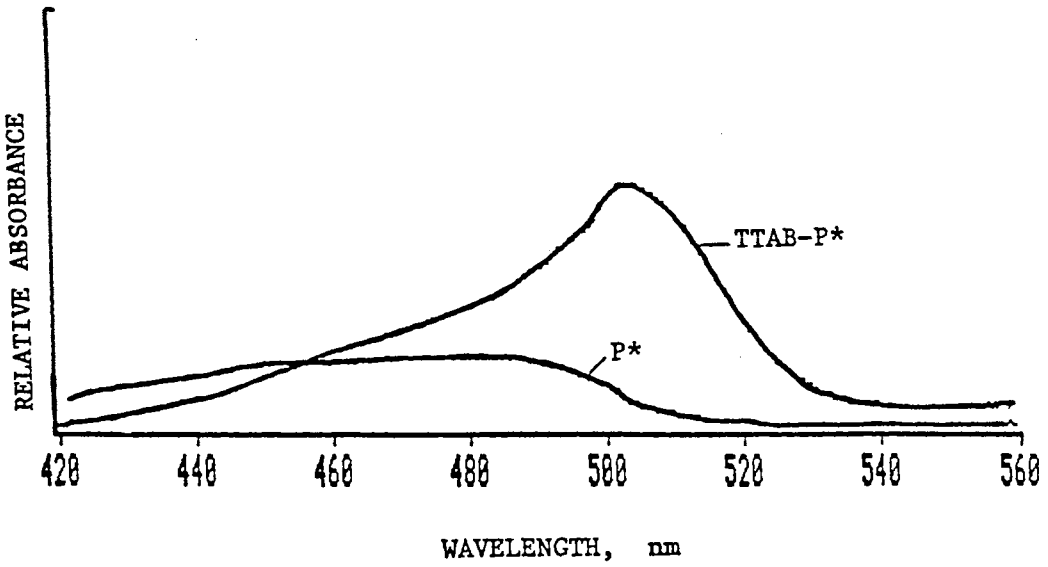

Figure 19. Absorption Spectra of Fluorescein-Labelled Phenobarbital with TTAB and without TTAB in Buffered Solution at pH 5.8.

The effects of TTAB on Ag* fluorescence were studied in buffered solutions adjusted to 0.010 M ionic strength with sodium chloride. Differences between the fluorescence lifetimes of TTAB-Ag* and Ag* as a function of pH are shown in Table IX. The change in lifetime calculated from the demodulation remained fairly constant, but the change in lifetime calculated from the phase-shift showed a definite increase with decreasing pH.

The effects of pH on the relative intensities of Ag* and TTAB-Ag* are shown in Figure 20, and the ratios of the intensities are listed in Table IX. Smaller relative enhancements were observed for the constant ionic strength solutions than for the buffered solutions without sodium chloride added (Table VIII).

Fluorescein is a weakly acidic molecule, with pK_{a1} and pK_{a2} values of 4.4 and 6.7, respectively (97). The completely dissociated form is highly fluorescent, and the fluorescence intensity of fluorescein solutions increases with increasing pH. As shown in Figure 20, in the low pH range, the fluorescence of Ag* is enhanced by association with TTAB, but above pH 7.2 TTAB causes a decrease in intensity relative to that in the absence of the micelle, which is higher because of increased dissociation of the fluorescein label.

TABLE IX

THE INTENSITY RATIOS OF TTAB-Ag* TO Ag* AND THE DIFFERENCES BETWEEN THE FLUORESCENCE LIFETIMES OF THE TWO AS A FUNCTION OF pH, IN CONSTANT IONIC STRENGTH SOLUTION

pH	Intensity Ratio[a]	τ_p[b]	τ_m[c]
5.8	1.38	0.37	0.43
6.0	1.30	0.37	0.52
6.2	1.15	0.36	0.46
6.4	1.11	0.29	0.46
6.6	1.19	0.35	0.44
6.8	1.30	0.31	0.45
7.0	1.07	0.29	0.46
7.2	0.98	0.33	0.46
7.4	0.98	0.26	0.46
7.6	0.97	0.27	0.44
7.8	0.88	0.26	0.47

[a] Intensities measured at λ_{ex} = 490 nm, and at the emission maximum of the solution, both at same pH.

[b] Fluorescence lifetime of TTAB-Ag* minus that of Ag* as calculated from the phase-shift lifetimes, in ns.

[c] Fluorescence lifetime of TTAB-Ag* minus that of Ag* as calculated from the demodulation lifetimes, in ns.

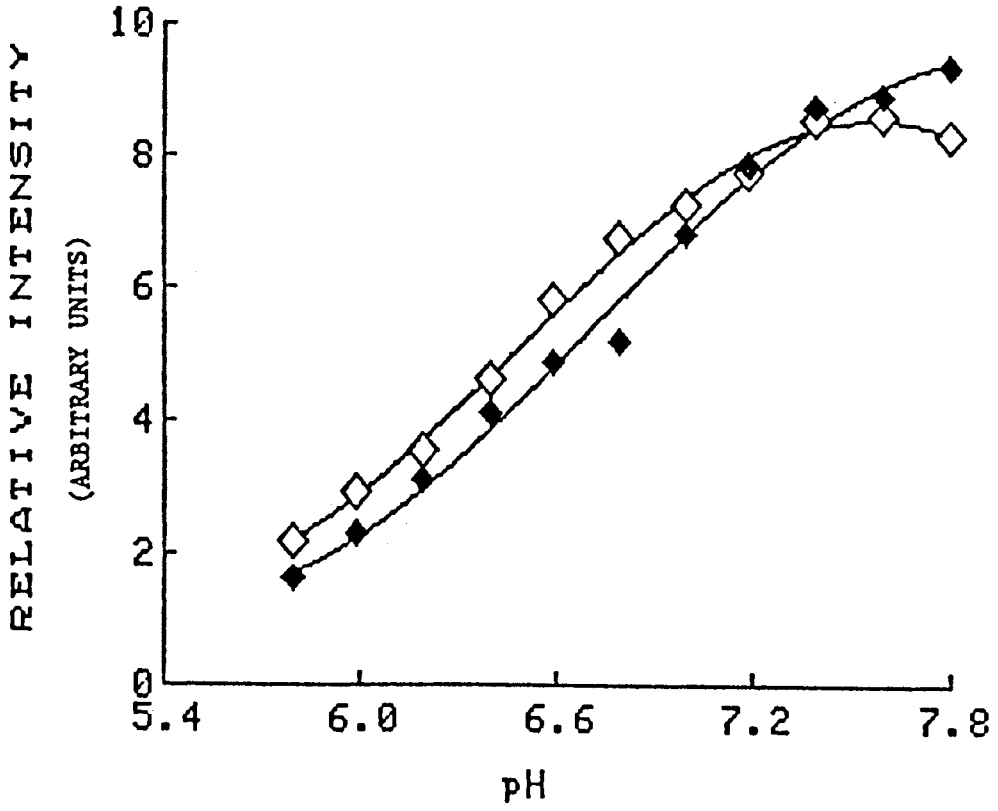

Figure 20. Fluorescence Intensity of Ag* (♦) and TTAB-Ag* (◊) as a Function of pH in Constant Ionic Strength Buffer.

excitation and emission spectra of Ag* with and without TTAB at pH 5.8 and pH 7.0 are shown in Figure 21. The ratio of the intensity of TTAB-Ag* to that of Ag*, measured at the wavelength maxima for the latter (λ_{ex} = 501 nm and λ_{em} = 525 nm) was found to be 2.7 at pH 5.8 and 1.7 at pH 7.0.

The fluorescence wavelength maxima and lifetimes of Ag* as a function of TTAB concentration were studied at pH 5.8 (Table X). Spectral shifts are almost negligible at TTAB concentrations below 0.6 mM. Fluorescence lifetimes decrease with increasing TTAB concentration up to around 1 mM, when they jump to a higher value that remains constant at higher concentrations. The initial decrease in lifetimes indicates quenching of the Ag* fluorescence at TTAB concentrations below its CMC. Above the CMC, the lifetimes achieve a maximum value corresponding to that of Ag* protected by micelle association. Table XI shows the results of a similar study at pH 7.0. Simliar trends are observed in the emission maxima and lifetimes, but the transitions occur at slightly lower TTAB concentrations. Relative intensities are also shown for both pH values, and indicate that there is indeed a quenching effect at TTAB concentrations below the apparent CMC.

The effects of β-CD on the fluorescence lifetime and polarization of Ag* at pH 7.4 were studied. The fluorescence lifetime of Ag* was measured over a β-CD range of 2 x 10^{-7} to 2 x 10^{-3} M. At low concentrations β-CD had no effect on the lifetime of Ag*. When the concentration ratio

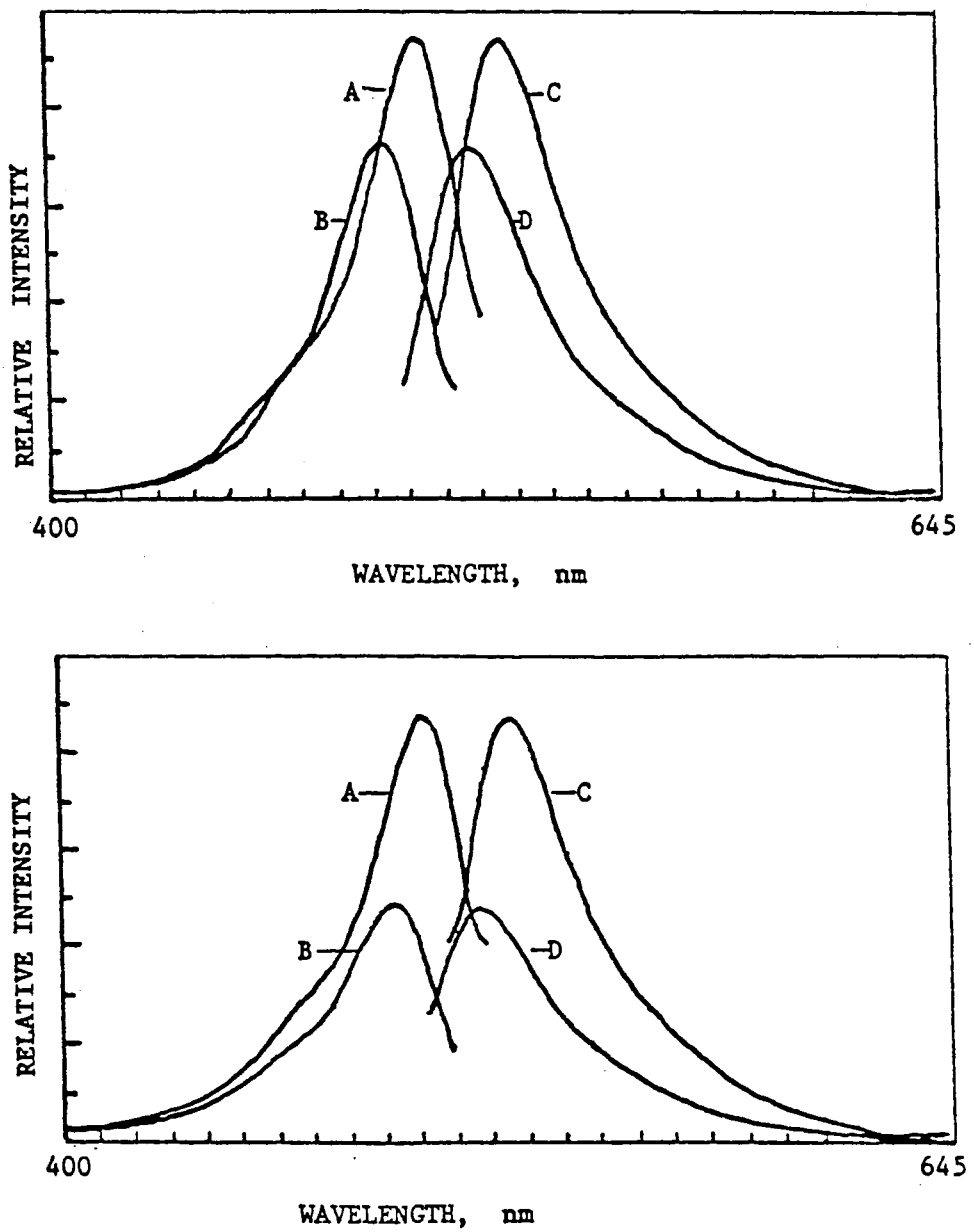

A = TTAB-Ag* excitation, B = Ag* excitation
C = TTAB-Ag* emission, D = Ag* emission
Note: The Intensity scales for the spectra at pH 7.0 and 5.8 are different. The intensity at 7.0 is higher.

Figure 21. Excitation and Emission Spectra of Ag* with and without TTAB in Constant Ionic Strength Buffer at pH 7.0 and pH 5.8.

TABLE X

FLUORESCENCE EXCITATION AND EMISSION MAXIMA AND THE DIFFERENCE BETWEEN THE FLUORESCENCE LIFETIMES OF TTAB-Ag* AND Ag* AS A FUNCTION OF TOTAL TTAB CONCENTRATION IN pH 5.8, CONSTANT IONIC STRENGTH SOLUTIONS

C_{TTAB} [a]	λ_{ex} [b]	λ_{em} [c]	τ_p [d]	τ_m [e]
0	491	517	-	-
0.46	492	518	0	0.06
0.58	492	518	-0.13	-0.04
0.69	496	525	-0.27	-0.06
1.0	502	525	0.32	0.45
3.1	501	525	0.36	0.48
7.0	501	525	0.36	0.49

[a] Analytical concentration of TTAB, in mM.

[b] Excitation maximum, in nm.

[c] Emission maximum, in nm.

[d] See (b), Table IX.

[e] See (c), Table IX.

TABLE XI

FLUORESCENCE EMISSIOM MAXIMA, INTENSITY RATIOS AND THE DIFFERENCE BETWEEN THE FLUORESCENCE LIFETIMES OF TTAB-Ag* AND Ag* AS A FUNCTION OF TOTAL TTAB CONCENTRATION IN pH 7.0, CONSTANT IONIC STRENGTH SOLUTION

C_{TTAB}[a]	λ_{em}[b]	Intensity Ratio[c]	τ_p[d]	τ_m[e]
0	516	-	-	-
0.69	521	0.28	-0.57	-0.17
0.81	525	0.42	-0.12	0.08
0.91	525	0.75	0.24	0.36
1.0	525	0.84	0.30	0.41
3.1	525	-	0.34	0.49
7.0	525	1.07	0.32	0.49

[a] Analytical concentration of TTAB, in mM.

[b] Emission maximum, in nm.

[c] Ratio of the intensity of TTAB-Ag* to Ag*, measured at λ_{ex} = 490 nm and at the emission maximum of the solution.

[d] See (b), Table IX.

[e] See (c), Table IX.

of β-CD to Ag* was greater than 100,000 to 1, the lifetime began to increase and was still increasing at a concentration ratio in excess of 8×10^5 : 1, as illustrated in Figure 22. This figure shows that fluorescein-labelled phenobarbital does not associate with β-CD until the cyclodextrin is in great excess, indicating a fairly weak interaction between the two species. The effect of β-CD on the polarization of a 1.9 nM Ag* solution is shown in Figure 23. The polarization increases with increasing concentration of β-CD up to a concentration of about 2.0 mM. This concentration is at a β-CD to Ag* concentration ratio of approximately 1.7×10^6 : 1. Because of the very weak interaction between Ag* and β-CD it is extremely unlikely that an inclusion complex is being formed. Phenobarbital is known to form inclusion complexes with β-CD (98), but it is bound via the aromatic ring. The fluorescein-labelled phenobarbital used in this work (see Figure 24 for the structure of Ag*) is labelled at the <u>para</u> position of the aromatic ring, preventing inclusion of this moiety. The fluorescein end of the Ag* is too large to fit into β-CD.

Conclusions

Changes observed in Ag* fluorescence upon association with micelles included pH-independent spectral shifts and pH-dependent fluorescence intensity and lifetime changes. Cyclodextrins did not induce spectral shifts in the Ag* fluorescence, and the induced lifetime changes were not as

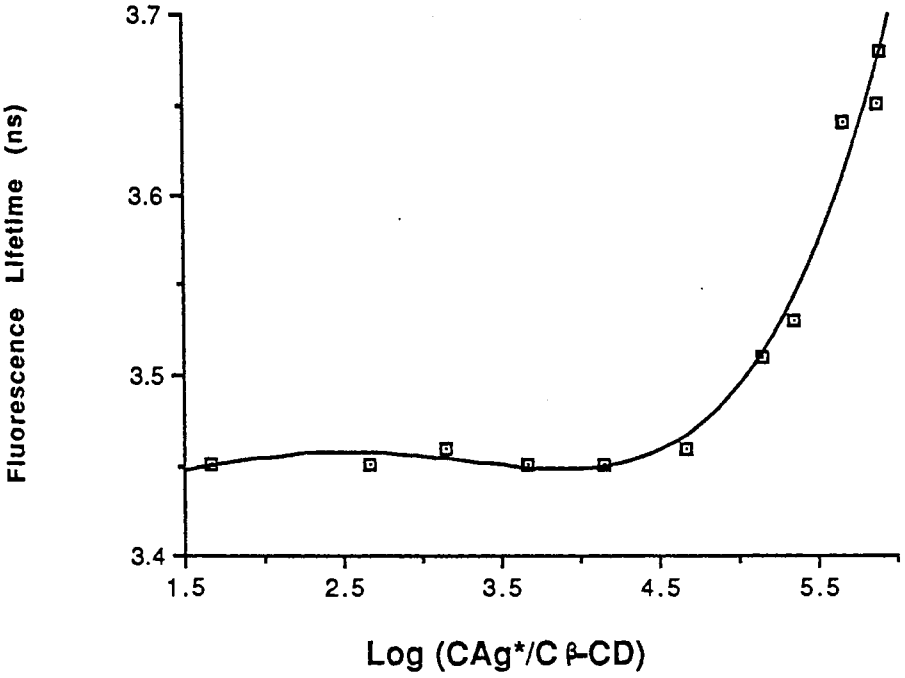

Figure 22. Fluorescence Lifetime of Ag* as a Function of Log (C_{Ag*} / $C_{\beta-CD}$) at pH 7.4.

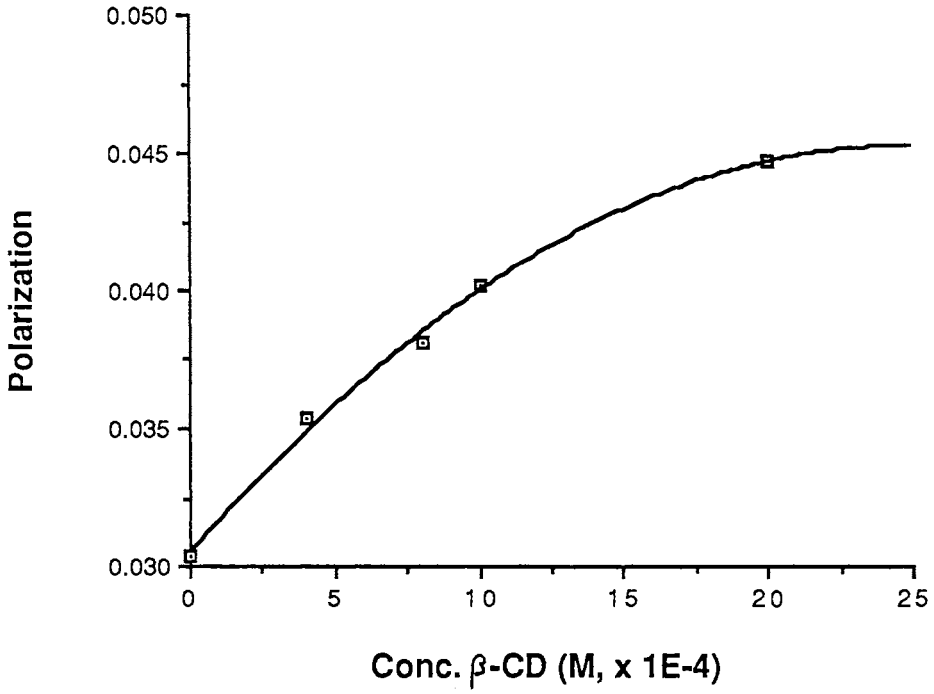

Figure 23. Fluorescence Polarization of 1.9 nM Ag* as a Function of $C_{\beta\text{-CD}}$ at pH 7.4.

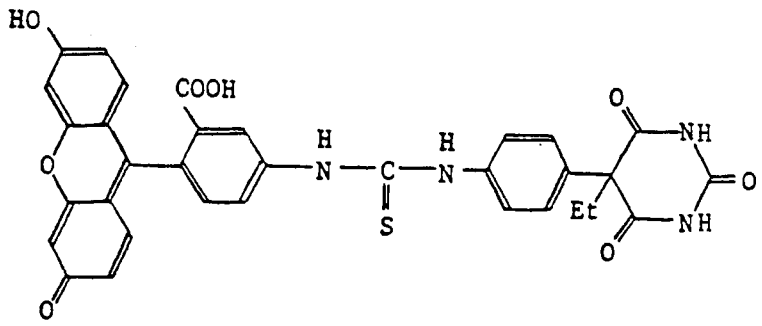

Figure 24. Structure of Fluorescein-Labelled Phenobarbital.

large as those observed for the micelle systems. However, large intensity enhancements were observed that might prove valuable in certain applications. Future research into the applications of auxillary binding reagents will require studies on the antibody-bound as well as the free labelled antigen. Therefore, it is difficult to predict which reagents will prove most valuable for a particular immunoassay technique. The studies described here demonstrate that significant changes in the fluorescence properties of fluorescein-labelled phenobarbital can be acheived by using micelles, and to a lesser degree, cyclodextrins.

Effects of Micelles and Cyclodextrins on Antibody-Bound Fluorescein-Labelled Phenobarbital

Results and Discussion

The interactions of micelles and cyclodextrins with Ag*-Ab, at the same auvillary binding reagent concentrations as used in the studies of free Ag*, were also investigated. The effect of Ab on Ag* in pH 7.4 phosphate buffer solution is used as a comparison in evaluating the effects of micelles and cyclodextrins. Various antibody preparations were compared. The results of these studies are discussed in Chapter V. The antibody preparation that gave the best results was used in subsequent studies.

The lifetime difference between Ag* and Ag*-Ab was found to be 0.37 ns in buffer solution. The effect of various micelles on the lifetime difference and the intensity ratio of Ag* to Ag*-Ab are shown in Table XII. The lifetime difference between Ag* and Ag*-Ab decreased substantially in the presence of the micelles. The smallest $\Delta\tau$ was seen in the presence of LDAO, and the largest $\Delta\tau$ was observed in the presence of TX-100. The intensity ratio of Ag* to Ag*-Ab was lower in the presence of the micelles than in their absence. The TX-100 micelles had the highest intensity ratio of all the micelles studied. No spectral shifts between the free and bound Ag* were seen in the presence of the micelles. These results show that the micelles actually decrease the ability to discriminate between the free and antibody-bound fluorescein-labelled phenobarbital.

The fluorescence excitation and emission spectra of Ag* in 2 mM β-CD in the presence and absence of Ab are shown in Figure 25. The excitation and emission maxima are essentially the same as in the absence of β-CD, as shown in Table XIII. The fluorescence intensities of both the free and bound Ag* are higher in β-CD than in buffer solution (Table XIII), although the intensity ratio of Ag* to Ag*-Ab at 520 nm was larger for the buffer solution.

The fluorescence polarization of Ag* as a function of the volume of Ab added is plotted in Figure 26 for 1.9 nM Ag* in both phosphate buffer and 2 mM β-CD at pH 7.4. In

TABLE XII

EFFECTS OF MICELLES ON THE FLUORESCENCE LIFETIME DIFFERENCES AND INTENSITY RATIOS BETWEEN Ag* AND Ag*-Ab

Added Species[a]	$\Delta\tau_{F-B}$[b]	Intensity Ratio[c]
none	0.37	2.02
CTAC (3.0)	0.08	1.04
TTAB (7.0)	0.09	1.02
LDAO (4.0)	0.13	1.35
TX-100 (0.25)	0.30	1.85

[a] Concentration in parentheses, mM.

[b] Fluorescence lifetime of Ag* minus that of Ag*-Ab as calculated from the phase-shift lifetimes, in ns.

[c] Ratio of the intensity of Ag* to Ag*-Ab, measured at λ_{ex} = 490 nm and λ_{em} = 530 nm.

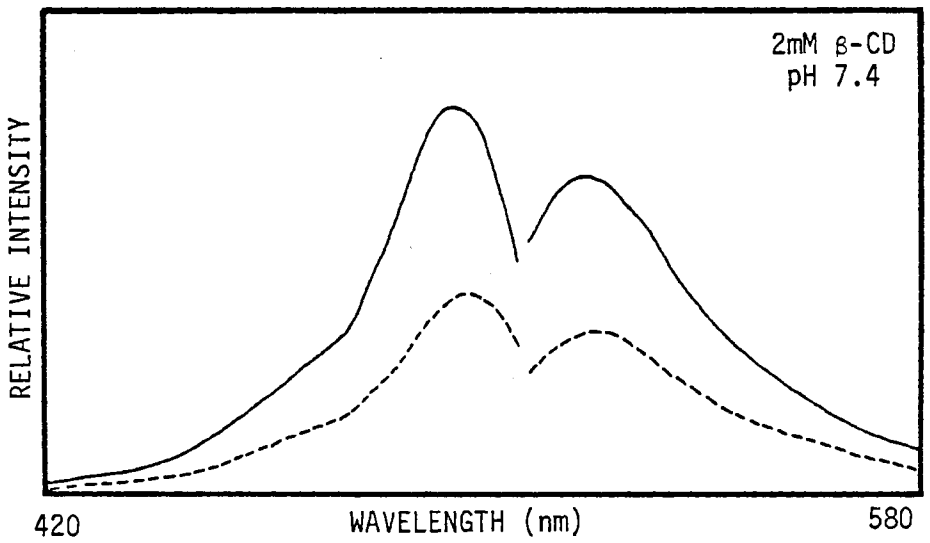

Figure 25. Fluorescence Excitation and Emission Spectra of Ag* in 2 mM β-CD in the Presence (----) and Absence (——) of Anti-Phenobarbital at pH 7.4

TABLE XIII

EFFECT OF β-CD ON THE SPECTRAL CHARACTERISTICS OF Ag* AND Ag*-Ab

Solution	λ_{ex}, max[a]	I max[b]	λ_{em}, max[a]	I max[c]	Intensity Ratio[d]
Buffer[e]					
Ag*	492	789	518	652	2.02
Ag*-Ab	496	405	520	322	
β-CD[f]					
Ag*	494	878	518	717	1.71
Ag*-Ab	494	522	520	420	

a Wavelength of maximum intensity, in nm.

b Excitation intensity measured at the excitation maximum, arbitrary units.

c Emission intensity measured at the emission maximum, arbitrary units.

d Ratio of the emission intensities of Ag* to Ag*-Ab, measured at λ ex = 494 nm and λ em = 520 nm.

e 0.010 M phosphate buffer, pH 7.4

f 2 mM β-CD, in 0.010 M phosphate buffer, pH 7.4.

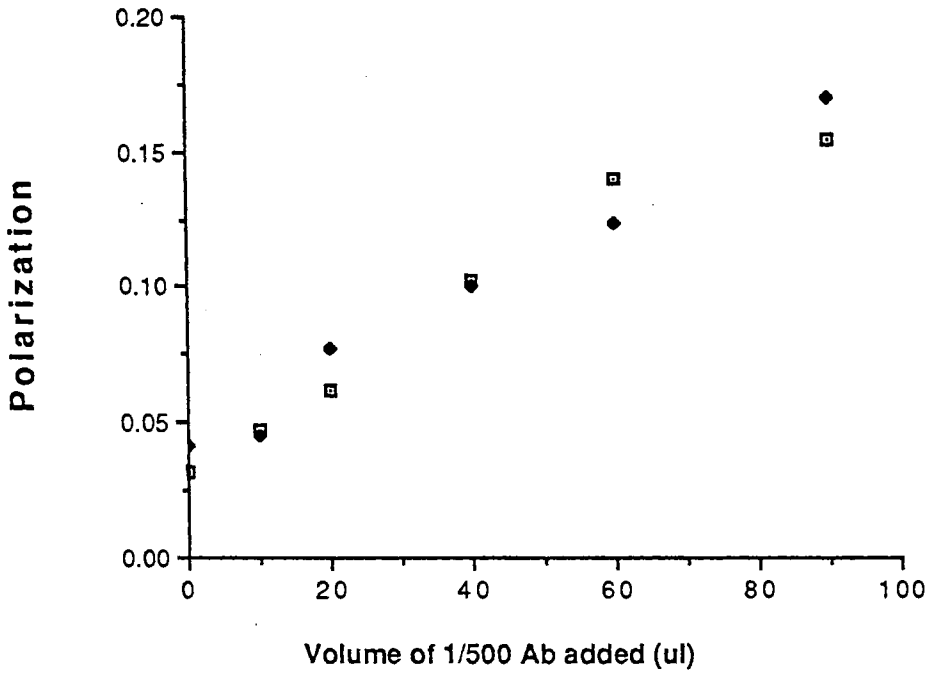

Figure 26. Fluorescence Polarization of 1.9 nM Ag* at pH 7.4 as a Function of Volume of 1:500 Ab added in both 2 mM β-CD (◆) and Phosphate Buffer (◘).

both cases, the polarization increases with increasing volume of Ab added. The points fall roughly on the same curve indicating no real advantage from including the β-CD in the system. The effect of β-CD on the fluorescence lifetime of Ag* over a range of Ag* concentrations was studied as a function of volume of Ab added. The results are shown in Figure 27. The difference in fluorescence lifetimes between the free and completely bound Ag* was approximately 0.44 ns except for a difference of 0.39 ns for the highest Ag* concentration (11.6 nM). The Ag* may not have been completely bound at this concentration. As the concentration of Ag* decreased from 11.6 to 1.2 nM the slope of the curves increased. In the buffer solution without β-CD, the curves for the same range of Ag* concentrations (in Chapter V) all tend to level out at about the same lifetime value. But in the presence of 2mM β-CD, the curves for 1.2 and 1.9 nM Ag* level out at lifetime values that are higher than expected: the 1.2 nM Ag* curve levels out about 0.10 ns higher than expected and the 1.9 nM Ag* curve at 0.04 ns higher. This effect indicates that β-CD plays a more predominant role at low concentrations of Ag* than at higher Ag* concentrations. The β-CD causes the system as a whole to have a higher overall lifetime but with a more pronounced effect when almost all of the Ag* is bound by the antibody.

The effect of γ-CD on the fluorescence lifetime of Ag* was studied and compared with the results of the studies of

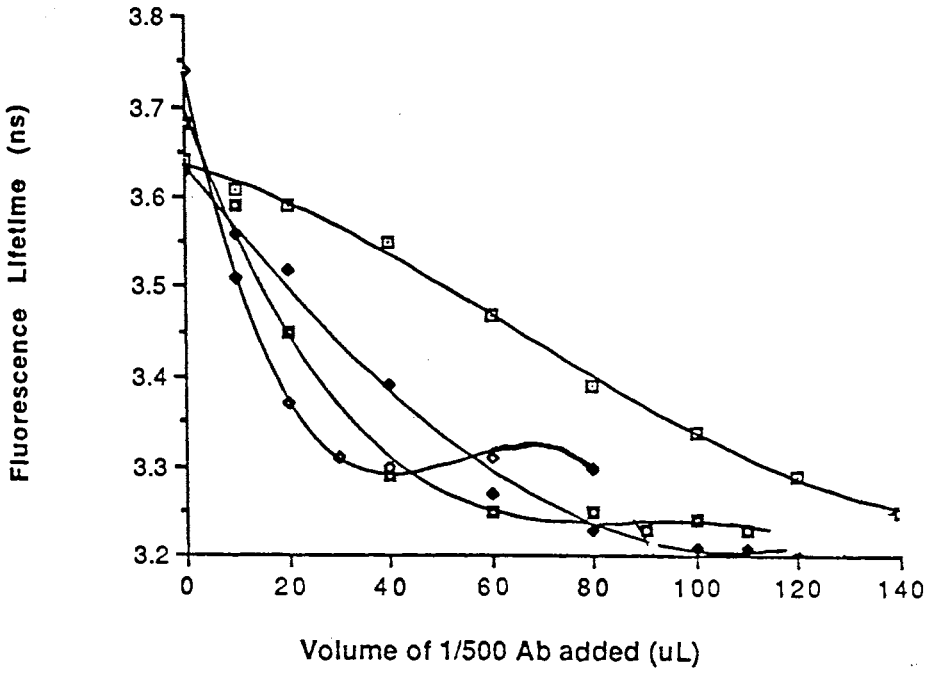

Figure 27. Antibody Dilution Profile in which Fluorescence Lifetime is Plotted as a Function of the Amount of 1:500 Dilution of Ab Added for a Series of Ag* concentrations in 2 mM, pH 7.4 β-CD. 11.6 nM (⧈), 5.0 nM (◆), 1.9 nM (■), 1.2 nM (◇)Ag*.

β-CD and phosphate buffer at a 1.9 nM Ag* concentration. Figure 28, in which the fluorescence lifetime is plotted as a function of the volume of 1:500 Ab added for 2 mM γ-CD, 2 mM β-CD and phosphate buffer, shows that the solutions γ-CD have a smaller lifetime difference between free and bound Ag* than either the β-CD or phosphate buffer solutions. The lifetime difference was found to be 0.32 ns.

Conclusions

The various micelles studied tended to have a detrimental effect on the ability to discriminate between the free and antibody-bound fluorescein-labelled phenobarbital. They increased the overall intensity of the system but decreased the intensity ratio of Ag* to Ag*-Ab relative to the intensity ratio in buffer solution. The least detrimental effects were seen in the presence of TX-100. The fluorophore seems to be adsorbed on the surface of the micelles thus allowing the micelles to associate with both Ag* and Ag*-Ab. The micelles may also denature the antibody to a certain extent. Micelles are not useful in the present PRFIA system but may be useful in a PRFIA with more hydrophobic labels and/or antigens.

The cyclodextrins had a much smaller effect on the Ag*-Ab than the micelles, showing only slight increases in overall lifetime and intensity of the system. The intensity ratio of Ag* to Ag*-Ab for both β-CD and γ-CD was lower than

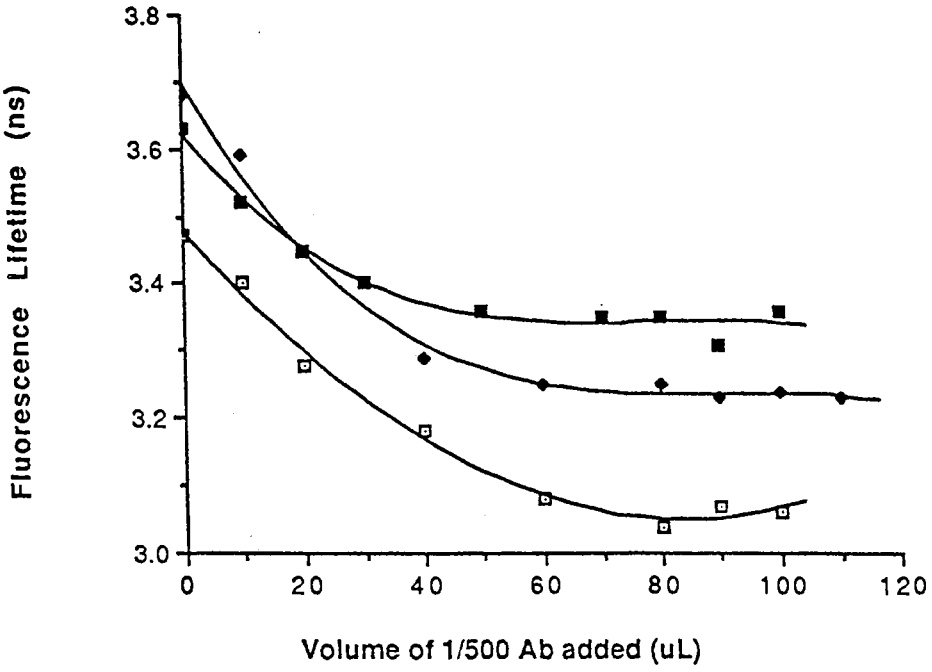

Figure 28. Fluorescence Lifetime of 1.9 nM Ag* as a function of the Amount of 1:500 Ab added for 2mM γ-CD (⧈), 2 mM β-CD (◆), and phosphate buffer (■) at pH 7.4.

that found in buffer solution, although the intensity ratio was still fairly high in β-CD; on the other hand, β-CD increased the lifetime difference between the free and antibody-bound Ag* slightly with respect to the buffer solution. However, these two effects tend to cancel each other out and therefore, β-CD is not very useful for the present PRFIA of phenobarbital. The cyclodextrins may be useful in PRFIA's with smaller, more hydrophobic labelled antigens.

CHAPTER V

OPTIMIZATION OF EXPERIMANTAL CONDITIONS IN THE PRFIA FOR THE DETERMINATION OF PHENOBARBITAL

Introduction

Fluoroimmunoassays (FIA) are widely used alternatives to radioimmunoassays (RIA) in the field of therapeutic drug monitoring. Unlike radioisotopes, fluorophores are sensitive to their chemical microenvironment enabling one to develop homogeneous (nonseparation) immunoassays. Any of several different fluorescence characteristics may change when the antibody binds to the labelled antigen. Homogeneous FIAs can take advantage of changes in fluorescence intensity, energy transfer, polarization, and fluorescence lifetimes (2-5). Both phase-resolved fluoroimmunoassays (PRFIA) and time-resolved fluoroimmunoassay (TRFIA) are based on fluorescence lifetimes; however, PRFIAs use fluorescence lifetimes to help in the discrimination between free and bound Ag*, while TRFIAs only use fluorescence lifetime differences to eliminate background fluorescence. PRFIAs may be either homogeneous or heterogeneous while, with two exceptions, all reported TRFIAs are heterogeneous (27,28, 44). The homogeneous TRFIAs were based on fluorescence intensity differences between the free and bound Ag*; only

PRFIAs use fluorescence lifetime selectivity as the basis of homogeneous detection. The first PRFIA was developed for the determination of phenobarbital (86). The phase-resolved technique was subsequently applied to the fluoroimmunochemical determination of human serum albumin (87) and human lactoferrin (89).

Phenobarbital was chosen as a model analyte for the initial development of PRFIA. Like other barbiturates, it acts upon the central nervous system as a suppressor of neuronal activity. Phenobarbital is used as a hypnotic and an anticonvulsive. Its therapeutic level is fairly narrow, ranging from 10 to 40 μg/ml. Serum levels between 40 and about 100 μg/ml are toxic but nonlethal. Concentrations above 100 μg/ml are usually considered lethal, although this level is not absolute since tolerance can occur (99-101). In addition, equivalent dosages do not produce equivalent serum levels from patient to patient. Thus, serum concentrations must be monitored to ensure effective pharmaceutical activity.

Experimental

Reagents

Fluorescein-labelled phenobarbital (Ag^*) was prepared *in situ*, see Chapter IV, (94) and the concentration of the chromatographically purified reaction product was estimated to be 30 uM (102). A preparation of anti-phenobarbital was obtained as gift from Syva. Goat anti-phenobabital was

obtained from International Immunology Corporation (Murrieta, CA) and sheep anti-phenobarbital (Ab) was purchased from Cambridge Medical Diagnostics (Billerica, MA). A protein concentration was not supplied with this Ab, thus all concentrations of this Ab in solutions are reported as µl of 1:500 dilution of Ab in 3.0 ml of buffered solution. Phenobarbital (Ag), Triton X-100, and pooled human sera were all purchased from Sigma Chemical Company. The pooled human sera was supplied as a lyophilized solid and reconstituted according to the manufacturer's instructions. All compounds were used without further purification.

Demineralized, distilled water was used for all preparations. Phosphate buffer was prepared from NaH_2PO_4 and Na_2HPO_4 solutions and contained 0.1% sodium azide as a preservative. The Ab stock solution was a 1:500 dilution of the Ab in phosphate buffer. The Ag* stock solutions ($3x10^{-6}$, $3x10^{-7}$ M) were prepared by diluting the appropriate volume of Ag* with phosphate buffer. The pooled human sera was diluted 300-fold with phosphate buffer. The Ag stock solution ($2.0x10^{-3}$ M) was prepared by dissolving the Ag in phosphate buffer and sonicating for one hour. A series of phenobarbital solutions were prepared by diluting the appropriate volume of Ag stock solution with 1:300 pooled human sera (or phosphate buffer for solutions without human sera). Standards and test solutions were prepared by the addition of 35 µl of $3x10^{-7}$ M Ag*, 50 µl of Ag of the appropriate concentration, and 35 µl of Ab to a cuvette

containing 2880 µl of 0.010 M phosphate buffer (pH 7.4, 0.010% TX-100) and incubating for one hour. The buffer solution containing the TX-100 was added to the cuvettes one day prior to preparing the standards and test solutions. Triton X-100 was used to prevent adsorption of the fluorophore onto the sides of the disposable polyethylene cuvettes (Precision Cells).

Apparatus and Procedures

All fluorescence measurements were made with an SLM 4800S spectrofluorometer (SLM Instruments, Inc.) with 450 W xenon arc source and photomultiplier tube (Hamamatsu R928) detection. An Apple IIe microcomputer was used for on-line data acquisition and for data analysis. An excitation modulation frequency of 30 MHz was used for all dynamic measurements. The sample compartment temperature was maintained at 25.0° ± 0.1° C with a Haake A81 temperature control unit. All fluorescence lifetimes are reported as the average of five measurements taken in the "100 average" mode, in which each measurement is the average of 100 samplings performed internally by the spectrofluorometer. A solution of acridine orange (U.S. Industrial Chemical Co.) in absolute ethanol was used as the reference for all direct lifetime measurements. The fluorescence lifetime of acridine orange was found to be 3.19 ± 0.02 ns versus a scatter solution. Steady state emission and excitation spectra were obtained in the "10 average" mode with slit

settings of 8 nm for the excitation monochromator entrance and exit and the modulation tank exit slits, and 16 nm for the emission monochromator entrance and exit slits. All other fluorescence measurements were made with the excitation monochromator entrance slit at 16 nm, the excitation monochromator exit slit at 0.5 nm, the modulation tank exit slit at 0.5 nm and a 530 nm bandpass filter (10 nm half-width, Oriel) instead of the emission monochromator.

Results and Discussion

Three different anti-phenobarbital preparations were studied. The first was a gift from Syva. No change in fluorescence intensity or lifetime was seen when this antibody was added to a solution of the fluorescein-labelled phenobarbital. Either the antibody was not binding the Ag* or it was just not producing any detectable changes in the fluorescence characteristics of the Ag* upon binding. The second antibody preparation was goat anti-phenobarbital from International Immunology. It produced a 0.10 ns lifetime difference between the free and bound Ag*. The third antibody preparation was sheep anti-phenobarbital from Cambridge Medical Diagnostics. It produced the largest lifetime change and also a large intensity change between the free and bound Ag*. This antibody was used in the remainder of the current work.

Spectra of free Ag* and completely Ab-bound Ag* are shown in Figure 29. The fluoresence intensity of the Ag* is

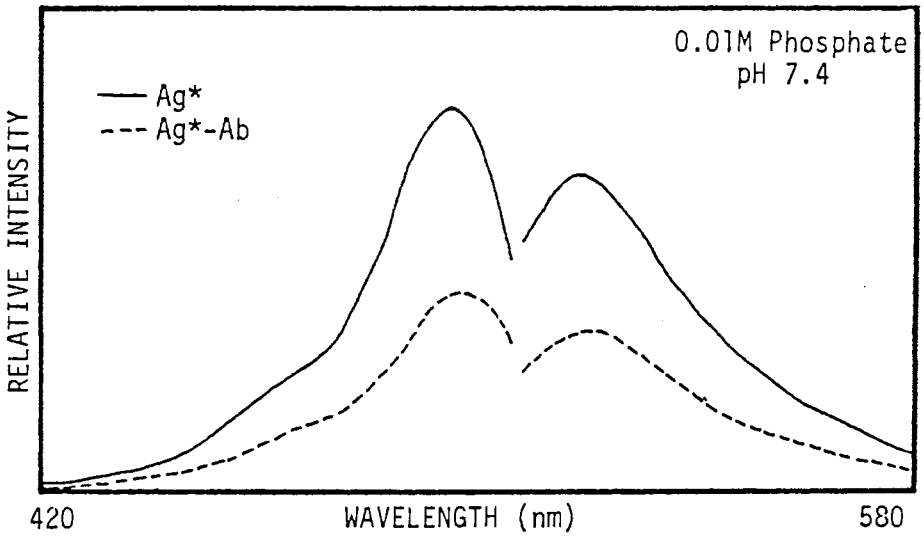

Figure 29. Fluorescence Excitation and Emission Spectra of Free (Ag*) and Antibody-Bound (Ag*-Ab) Labelled Phenobarbital in Phosphate Buffer Solution at pH 7.4.

quenched when the antibody binds the Ag*. The ratio of the fluorescence emission intensities at 525 nm of the free to the bound Ag* was 2.7. The excitation and emission maxima remain constant, with the excitation maximum at 490 nm and the emission maximum at 525 nm.

The fluorescence lifetime of Ag*, as a function of the volume of Ab added is plotted in Figure 30 for four different concentrations of Ag*. In all cases, the difference in fluorescence lifetime between the free and completely bound Ag* was approximately 0.35 ns. As the concentration of Ag* decreased from 11.6 nM to 1.2 nM, the slope of the curves increased. Thus, lower concentrations of Ag* require less Ab to become ~50% bound and, consequently, the introduction of a small amount of Ag into the system induces a larger change in the fluorescence signal in the immunoassay that uses a lesser amount of Ag*. However, the signal to noise ratio decreases as the concentration of Ag* decreases; therefore, a compromise must be reached between (1) improved sensitivity, and (2) deteriorating signal-to-noise ratio. Initially, a 1.9 nM concentration of Ag* was chosen and 20 μL of 1:500 Ab in 3.0 mL total volume bound approximately 50% of this concentration of Ag*. The concentration of Ag* was later increased to 3.5 nM to improve the S/N ratio and the amount of Ab added was increased accordingly. Increasing the concentration of Ag* also widens the dynamic range of the calibration curve.

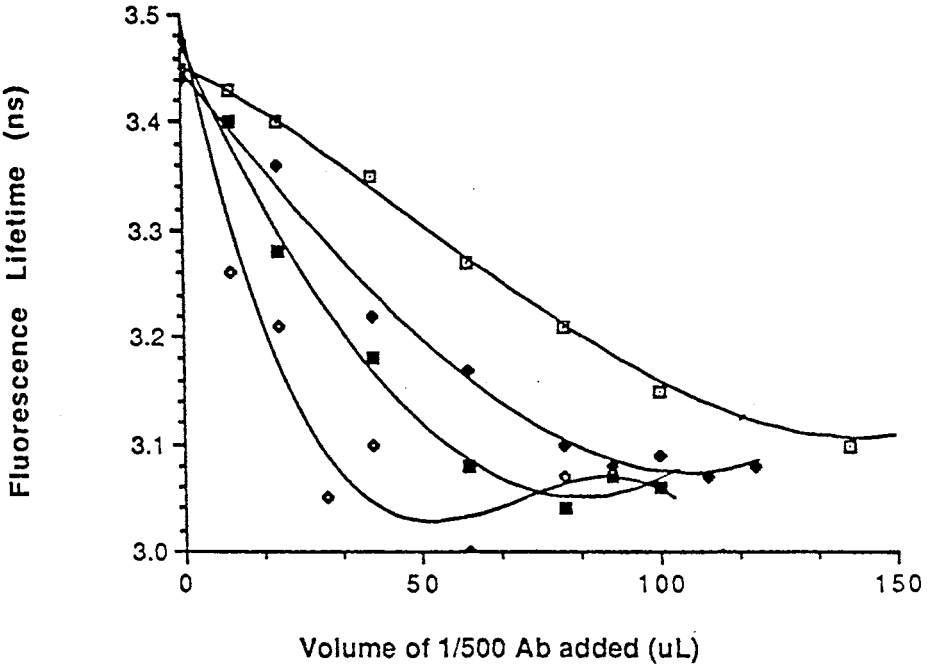

Figure 30. Antibody Dilution Profile, with Fluorescence Lifetime Plotted as a Function of Volume of 1:500 Ab Added for a Series of Ag* Concentrations. 11.6 nM (⧈), 5.0 nm (◆), 1.9 nM (■), 1.2 nM (◇) Ag*.

Figure 31 shows a plot of PRFI as a function of the ϕ_D for free Ag*, 100% bound Ag* and a calibration blank, which contained 1.9 nM Ag*, 20 µL of 1:500 Ab, and no Ag. All three solutions have phase maxima at a ϕ_D setting of around 115°. The observed phase angle difference between the free and bound Ag* was 3.84°, which corresponds to a lifetime difference of 0.36 ns. This is consistent with the lifetime differences that were obtained from direct lifetime determinations (Figure 30).

The PRFI intensity ratio of the 60 nM standard to the calibration blank for 3.5 nM Ag* and 35 µL of 1:500 Ab as a function of ϕ_D is shown in Figure 32. A ϕ_D of 45° gave the highest intensity ratio. At ϕ_D settings on either side of 45°, a decrease in the intensity difference between the standard and the blank was seen.

Calibration curves were produced by plotting the ratio of the intensities (PRFI or steady-state) of each standard solution to that of the calibration blank as a function of the Ag concentration. Use of the intensity ratio helped to minimize the effects of variations in different sets of standard solutions and reagents, and of day-to-day variations in the tuning of the fluorometer. The calibration curves were fit with a third-order polynomial function. Each of the curves shown in Figures 33 and 34 is the average of four curves, generated from triplicate measurements of each standard in the 100 average mode. The pooled standard deviation and relative standard deviations

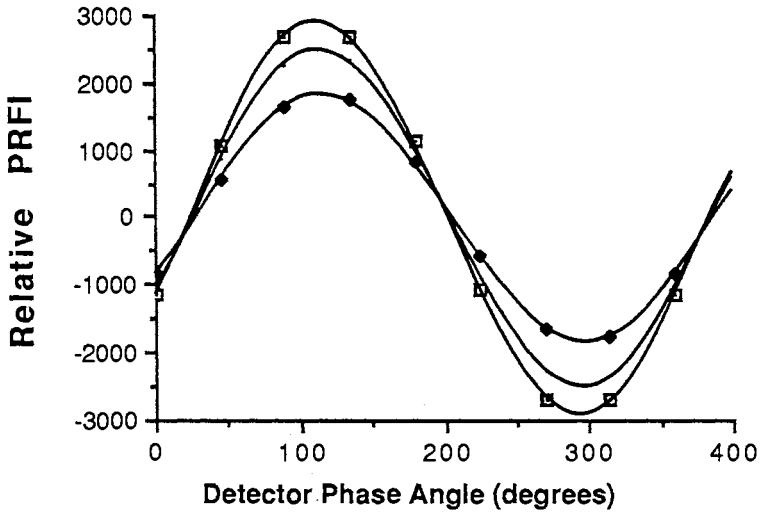

Figure 31. Phase Angle Diagram in Which Relative PRFI of 1.9 nM Ag* in the Presence (◆) and Absence (□) of Ab is Plotted as a Function of the Detector Phase Angle Setting (ϕ_D).

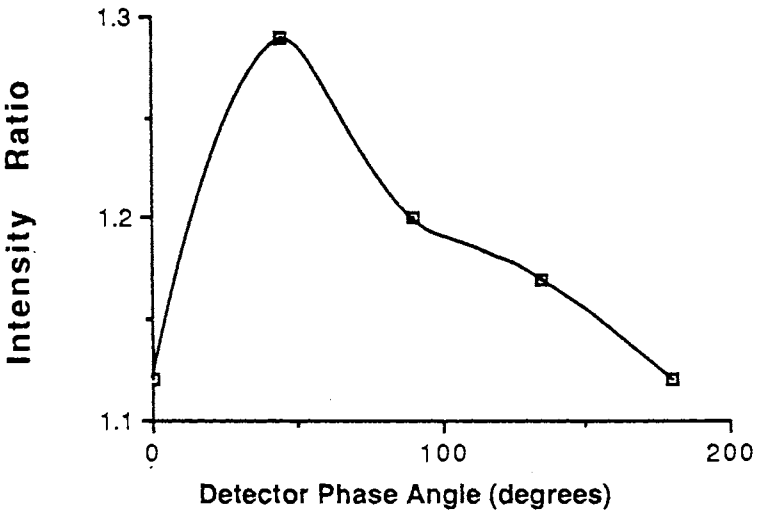

Figure 32. Ratio of the PRFI of Ag* in the Presence of Ag (60 nM) to the PRFI in the Absence of Ag when C_{Ag^*} = 3.5 nM and $Vol._{Ab}$ = 35 µL, as a function of Detector Phase Angle.

for each type of calibration curve studied are shown in Table XIV, which also shows the estimated limit of detection if it was determined. The calibration curve isn't linear between the lowest standard and the calibration blank and the third-order polynomial function was unable to fit a line between these two points without distorting the rest of the curve. The nonlinearity is probably due to two factors. First, because the intensity ratio is used, the blank value is equal to 1.00 by definition. Second, immunoassay calibration curves are typically "S" shaped and thus the curve should be expected to level out as the concentration of Ag approaches zero. This appears to be happening somewhere between the 1.0 nM Ag standard and the blank. No other standards were run between these points so the curve is hard to fit in this region. Because of the nonlinearity, the limit of detection was estimated from the signal of the lowest standard plus three times its standard deviation. The actual detection limit is likely to be lower than this value but it can be used as an upper estimate.

Effects of the Ag^* concentration on the linear range and shape of the calibration curve are shown in Figure 33. Increasing the Ag^* concentration from 1.9 to 3.5 nM increased the linear range and gave a calibration curve with a better fit. The pooled standard deviation decreased from 0.028 to 0.020 intensity ratio units as the concentration of Ag^* increased. These represent a coefficient of variation range of 2.8 to 2.5% and 1.9 to 1.5%, respectively,

TABLE XIV

ANALYTICAL PARAMETERS FOR THE TYPES OF CALIBRATION CURVES STUDIED

Type	Conc. Ag*[a]	Conc. TX-100[a]	pooled SD[b]	RSD[c]	LOD[d]
PRFS	1.7 nM	0.010%	0.028	2.8 - 2.5	
PRFS	3.5 nM	0.010%	0.020	1.9 - 1.5	1.6 nM
Steady State	3.5 nM	0.010%	0.034	2.9 - 2.5	
PRFS in sera	3.5 nM	0.010%	0.050	3.8 - 4.9	
PRFS in sera	3.5 nM	0.075%	0.024	1.6 - 2.0	2.6 nM
PRFS % Free[e]	3.5 nM	0.075%	2.68	6.2 - 3.7	2.0 nM

[a] Concentration in cuvette.
[b] Pooled standard deviation.
[c] Relative standard deviation (%) over the range of standards used in the calibration curve.
[d] Estimated limit of detection.
[e] Data analyzed in a manner analogous to the previously reported PRFIA.

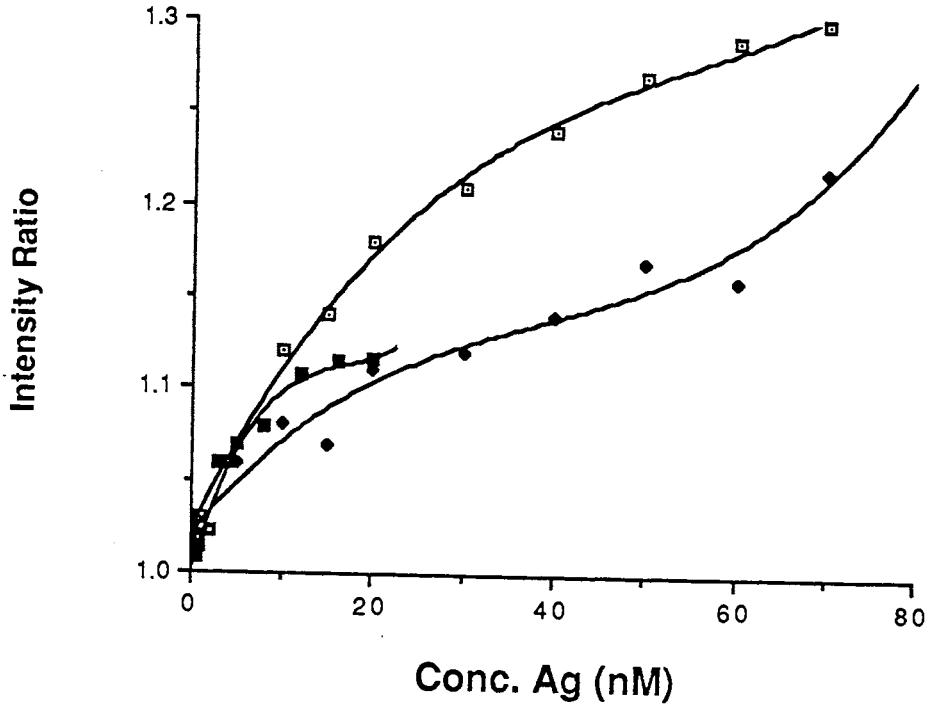

Figure 33. Phase-Resolved (■ 1.9 nM Ag*, ⊡ 3.5 nM Ag*) and Steady-State (♦ 3.5 nM Ag*) Calibration Curves. PRFI Ratio (as in Figure 32) as a Function of Conc. Ag. Measurements Were Made at Φ D = 45°, with 20 µl of Ab Added to the 1.9 nM Ag* Solutions and 35 µl of Ab to the 3.5 nM Ag* Solutions.

over the range of intensity ratios for the calibration curves. The estimated limit of detection for the 3.5 nM Ag* calibration curve was found to be 1.6 nM Ag. Figure 33 also shows a steady-state calibration curve at 3.5 nM Ag*. The steady-state calibration curve has lower sensi- tivity and a higher standard deviation than the PRFS calibration curve.

Figure 34 shows phase-resolved calibration curves for phenobarbital in pooled human sera, at a 1:18,000 fold dilution. When the working standards were prepared in pooled human sera the imprecision of the data points increased. Increasing the amount of Triton X-100 in the buffer reduced this effect. However, increasing the concentration of TX-100 also decreased the intensity ratio of the standards, which led to a decrease in the sensitivity. The intensity ratio of a 65 nM Ag standard was found to decrease gradually from 1.25 to 1.14 over a TX-100 concentration range of 0.010% (0.20 mM) to 0.100% (1.58 mM). When calibration curves were run with 0.075% TX-100 added to the buffer, the pooled standard deviation decreased from 0.050 to 0.024 intensity ratio units as shown in Table XIV. The relative standard deviation decreased correspondingly from ~5% to ~2%. The detection limit for the calibration curves with 0.075% TX-100 was estimated to be 2.6 nM Ag from the signal of the lowest standard plus three times its standard deviation. This value corresponds to a concentration of 10.9 µg/ml in the undiluted sample.

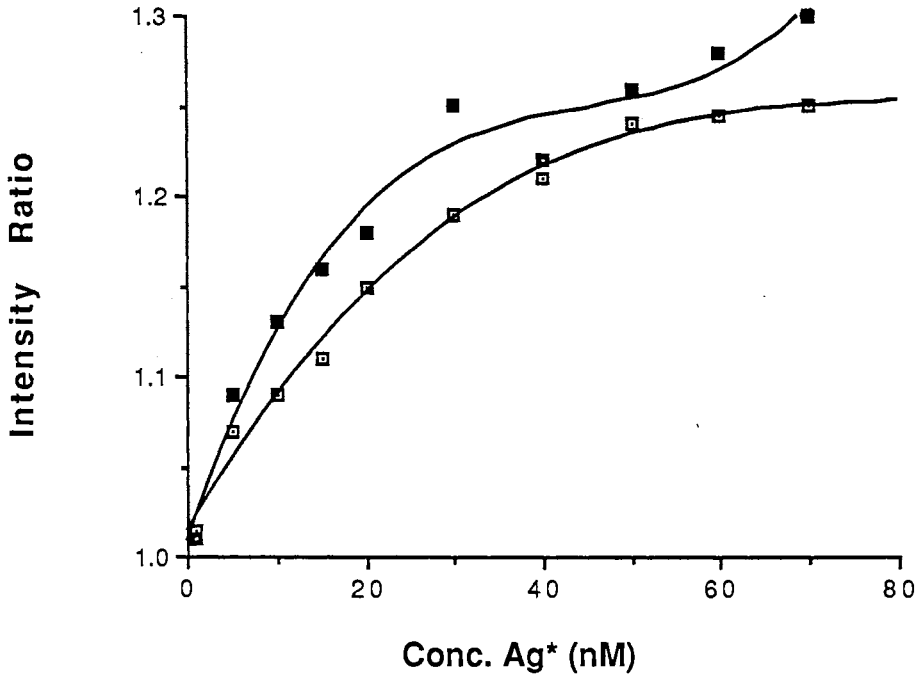

Figure 34. Effect of TX-100 on Phase-Resolved Calibration Curves of Ag in 1:18,000 Dilution of Pooled Human Sera. PRFI ratio (as in Figure 32) as a function of Conc. Ag. Measurements were made at Φ D = 45 , with Conc. Ag* = 3.5 nM, and 35 µl 1:500 Ab. 0.010 % (■), 0.075% (⧈) TX-100.

The effect of the dilution factor of the pooled human sera on the intensity ratio of the calibration standards was also studied. As seen in Figure 35, the intensity ratio of the standards tends to decrease, as the level of sera in the calibration standards is increased. The lowest concentration standards show little or no change in intensity ratio. As the concentration of Ag in the standards increases, the pooled sera has a proportionately greater effect on the intensity ratio. However, if a lower detection limit is desired, the dilution factor of the immunoassay could be decreased without significantly adverse effects on the low range of the calibration curve.

Two phenobarbital test solutions of differing concentrations of Ag were prepared. The results of the determination of phenobarbital in these test solutions are shown in Table XV. Three replicates of each solution were analyzed and the mean for each solution was reported.

Conclusions

The differences in the fluorescence intensities of the free and Ab-bound labelled phenobarbital are much larger than those found in the previous PRFIA of phenobarbital (7). The change in the fluorescence lifetimes is also larger. Previously, only a small intensity difference and a lifetime difference of 0.10 ns was reported. In the current system there is about a 50% change in intensity and a lifetime difference of 0.36 ns. The previous PRFIA used reagents

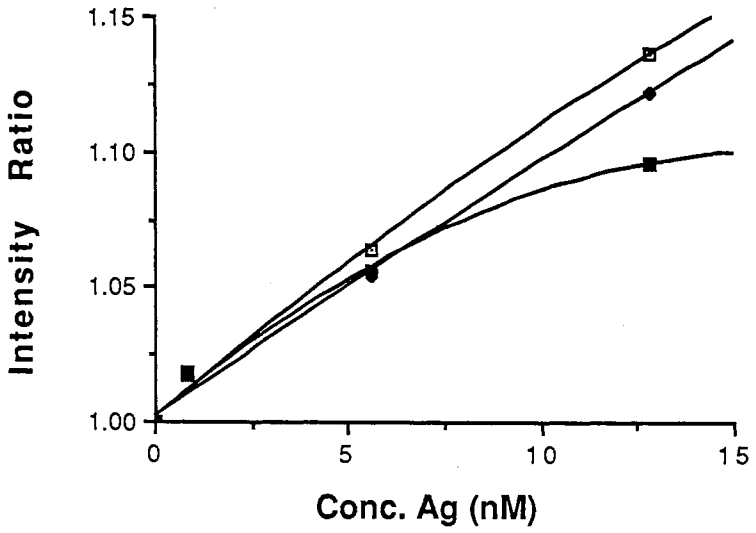

Figure 35. Effect of Pooled Sera Dilution Factor on the Intensity Ratio of Calibration Standards. PRFI ratio (as in Figure 32) as a function of Conc. Ag for pooled sera dilution factors of ⊡ 1:18,000, ◆ 1:9,000, ■ 1:6000. Solution conditions: 3.5 nM Ag*, 35 µl 1:500 Ab, 0.075%-TX-100.

TABLE XV

DETERMINATION OF UNKNOWN TEST SOLUTIONS

sample	true value[a]	found[b]	rel. error[c]	RSD[d]
1	13.3 nM	13.4 nM	0.8	1.7
2	50.0 nM	51.1 nM	2.2	1.3
avg.			1.5	1.5

[a] Concentration added to cuvette.

[b] Experimentally determined value, average of three identically prepared solution, concentration in cuvette.

[c] Relative error of determination (%) for the mean concentration.

[d] Relative standard deviation (%) of the three replicates analyzed.

from a FIA kit that was commercially avaliable at that time. The current PRFIA uses labelled phenobarbital prepared *in situ*, in which the fluorescein moiety was attached to the *para* position of the aromatic ring of phenobarbital. The anti-phenobarbital antibody preparation, purchased from Cambridge Medical Diagnostics, was raised by injecting animals with a preparation of phenobarbital attached to a carrier molecule via the aromatic ring of phenobarbital. Thus, the label is unlikely to interfere with antibody binding to the labelled phenobarbital.

The method of data analysis in the previous PRFIA (86) involved measuring the PRFI of each standard or sample at five different detector phase angles and generating a series of linear simultaneous equations. The series of equations was "solved" for the fractions of free and bound Ag* by using a Gauss-Newton iterative procedure on a microcomputer. The PRFIA calibration curve for phenobarbital was generated by plotting the % Free Ag* versus Ag concentration, followed by third-order polynomial fitting. This multiple phase-angle approach involves much more data collection and analysis than the current PRFIA. In order to compare the current system of reagents to the previous PRFIA, data were collected and analyzed in an analogous manner using two detector phase angles. The results are shown in Table XIV. The detection limit for the old method was lower than the detection limit for the intensity ratio calibration curve, but a data point for the calibration blank was included in

the fit since a nontrivial value could be obtained using the multiple phase-angle approach. However, the mutiple phase-angle approach is not very amenable to automation. The current PRFIA could be easily automated using flow injection analysis. Serum samples are generally better behaved in flow systems, so it may also be possible to reduce the TX-100 concentration in the flow system in order to get higher sensitivity and a lower detection limit.

CHAPTER VI

CONCLUSIONS

Homogeneous phase-resolved fluoroimmunochemical determinations are advantageous in that they do not require a separation step or any other special sample handling techniques. They are also the only FIA which uses fluorescence lifetime selectivity as the basis of homogeneous detection. The first PRFIA for haptens (86) involved fairly complicated and time-consuming data collection and analysis; which was required because there was very little difference in the fluorescence intensity and lifetime between the free and antibody-bound species. One of the main advantages of homogeneous FIAs is that they are usually easliy automated. The data collection and analysis scheme of the first PRFIA, in all practicality, precludes its automation. In order to better demonstrate the applicability of PRFS to immmunoassays for the determination of haptens, a simplified PRFIA with a larger change in signal between the free and bound labelled antigen was needed.

This work decribes the attempts that were made to improve the discrimination between the Ag* and Ag*-Ab. The first section focused on the use of micelles and cyclodextrins (auxillary binding reagents) to increase the

difference in fluorescence signals. It was thought that the auxillary binding reagents might associate with the free Ag* and not with Ag*-Ab, thereby increasing the difference between their fluorescence signals. Unfortunately, the micelles and cyclodextrins associate with both Ag* and Ag*-Ab. The auxillary binding reagents decreased the intensity ratio of free Ag* to Ag*-Ab, relative to the intensity ratio in buffer. The micelles and γ-CD also decreased the lifetime difference between the free Ag* and Ab-Ag*. The β-CD, on the other hand, increased the lifetime difference by about 0.05 ns. When the two effects are considered together, no gain in the ability to discriminate between Ag* and Ag*-Ab was found with β-CD. The micelles may be useful with other haptens or labels; β-CD would probably be useful if the aromatic ring of phenobarbital was accessable to it, perhaps by labelling via the ethyl group.

The second part of this work involved the optimization of the experimental conditions and reagents used in the PRFIA of phenobarbital. The effects of several different antibody preparations on Ag* were studied. It was found that the intensity and lifetime differences could be increased dramatically by judicious choice of the antibody preparation. Because of the larger differences between the signals of Ag* and Ag*-Ab, a simplified data collection and analysis scheme was implemented. The automation of this new PRFIA for phenobarbital should be fairly simple using an unsegmented continuous-flow system.

BIBLIOGRAPHY

1. Chard, T. An Introduction to Radioimmunoassay and Related Techniques; 3rd Revised Edition; Elsevier: Amsterdam 1987; pp 1-10, 130-136.

2. Nakamura, R. M. Clin. Lab. Assays: [pap. Annu. Clin. Lab. Assays Conf.] 4th 1983, 33-60.

3. Smith, D. S.; Al-Hakiem, M. H. H.; Landon, J. Ann. Clin. Biochem. 1981, 81, 253-274.

4. Hemmila, I. Clin. Chem. 1985, 31, 359-370.

5. Smith, D. S.; Hassan, M.; Nargessi, R. D. In Modern Fluorescence Spectroscopy; Whery, E. L., Ed.; Plenum: New York, 1981; Vol. 3, Chapter 4.

6. Yalow, R. S.; Berson, S. A. J. Clin. Invest. 1960, 39, 1157-1175.

7. Miles, L. E. M.; Hales, C. N. Nature 1968, 219, 186-189.

8. Ekins, R. P.; Dakubu, S. Pure Appl. Chem. 1985, 57, 473-482.

9. ACS Committee on Environmental Improvement Anal. Chem. 1980, 52, 2242-2249.

10. International Federation of Clinical Chemistry Committee on Standards Clin. Chem. 1976, 22, 532-540.

11. Ekins, R. In Monoclonal Antibodies and Developments in Immunoassay; Albertini, A., Ekins, R., Eds.; Elsevier/North Holland Biomedical Press: Amsterdam, 1981; Chapter 1.

12. Dakabu, S.; Ekins, R.; Jackson, T.; Marshall, N. J. In Practical Immunoassay: The State of the Art; Butt, W. R., Ed.; Marcel Dekker, Inc.: New York, 1984; pp 71-101.

13. Hood, L. E.; Weissman, I. L.; Wood, W. B. "Immunology"; Benjamin/Cummings: London, 1978; p 4.

14. Harris, C. C.; Yolken, R. H.; Krokan, H.; Hsu, I. C. Proc. Natl. Acad. Sci. USA 1979, 76, 5336.

15. Shalev, A.; Greenberg, G. H.; McAlpine, P. J. J. Immunol. Methods 1980, 38, 125.

16. Woodhead, J. S.; Simpson, J. S. A.; Weeks, I.; Patl, A.; Campbell, A. K. In Monoclonal Antibodies and Developments in Immunoassay; Albertini, A., and Ekins, R. P., Eds.; Elsevier/North Holland Biomedical Press: Amsterdam, 1981; p 135.

17. Hemmila, I.; Dakubu, S.; Mukkala, V.-M.; Siitari, H.; Lovgren, T. Anal. Biochem. 1984, 137, 335-343.

18. Soini, E.; Hemmila, I. Clin. Chem. 1979, 25, 353-361.

19. Leung, C. S-H.; Meares, C. F. Biochem. Biophys. Res. Commun. 1977, 75, 149.

20. Wieder, I. In Immunofluoresence and Related Staining Techniques; Knapp, W., Holubar, K., Wick, G., Eds.; Elsevier/North-Holland Biomedical Press: Amsterdam, 1978; pp 67-80.

21. Ringbom, A. Complexation In Analytical Chemistry Wiley-Interscience: New York, 1963; pp.

22. Khosravi, M. J.; Diamandis, E. P. Clin. Chem. 1987, 33, 1994-1999.

23. Chan, M. A.; Bellem, A. C.; Diamandis, E. P. Clin. Chem. 1987, 33, 2000-2003.

24. Reichstein, E.; Yehezkel, S.; Ramjeesingh, M.; Diamandis, E.P. Anal. Chem. 1988, 60, 1069 - 1074.

25. Evangelista, R.; Pollack, A.; Allore, B.; Templeton, E. F.; Morton, R. C.; Diamandis, E. P.Clin. Biochem. 1988, 21, 173-178.

26. Diamandis, E. P.; Morton, R. C. J. Immunol. Met. 1988, 112, 43-52.

27. Hemmila, I.; Malminen, O.; Mikola, H.; Lovgren, T. Clin. Chem. 1988, 34, 2320-2322.

28. Barnard, G.; Kohen, F.; Mikola, H., Lovgren, T. Clin. Chem. 1989, 35, 555-559.

29. Marshall, N. J.; Dakubu, J.; Jackson, T.; Ekins, R. P. In Monoclonal Antibodies and Developements in Immunassay Albertini, A., Ekins, R. P., Eds.; Elsevier/North Holland: Amsterdam, 1981; pp 101-108.

30. Bador, R.; Dechaud, H.; Claustrat, F.; Desuzinges, C. Clin. Chem. 1987, 33, 48-51.

31. Hemmila, I. Anal. Chem. 1985, 57, 1676-1681.

32. Hemmila, I.; Holttinen, S.; Pettersson, K.; Lovgren, T. Clin. Chem. 1987, 33, 2281-2283.

33. Kricka, L.J. Ligand-Binder Assays; Marcel Dekker: New York, 1985; pp 15-38, 70.

34. Diamandis, E. P.; Morton, R. C.; Reichstein, E.; Khosravi, M. Anal. Chem. 1989, 61, 48-53.

35. Dechaud, H.; Bador, R.; Claustrat, F.; Desuzinges, C.; Mallein, R. Clin. Chem. 1988, 34, 501-504.

36. Diamandis, E. P.; Bhayana, V.; Conway, K.; Reichstein, E.; Papanatasiou-Diamandis, A. Clin. Biochem. 1988, 21, 291-296.

37. Reichstein, E.; Morton, R. C.; Diamandis, E. P. Clin. Biochem. 1989, 22, 23-29.

38. Khosravi, M. J.; Morton, R. C.; Diamandis, E. P. Cli Chem. 1988, 34, 1640-1644.

39. Khosravi, M. J.; Chan, M. A.; Bellem, A. C.; Diamandis, E. P. Clin. Chim. Acta 1988, 175, 267-276.

40. Lovgren, T.; Hemmila, I.; Pettersson, K.; Halonen, P. In Alternative Immunoassays; Collins, W. P., Ed.; John Wiley: New York, 1985; pp 203-217.

41. Soini, E.; Kojola, H. Clin. Chem. 1983, 29, 65-68.

42. Kuo, J. E.; Milby, K. H.; Hinsberg, W. D.; Poole, P. R.; McGuffin, V. L.; Zare, R. N. Clin. Chem. 1985, 31, 50-53.

43. Dechaud, H.; Bador, R.; Claustrat, F.; Desuzinges, C. Clin. Chem. 1986, 32, 1323-1327.

44. Diamandis, E. P. Clin. Biochem. 1988, 21, 139-150.

45. Wilmott, N. J.; Miller, J. N.; Tyson, J. F. Analyst 1984, 109, 343-345.

46. Bailey, M. P.; Rocks, B. F.; Riley, C. Analyst 1984, 109, 1449-1450.

47. Vilpo, J. A.; Rasi, S.; Suvanto, E.; Vilpo, L. M. Anal. Biochem. 1986, 154, 436-440.

48. Sidki, A. M.; Smith, D. S.; Landon, J. Clin. Chem. 1986, 32, 53-56.

49. Bertoft, E.; Eskola, J. U.; Nanto, V.; Lovgren, T. FEBS Letters 1984, 173, 213-216.

50. Eskola, J. U.; Nanto, V.; Meurling, L.; Lovgren, T. N.-E. Clin. Chem. 1985, 31, 1731-1734.

51. Rasi, S.; Suvanto, E.; Vilpo, L. M.; Vilpo, J. A. J. Immunol. Met. 1989, 117, 33-38.

52. Helsingius, P.; Hemmila, I.; Lovgren, T. Clin. Chem. 1986, 32, 1767-1769.

53. Alfthan, H. J. Immunol. Meth. 1986, 88, 239-244.

54. Dobson, S.; White, A.; Hoadley, M.; Lovgren, T.; Ratcliffe, J. Clin. Chem. 1987, 33, 1747-1751.

55. Halonen, P.; Meurman, O.; Lovgren, T.; Hemmila, I.; Soini, E. Current Topics in Microbiology and Immunology; Vol 104, "New Developements in Diagnostic Virology"; Bachmann, P.A., Ed.; Springer-Verlag: Berlin, 1983; pp 133-146

56. Pettersson, K.; Siltari, H.; Hemmila, I.; Soini, T.; Lovgren, T.; Hanninen, V.; Tanner, P.; Stenman, U.-H. Clin. Chem. 1983, 29, 60-64.

57. Stenman, U.-H.; Alfthan, H.; Myllynen, L.; Seppala, M. The Lancet 1983, 9, 674-649.

58. Alfthan, H.; Schroder, J.; Fraser, R.; Koskimies, A.; Halila, H.; Stenman, U.-H. Clin. Chem. 1988, 34, 1758-1762.

59. Kaihola, H.-L.; Irjala, K.; Vilkari, J.; Nanto, V. Clin. Chem. 1985, 31, 1706-1709.

60. Kreutzer, H. J. H.; Tertoolen, J. F. W.; Thijssen, J. H. H.; der Kinderen, P. J.; Koppeschaar, H. P. F. Clin. Chem. 1986, 32, 2085-2090.

61. Lovgren, T.; Hemmila, I.; Pettersson, K.; Eskola, J. U.; Bertoft, E. Talanta 1984, 10, 909-916.

62. Lawson, N.; Mike, R.; Wilson, R.; Pandov, H. Clin. Chem. 1986, 32, 684-686.

63. Torresani, T. E.; Scherz, R. Clin. Chem. 1986, 32, 1013-1016.

64. Parnham, A. J.; Tarbit, I. F. Clin. Chem. 1987, 33, 1421-1424.

65. Stenman, U.-H.; Alfthan, H.; Koskimies, A.; Seppala, M.; Pettersson, K.; Lovgren, T. Ann. N. Y. Acad. Sci. 1985, 442, 544-550.

66. Toivonen, E.; Hemmila, I.; Marniemi, J.; Jorgensen, P. N.; Zeuthen, J.; Lovgren, T. Clin. Chem. 1986, 32, 637-640.

67. Pesonen, K.; Alfthan, H.; Stenman, U.-H.; Viinikka, L.; Perheentupa, J. Anal. Biochem. 1986, 157, 208-211.

68. Meurman, O. H.; Hemmila, I. A.; Lovgren, T. N.-E.; Halonen, P. E. J. Clin. Micro. 1982, 16, 920-925.

69. Siitari, H.; Hemmila, I. ; Soini, E.; Lovgren, T.; Koistinen, V. Nature 1983, 301, 258-260.

70. Suonpaa, M. U.; Lavi, J. T.; Hemmila, I. A.; Lovgren, T. N.-E. Clin. Chim. Acta 1985, 145, 341-348.

71. Niemi, S.; Maentausta, O.; Bolton, N. J.; Hammond, G. L. Clin. Chem. 1988, 34, 63-66.

72. Boerman, O. C.; Thomas, C. M. G.; Segers, M. F. G.; Kenemans, P.; Lovgren, T.; Zurawski, V. R.; Haisma, H. J.; Poels, L. G. Clin. Chem. 1987, 33, 2191-2194.

73. Kostinen, R.; Stenman, U.-H.; Alfthan, H.; Seppala, M. Clin. Chem. 1987, 33, 1126-1128.

74. Eskola, J. U.; Nevalainen, T. J.; Lovgren, T. N.-E. Clin. Chem. 1983, 29, 1777-1780.

75. Schmidt, B.; Steinmetz, G. Clin. Chem. 1987, 33, 1070.

76. Thomas, C.M.G.; van den Berg, R.J.; Seyers, M.F.G. Clin. Chem. 1987, 33, 120.

77. Butzow, R.; Alfthan, H.; Stenman, U.-H.; Sulkkari, A.-M; Bohn, H.; Seppala, M. Clin. Chem. 1988, 34, 1591-1593.

78. Dakubu, S.; Hale, R.; Lu, A.; Quick, J.; Solas, D.; Weinberg, J. Clin. Chem. 1988, 34, 2337-2340.

79. Bailey, M. P.; Rocks, B. R.; Riley, C. Analyst 1985, 110, 603-604.

80. Keelan, J. A.; France, J. T.; Barling, P. M. Clin. Chem. 1987, 33, 2292-2295.

81. Demas, J. N. Excited State Lifetime Measurements; Academic Press: New York, 1983.

82. Lakowicz, J. R. Principles of Fluorescence Spectroscopy; Plenum Press: New York, 1983.

84. Bright, F. V.; Ph.D. thesis "Theory and Applications of Phase-Resolved Fluorescence Spectroscopy (PRFS) for Implementation of Fluorescence Lifetime Selectivity in Multicomponent Fluorometric Determinations"; 1985, Oklahoma State University, Stillwater.

85. McGown, L. B.; Bright, F. V. Anal. Chem. 1984, 56, 1400A-1415A.

86. Bright, F. V.; McGown, L. B. Talanta 1985, 32, 15-18.

87. Tahboub, Y. R.; McGown, L. B. Anal. Chim. Acta 1986, 182, 185-191.

88. Doumas, B. T.; Watson, W. A.; Biggs, H. G. Clin. Chim. Acta 1971, 31, 87-96.

89. Nithipatikom, K. ;McGown, L. B. Anal. Chem. 1987, 59, 423-427.

90. James, A. D.; Robinson, B. H.; White, N. C. J. Colloid Interface Sci. 1977, 59, 328-336.

91. Nelson, G.; Patonay, G.; Warner, I. M. Anal. Chem. 1988, 60, 274-279.

92. Halfman, C. J.; Wong, F. C. L.; Jay, D. W. Anal. Chem. 1985, 57, 1928-1930.

93. Halfman, C. J.; Jay, D. W. Anal. Chem. 1986, 32, 1677-1681.

94. Bright, F. V.; Bunce, R. A.; McGown, L. B. Org. Prep. Proc. Intl. 1986, 18, 209-212.

95. Fendler, J. H.; Fendler, E. J. Catalysis in Micelles and Macromolecular Systems; Academic Press: New York, 1975; Chapters 1-2.

96. Malliaris, A.; LeMoigne, J.; Sturm, J.; Zann, R. J. Phys. Chem. 1985, 89, 2709-2713.

97. Martin, M.; Lindquist, L. J. Lumin. 1975, 10, 381.

98. Han, S. M.; Purdie, N. Anal. Chem. 1984, 56, 2825-2827.

99. Johns, M. P. Drug Therapy and Nursing Care; Mcmillan: New York, 1979; pp. 567-569.

100. Baselt, R. C. Analytical Procedures for Therapeutic Drug Monitoring and Emergency Toxicology; Biomedical Publications: Davis, CA, 1980; p. 10.

101. Mofenson, H. C.; Curaccio, T. R.; Greensher, J. In Conn's Current Therapy 1987; Rakel, R. E., Ed.; Saunders: Philadelphia, PA, 1987; p. 992.

102. Keimig, T. L.; McGown, L. B. Talanta 1986, 33, 653-656.

VITA

Teresa L. Keimig

Candidate for the Degree of

Doctor of Philosophy

Thesis: PHASE-RESOLVED FLUOROIMMUNOCHEMICAL METHODS FOR THE DETERMINATION OF PHENOBARBITAL

Major Field: Chemistry

Biographical:

Personal Data: Born in Canby, Minnesota, February 17, 1960, the daughter of Joseph H. and Catherine T. Keimig.

Education: Graduated from Fergus Falls Senior High School, Fergus Falls, Minnesota, in June 1978; attended Moorhead State University from September, 1978 until May 1980; recieved Bachelor of Science Degree in Chemistry from the University of South Dakota in May 1982; recieved Master of Science Degree in Chemistry from the University of Iowa in May, 1984; completed requirements for the Doctor of Philosophy Degree at Oklahoma State University in December, 1989.

Professional Experience: Laboratory Technician, South Dakota Geological Survey, Vermillion, South Dakota, 1981-1982; Graduate Teaching Assistant, Department of Chemistry, University of Iowa, Iowa City, Iowa, 1982-1984; Graduate Teaching Assistant, Department of Chemistry, Oklahoma State University, Stillwater, Oklahoma, 1984, 1987-1989; Graduate Research Assistant, Department of Chemistry, Oklahoma State University, Stillwater, Oklahoma, 1985-1987.